A Self-Contained Pocket APRS Transmitter

QEX
INCLUDING: COMMUNICATIONS QUARTERLY

Mark J. Wilson, K1RO
Publisher

Doug Smith, KF6DX
Editor

Robert Schetgen, KU7G
Managing Editor

Lori Weinberg, KB1EIB
Assistant Editor

L. B. Cebik, W4RNL
Zack Lau, W1VT
Ray Mack, WD5IFS
Contributing Editors

Production Department
Steve Ford, WB8IMY
Publications Manager

Michelle Bloom, WB1ENT
Production Supervisor

Sue Fagan
Graphic Design Supervisor

Mike Daniels
Technical Illustrator

Joe Shea
Production Assistant

Advertising Information Contact:
Joe Bottiglieri, AA1GW, *Account Manager*
  860-594-0329 direct
  860-594-0200 ARRL
  860-594-4285 fax

Circulation Department
Kathy Capodicasa, *Circulation Manager*
Cathy Stepina, *QEX Circulation*

Offices
225 Main St, Newington, CT 06111-1494 USA
Telephone: 860-594-0200
Telex: 650215-5052 MCI
Fax: 860-594-0259 (24 hour direct line)
e-mail: **qex@arrl.org**

Subscription rate for 6 issues:
  In the US: ARRL Member $24,
  nonmember $36;

  US by First Class Mail:
  ARRL member $37, nonmember $49;

  Elsewhere by Surface Mail (4-8 week delivery):
  ARRL member $31, nonmember $43;

  Canada by Airmail: ARRL member $40,
  nonmember $52;

  Elsewhere by Airmail: ARRL member $59,
  nonmember $71.

Members are asked to include their membership control number or a label from their *QST* when applying.

In order to ensure prompt delivery, we ask that you periodically check the address information on your mailing label. If you find any inaccuracies, please contact the Circulation Department immediately. Thank you for your assistance.
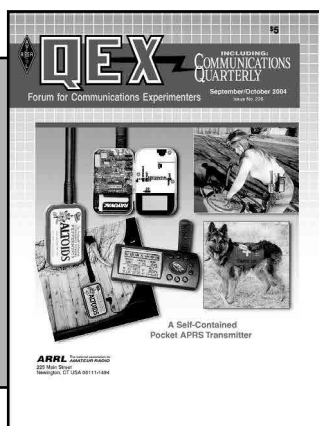
About the Cover

Pocket Tracker: APRS for all occasions (Story on page 3).

A Self-Contained Pocket APRS Transmitter

Features

Columns

Sept/Oct 2004 *QEX* Advertising Index

Empirical Outlook

The Logistics of *QEX*

In the last issue, we had a look behind the scenes at *QEX*. Now here is a little bit more about the technical and logistical details that keep it going.

QEX is a voracious animal. It gobbles up a great deal of technical material from many sources. We publish about twice as much technical material as *QST* does, on a monthly basis. We can't rest for a minute. Our staff writes a rather small percentage of what we publish, so we count on articles submitted from outside to fill the pages of every issue. *QEX* is therefore largely what you make it.

Our Basic Editorial Approach

Our need for articles is great, so don't be bashful. We need material at all skill levels. We actively support a variety of topics, from simple construction projects to the advancement of theory. We consider previously published material, but we usually need to obtain permission, unless it is from a club newsletter or the like.

The content of each issue is not planned far in advance, and may change until the issue is sent to the printer. Therefore, we can't always predict when your article will appear until well after it's edited. Expect up to twelve months to elapse between submission and publication. Authors are compensated for published articles at the rate of $50 per published page or part thereof.

Perhaps half the author's battle is deciding to write an article and choosing a subject.

Ask yourself a few questions: What subject do you know well enough to help others understand? Have you recently completed a construction project others might find interesting or want to duplicate? Do you have experimental results to pass along to others? Is there something new about your subject or your presentation? Will your article interest other amateurs?

We prefer to review a completed manuscript. Letters of inquiry involve longer turnaround times, and reviewing an outline gives no guarantee that the final manuscript will make a good article. The only advantage in submitting an outline is that you will find out beforehand if there is no interest in publishing an article on the subject you have chosen. There may be many reasons for that, including a surplus of articles on your topic.

We like to get your submissions via regular mail with hard copy and a diskette or CD. Use Word format for the text and put figures in separate files. Include figure captions at the end of the manuscript. We can use hand-drawn figures as long as they are clear enough for our artist to redraw them. Electronic figure files (screen captures, charts, etc) should be at least 1000 pixels in the largest dimension to reproduce well. Of course, photographs are good, too, as long as they are in focus with sufficient depth of field, good exposure) and of sufficient resolution. We print at 300 dots per inch. For single, double and triple column photos, that is 750, 1500 and 2250 pixels wide, respectively. This means about 1.2 megapixel for a single-column in the magazine. Potential authors can find more information on our Web page at **www.arrl.org/qst/aguide/**. Keep those projects going and the articles coming!—*73, Doug Smith, KF6DX;* **dsmith@arrl.org**

In This Issue

Jim Hall, W7TVI, and Tony Barrett, N7MTZ, bring us their design for a pocket APRS transmitter. It weighs only a few ounces, runs from an inexpensive battery for days and opens a world of possibilities for experimenters. Brian Cake, KF2YN, returns with a third segment on twin-C antennas.

Steve Gradijan, WB5KIA, describes how to "Build a Super Transceiver."

Al Christman, K3LC, describes the control networks that make his 4-square array hit the compass points. Contributing Editor L.B. Cebik, W4RNL, brings another segment of his "Tale of Three Yagis" in "Antenna Options." Look for installments of "Outside the Box" and "Tech Notes" by Contributing Editor Ray Mack, WD5IFS.—*73 de Doug Smith, KF6DX,* **kf6dx@arrl.org**. □□

A Pocket APRS Transmitter

*Here's a great project for APRS.
Its widespread use could save many lives*

By Jim Hall, W4TVI, and Tony Barrett, N7MTZ

One day Tony, N7MTZ, walked into the shack and said "Wouldn't it be neat if we could build an inexpensive APRS transmitter that weighed only a few ounces, would operate off a 9 V battery for several days and had an integrated GPS interface? A transmitter like that would open APRS operation to a whole range of personal activities such as biking, hang gliding, backpacking, skiing or snowmobiling. It would also be a great asset for emergency or Search-and-Rescue situations.[1] Just put the transmitter and a GPS receiver on

[1]Notes appear on page 11.

anything (person, vehicle, even a search dog) to automatically track it. (See Fig 1 and the sidebar, "An APRS "Killer App?") And it would be a natural for Near-Space ballooning.[2] The concept was so compelling that we immediately agreed we should attempt to build such a unit. The Pocket APRS Transmitter presented here is the result of our effort.

Discussions with other hams revealed that a Pocket APRS Transmitter is also good for those who can't justify the cost of a separate transceiver dedicated to APRS and those shy about interfacing an APRS encoder to their transceiver.

Design Considerations

Transmitter design objectives:
- Output frequencies: 144.39 and 144.34 MHz (with crystal stability).
- An integrated APRS encoder for automatic position transmission.
- Low cost.
- Small size (fit in a standard mint tin with a 9-V battery).
- 200-250 mW output.
- Battery life: At least 4 days with a standard 9 volt alkaline battery.
- Simple to assemble, align and configure.
- Use modern, readily available parts.
- FM modulation: 5 kHz peak deviation with low distortion.
- Meet FCC spurious-emission requirements.

The RF output power requirement was a major question. The final output power goal was based on the

7960 W Bayhill Ct
Boise, ID 83704
jahall@perseidsystems.com

5389 Kyle Ave
Boise, ID 83704
tonybarrett@sunvalley.net

need to minimize dc input power and the fact that most urban areas have a well-developed APRS repeater infrastructure. In such areas, APRS stations using handheld power levels have demonstrated good results. For emergency or other special situations out of repeater range, it is easy to configure a standard mobile APRS station to provide digi-peater capability.[1] For Near Space Ballooning, our local team has successfully used APRS transmitters with only a few hundred milliwatts of RF power to cover distances up to 200 miles on many of their flights.[2]

A second question was the architecture for the FM transmitter. We could have used a crystal oscillator followed by a phase modulator.[3] Experiments showed that the output frequency of a simple phase modulator would need to be multiplied by at least nine to achieve the required deviation with reasonably low distortion. This would mean using a 16 MHz crystal oscillator/phase modulator followed by at least two frequency-multiplier stages. Narrow-band filters would be required to reduce spurious frequencies to levels meeting FCC requirements. The required circuit complexity ruled out this approach for our application.

Another popular method uses a voltage controlled oscillator (VCO) operating directly at the desired output frequency, phase locked to a crystal oscillator.[3] Frequency modulation of the VCO is still possible at modulation frequencies greater than the feedback-loop bandwidth. RF filtering is simplified with this method, because RF is generated directly at the output frequency. This approach was selected for the Pocket APRS Transmitter.

Most modern electronic components and designs use surface-mount technology (SMT).[4] The small size of SMT components permits a more compact design, while improving electrical performance by reducing parasitic inductance and capacitance. SMT was a natural choice for this project, given our goal of a small pocket transmitter using modern, commercially available parts. We did, however, use through-hole parts where they were less expensive than SMT and readily available.

The TinyTrak3 (TT3) GPS position encoder (**www.byonics.com**) provides an off-the-shelf, single-chip interface between an external GPS receiver and the FM transmitter. Its power requirements are low and by using SMT parts, it was made to fit in less than half the board space of a standard through-hole TT3. This size reduction is accomplished even with a standard TT3 DIP packaged micro-

controller. As a result, we were able to keep our TT3 circuit schematically identical to the standard through-hole TT3, use a genuine TT3 PIC, and support all TT3 features.

Fig 2C shows an internal view of the Pocket APRS Transmitter. The internal 9-V battery compartment is at the bottom of the photo. The TT3 is above that in the area dominated by its DIP micro-controller. The transmitter is at the top and occupies the area from the crystal to the BNC output connector.

Operation

Fig 3 shows a block diagram of the Pocket APRS Transmitter. The TT3 receives position data from an external GPS receiver and produces an audio

signal representing the GPS position report in one of several user-selectable APRS packet data formats. This audio signal is applied to the FM pre-emphasis circuit, which attenuates lower audio frequencies, spreading modulation energy more evenly across the audio band. The output of the pre-emphasis circuit modulates the frequency of the VCO.

The VCO is a transistor oscillator operating directly at 144 MHz. It drives a single-stage 144 MHz amplifier. The amplifier output passes through a low-pass filter that attenuates harmonics of the desired 144 MHz signal and then through a diplexer circuit and finally to the RF output connector.

A sample of the VCO output drives

(A)

(B)

(C)

(D)

Fig 1—At A, Tony's wife, Delora, prepares to go mountain biking with the Pocket APRS Transmitter at her waist. B shows a search dog, Xena, with the first attempt to secure a Pocket APRS Transmitter to her vest. The horizontal antenna isn't ideal, but it works over a mile and isn't likely to get caught on anything. The authors are thinking about a tag a user could remove so the TinyTrak3 would send a different status message. This is a standard feature of the Tinyrak3 / Pocket APRS Transmitter requiring only an added switch. Serious field work calls for a rugged, weatherproof package. C shows a weatherproof plastic case available at many sporting-goods stores for about $7. It includes an O-ring seal and the lanyard shown. The FPS receiver connects to the two-conductor cable. D shows a pocket tracker stuck to the inside of a vehicle window with suction cups. It has ridden there for thousands of miles. A similar arrangement with a ⅝ λ antenna routinely reaches a directly to a digipeater 45 air miles away.

a PLL IC.[5] Fig 4 shows the PLL IC in more detail. In the IC, programmable frequency divider N divides the 144 MHz VCO signal down to 5 kHz. This 5 kHz signal is applied to input A of the phase detector. An 8 MHz crystal reference oscillator drives programmable frequency divider R, which divides the 8 MHz signal down to 5 kHz. This 5 kHz signal is applied to input B of the phase detector. The phase-detector output consists of pulses that vary in width and sign (positive or negative going) depending on whether input A is leading or lagging input B.

The PLL IC frequency dividers are controlled by a serial data input signal generated by a second dedicated PIC microcontroller. Each time the transmitter is keyed by the TT3, this PIC generates a serial data stream, programming the N and R dividers as well as other PLL IC parameters. The R divider is set to divide by 1600 (8 MHz reference divided by 5 kHz). For an output frequency of 144.39 MHz (the most popular APRS 2 meter operating frequency), the N divider is set to divide by 28,878 (144.39 MHz divided by 5 kHz).

The output of the phase detector passes through a 120 Hz active low-pass filter. This filter attenuates the fundamental and harmonics of the phase detector output pulses and delivers a dc voltage proportional to the phase difference between the two 5-kHz phase-detector inputs. Since these 5 kHz signals are derived from the 144 MHz VCO and 8 MHz crystal reference oscillator, the active-filter dc output is also proportional to the phase difference between these two signals.

The dc output of the active filter drives voltage-variable capacitors (Varactor diodes[6]) that are part of the VCO frequency-determining circuit. Increasing the Varactor voltage increases the VCO frequency, while decreasing it decreases the VCO frequency.

When the VCO starts to drift upward in frequency, the phase of its output will start to lead that of the reference frequency by an increasing amount. The phase detector is programmed to decrease the VCO Varactor voltage, tuning the VCO back down to the desired frequency. Similarly, if the VCO starts to drift downward in frequency, the Varactor voltage increases, tuning the VCO back up to the desired frequency. In this way, the feedback loop formed by the VCO, PLL IC and active filter, locks the VCO into a fixed frequency
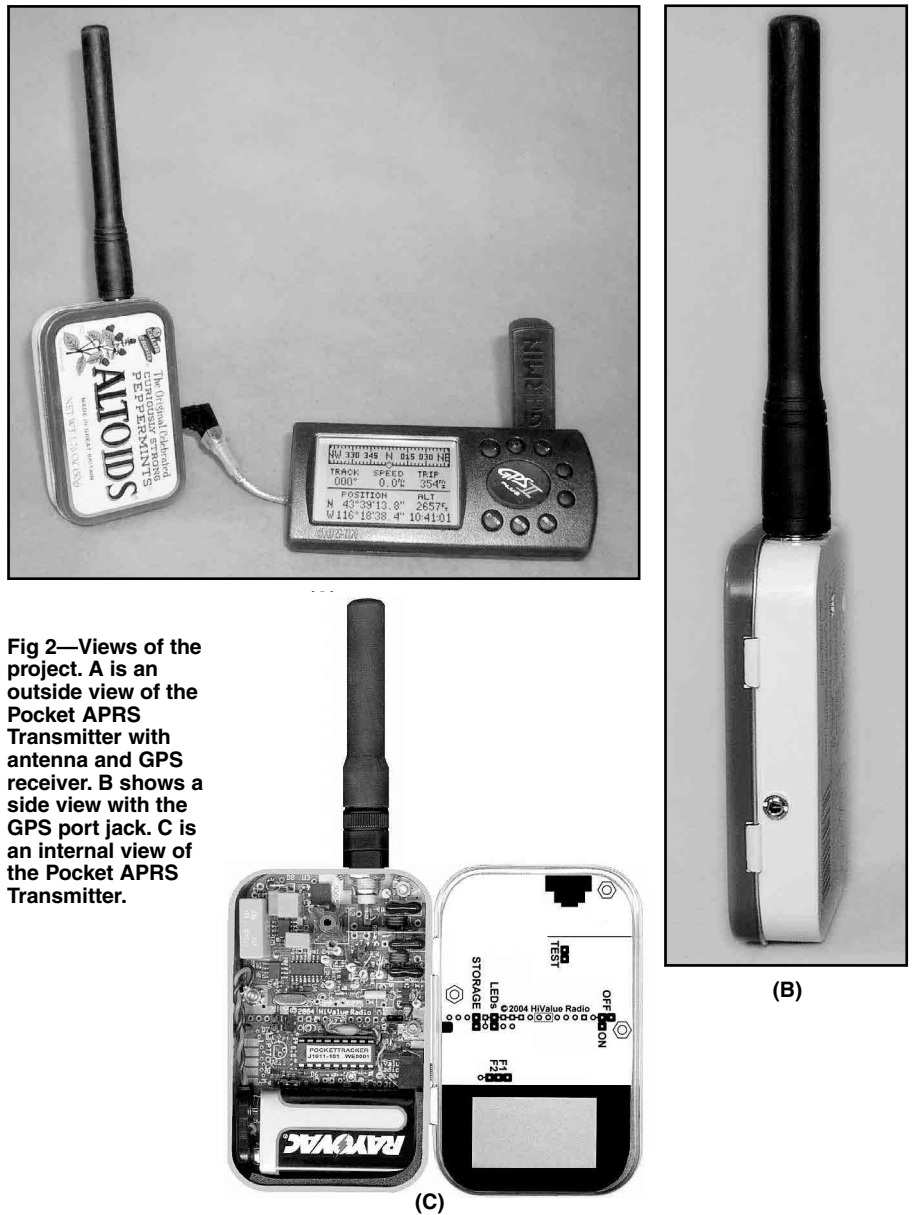
Fig 2—Views of the project. A is an outside view of the Pocket APRS Transmitter with antenna and GPS receiver. B shows a side view with the GPS port jack. C is an internal view of the Pocket APRS Transmitter.

An APRS "Killer App?"

Have you heard the term "Killer App"? It's an application that brings hitherto underused technology into common usage. For example, one could argue that Microsoft *Office* was a "killer app" for the *Windows* operating system.

Scene 1: APRS began when hams wanted to track the progress of the runner who makes the trek from Annapolis to West Point for the annual Army versus Navy football game. Since then, it has developed into a fascinating Amateur Radio activity used by hams to report their positions or those of their vehicles to other hams or Web sites. While this is fun, it is not a *compelling* use for the technology.

Scene 2: Some years ago, as I was driving to ARRL HQ for work, I heard a news story about a fire at a group home in Hartford, Connecticut. Medical attention was delayed for some of the injured because the Emergency Medical Technicians (EMTs) had trouble locating the patients at the site.

I had a vision. If we had small, inexpensive APRS transmitters, they could be distributed to police and fire departments. Then, police or firefighters could place them with injured persons. EMTs with cell-phones and notebook computers could read the positions from APRS Web sites and use GPS location to navigate within a few feet of those needing medical attention.

Scene 3: Jim Hall, W7TVI, and Tony Barrett, W7MTZ, develop the Pocket APRS Transmitter for search and rescue work in the Pacific Northwest. Mass production of the pocket transmitter could make it inexpensive enough for the vision to become reality.—*Bob Schetgen, KU7G, QEX Managing Editor*

relationship with the crystal controlled reference oscillator.

Design

The schematic for the Pocket APRS Transmitter is shown in Fig 5. The VCO consists of Q4 and its associated circuitry. The common-collector configuration in conjunction with base-to-emitter capacitor C27 produces a negative resistance looking into the base of Q4. The series-tuned circuit at the base of Q4 determines the oscillation frequency. This tuned circuit consists of the capacitance formed by C26 in parallel with the series combination of C25 and the two Varactor diodes (D9) plus inductor L3. A quite linear frequency versus diode voltage characteristic is obtained by using hyperabrupt Varactor diodes (capacitance nearly proportional to the square of the applied voltage) for D9. RF choke L1 provides a dc path for bias to D9, but it isolates D9 from the active filter and pre-emphasis network at RF frequencies. L2 completes the dc path for the upper diode in D9.

The nominal operating frequency of the VCO is adjusted using slug-tuned coil L3, with +2.5 V applied to D9. The sensitivity of the Varactor circuit is such that the VCO frequency varies by about 450 kHz for a 1 V change in the voltage applied to D9. It was a conscious decision to set the VCO frequency sensitivity so. The transmitter circuits operate from a 5-V supply, which limits the D9 drive-voltage range. It's from about +0.5 V to +4.5 V. This voltage range must tune the VCO frequency far enough to compensate for frequency variations caused by temperature, vibration, antenna SWR and voltage. On the other hand, the frequency sensitivity should not be too great, as that can introduce undesired FM noise. 450 kHz per volt was chosen as a good compromise.

The VCO output is taken from the emitter of Q4. C28 was chosen to optimize power transfer from Q4 to the 50 Ω (nominal) input impedance of the following circuitry. RF choke L6 isolates the RF output from R27. The RF power output of the VCO is around +14 dBm into 50 Ω.

The VCO RF output is coupled via a resistive divider (R29 and R30) to the input of a common-emitter RF amplifier Q5, which operates as Class C. Inductive emitter degeneration (L10) helps stabilize operation against changes in drive power and output loading. The input impedance of Q5 is a series R C circuit. L7 tunes out the capacitive component, yielding a resistive input impedance. R30 also pro-

vides the dc path to ground for Q5 base current.

The collector of Q5 is isolated from the power supply at RF by the parallel-resonant circuit L9/C30. The combination of L8 and R31 provide a resistive collector termination at frequencies between 3 and 50 MHz, eliminating a tendency of Q5 to oscillate at those frequencies.

The RF output of Q5 passes through a standard five-section, 0.25 dB-ripple Chebychev low-pass filter that ensures all harmonics are at least 45 dB below the 144 MHz fundamental. The first inductor in the filter (L11) was modified slightly (65 nH, not the theoretical 73 nH) to provide a collector load of about 40 Ω, maximizing RF power output. The output of the low-pass filter connects to a simple diplexer[3] circuit (L13, R32, C35) that resistively terminates the low-pass filter at frequencies below 50 MHz. This further reduces any tendency of Q5 to oscillate at low frequen-

cies. The 144 MHz output signal passes through the diplexer to the BNC output connector with minimal loss. The RF output power delivered to a 50 Ω load is typically around 200 mW.

A sample of the VCO output is taken via R28, supplying the N divider input for the PLL IC (U4 pin 4). An 8-MHz crystal (×1), connected between U4 pins 1 and 2, determines the PLL reference frequency. The crystal we used is specified to oscillate in parallel resonance at 8.0 MHz with a 20 pF load. The actual oscillation frequency was measured to be about 1.1 kHz high. This is largely because the actual crystal load capacity obtained with the series combination of C9 and C10 in parallel with the input capacity of U4 is only about 15.7 pF. It is impossible to increase the crystal loading to 20 pF without exceeding the maximum value (30 pF) allowed by the PLL data sheet for C9 and C10. Programming U4 with a slightly lower N
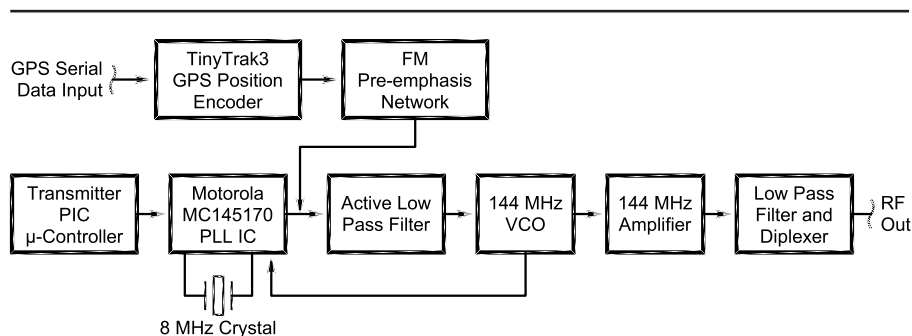

Fig 3—Pocket APRS Transmitter simplified block diagram.
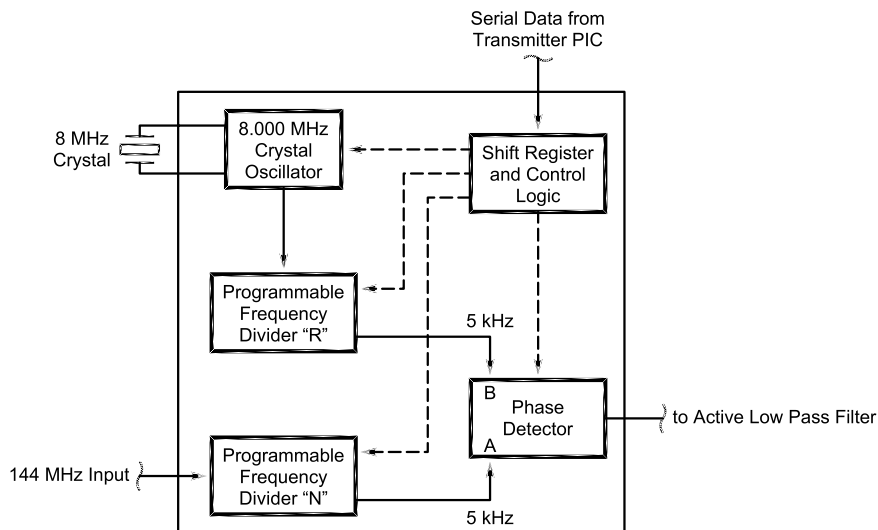

Fig 4—A simplified block diagram of the Motorola MC145170 PLL IC.

division ratio compensates for this and other frequency inaccuracies caused by the crystal. Although this means the phase-detector input isn't at exactly 5 kHz, this is of no practical consequence.

The PLL IC memory is volatile and must be reprogrammed each time the TT3 applies power to the transmitter. This is accomplished with an inexpensive PIC micro-controller (U6). The PIC is programmed for the transmitter to operate on either of two popular APRS frequencies. With no connection to U6 pin 7, the internal U6 pull-up resistor holds pin 7 high, and the transmitter operates on 144.390 MHz. 144.340 MHz operation is selected by grounding this pin. Different frequencies can be selected by modifying the PIC firmware.[7] The only constraint is that the two frequencies selected

should be within about 150 kHz of each other to ensure enough tuning range remains to compensate for environmental changes in VCO frequency.

Theoretically, the TT3 chip could perform the functions of U6 in addition to its normal GPS position-encoding duties. However, this would require a non-standard TT3 chip and could easily add more incremental cost than the cost of U6.

The phase-detector output (U4 pin 13) drives active low-pass filter U5a. This filter is a 2 pole, multiple feedback (MFB), Butterworth design with a 3 dB bandwidth of 120 Hz and a dc gain of 5.3. This filter was designed using *FilterPro*, (available for free download at **www.ti.com**). The non-inverting input to U5a is biased with a fixed +2.5 V from voltage divider

R18, R19. When the VCO is tuned to the programmed operating frequency with L3: the phase detector output is +2.5 V, the active filter output (U5a pin 1) is +2.5 V and the voltage applied to VCO Varactor (D9) is +2.5 V. When the VCO starts to drift off frequency, the varactor bias is changed up or down to maintain the correct frequency as determined by dividers N and R.

Actual operation of the PLL is a bit more complex than the simple description given above. In control system terminology, the feedback loop used in this transmitter is a Type 1 system (one loop integration). This type of feedback system forces the two frequencies at the input of the phase detector to be exactly equal. However, a static phase difference is allowed between the two phase-detector input

Table 1

Parts List

C15—470 nF ±2% metalized polypropylene [BC2083-ND].
C16—22 nF ±2% metalized polypropylene [BC2144-ND].
C22—1 nF ±2% metalized polypropylene [BC2177-ND].
C23—100 nF ±2% metalized polypropylene [BC2054-ND].
C32, C34—30 pF mica ±5% [338-1056-ND].
C33—47 pF mica ±5% [338-1053-ND].
D8—Diode, silicon, 1A, 200V [1N4003MSCT-ND].
J4, J9, J11—Jumper shunts with handles [A26242-ND].
J8—3-Conductor stereo $^3/_{32}$" subminiature phone jack RadioShack 274-245.
J10—9-V battery clip (123-5006).
J12—BNC connector, female Allied Electronics 713-9085.
L1, L2, L4, L5, L6, L8—3.3 µH ±10%, axial molded unshielded choke [DN2532-ND].
L3—6.5 turn, unshielded variable inductor (434-1012-6.5C).
L7—0.12 µH ±10%, axial molded unshielded choke [DN2596-ND].
L9—0.1 µH ±10%, axial molded unshielded choke [DN2594-ND].
L10—5 nH, 26 AWG wire, see instructions at **www.byonics.com/pockettracker**. Form using #26 AWG wire listed below.
L11—65 nH, #20 AWG magnet wire, 3 inches, 3 turns on $^3/_{16}$" drill. Wind using #20 AWG wire below.
L12—73 nH, #20 magnet wire, 3", 3 turns on $^{13}/_{64}$" drill. Wind using #20 AWG wire below.
L13—0.22 µH ±10%, axial molded unshielded choke [M9R22-ND].
U1—PIC 16F628-20/p programmed with TinyTrak3 firmware version 1.1 Available at **www.byonics.com**.
UX1—18-pin DIP socket (571-3902615).
X1—8.000-MHz crystal, 20 pF, HC-49/UA [X021-ND].
Y1—10-MHz ceramic resonator [X906-ND].

Miscellaneous parts included in the kit:
12-pin strip of breakaway header posts, square 25 mil (517-2312-6111TG).
#20 AWG polyurethane coated magnet wire, 6.0 inches long, Allied Electronics 293-0316.
#26 AWG black wire, 4 inches long [K386-ND].
#26 AWG red wire, 4 inches long [K387-ND].
#26 AWG yellow wire, 6 inches long [K388-ND].
#26 AWG blue wire, 4 inches long [K327-ND].
#26 AWG white wire, 4 inches long [K389-ND].
RF shield plate, 10-mil-thick tin plated copper, 0.941×0.560 inches, chemically milled. Custom fabricated, contact N7MTZ*.
Battery pad (top), $^1/_8$" thick gray foam, 0.8"×1.5", adhesive backed custom fabricated, contact N7MTZ*.
Battery pad (side), $^1/_8$" thick gray foam, 0.75" × 2.8", adhesive backed custom fabricated, contact N7MTZ*.
Lid label, printed, laminated, adhesive backed custom fabricated, contact N7MTZ*.
Insulating liner material, 3.8"×2.5" white polycarbonate, 5 mils thick, printed and punched custom fabricated, contact N7MTZ*.
#4-40 ×$^3/_8$" long flathead screws (3), nuts (6), lockwashers (3) from The Nutty Company, PO Box 473, 135 Main St (Rte 34), Derby, CT 06418; Toll Free 800-4-NUTTY, 1 (800-468-8891), (203) 734-1604, fax (203) 735-1097; **www.nuttycompany.com**; e-mail **sales@nuttycom.**

Notes
Part numbers in (parenthesis) are for Mouser. Part numbers in [brackets] are for Digi-Key.
A complete set of parts, including U1, is available as a kit from **www.byonics.com**. The kit does not include: battery, tin, antenna, GPS receiver, PC / GPS cable(s) and connectors. Check the Web site for availability.
*A PC Board is available with all surface-mount parts soldered in place, including a programmed U6. Contact N7MTZ via e-mail at: **tonybarrett@sunvalley.net**.
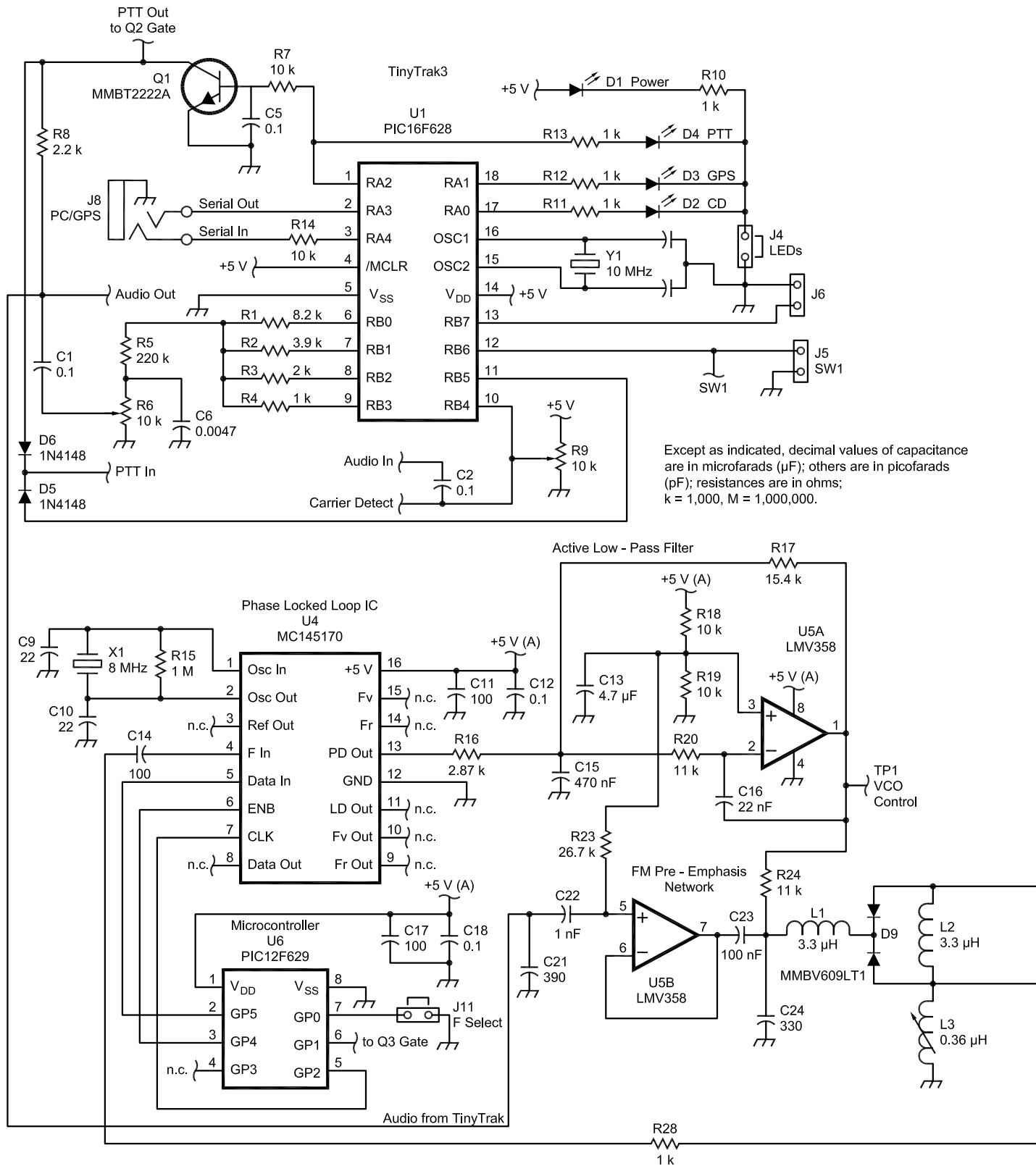
Fig 5—The Pocket APRS Transmitter schematic. Table 1 is a parts list. Traces and pads are on the PCB for C2, C3, C6, D1, D2, D5, D6, D7, J1, J2, J3, J5, J6, R8, R9, R10, R11and U2 but these parts are not included with the Byonics PCB. If loaded, J1 and J2 can be wired as the user desires.

Radio V+

J7

Serial V+

J3
Power In

U2
LM7805

+5 V

2   D7
1N4148   C3
0.1

1   In   Reg   Out   3
Adj

C4
0.1

2

J1 F

J2 M

U3
LF50CDT

+5 V to
TinyTrak

D8
1N4003

1   In   REG   Out   3
Gnd

S   D

+5 V (A)

J9
Power Switch

C7
0.1

2

C8
4.7 µF

R21
10 k

Q2
NDS352AP

G

F1
1/4 A

Power Supply

PTT to
Q1 Collector

J13
PTT Test
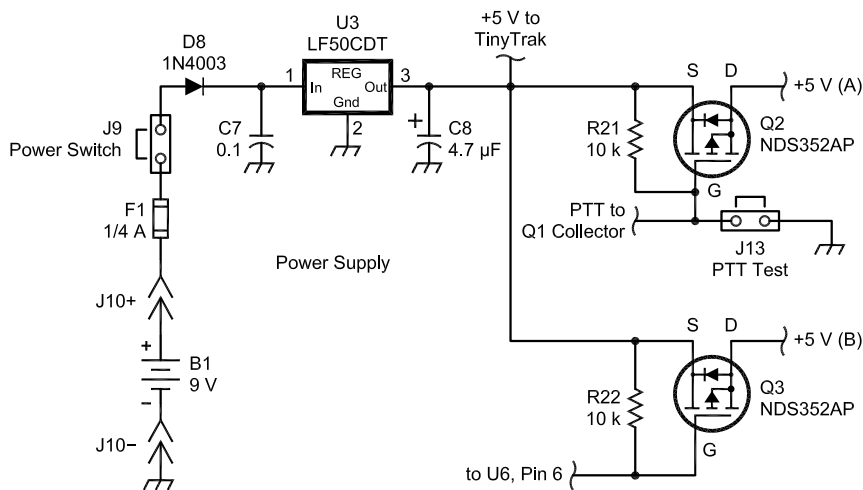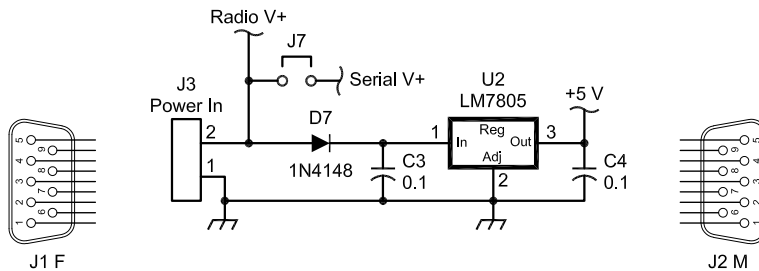
Except as indicated, decimal values of capacitance
are in microfarads (µF); others are in picofarads
(pF); resistances are in ohms;
k = 1,000, M = 1,000,000.

J10+

+

B1
9 V

–

S   D

+5 V (B)

R22
10 k

Q3
NDS352AP

G

J10–

to U6, Pin 6

VCO

+5 V (A)

L5

C19
390

3.3 µH

C20
390

RF Amplifier

+5 V (B)

C39
390

R34
63.4

L8
3.3 µH

R25
3.16 k

R26
2.37 k

L4
3.3 µH

C30
12

L9
0.1 µH

Low - Pass Filter

J12
144 MHz
Out

C25
1.3

C26
1.3

C27
56

Q4
NE46134

C28
10

R29
10

L7
0.12 µH

Q5
NE46134

C31
390

C32
30

L11
65 nH

C33
47

L12
73 nH

C34
30

C35
68

R32
51.1

R30
63.4

L6
3.3 µH

L10
5 nH

L13
0.22 µH

R27
38.3
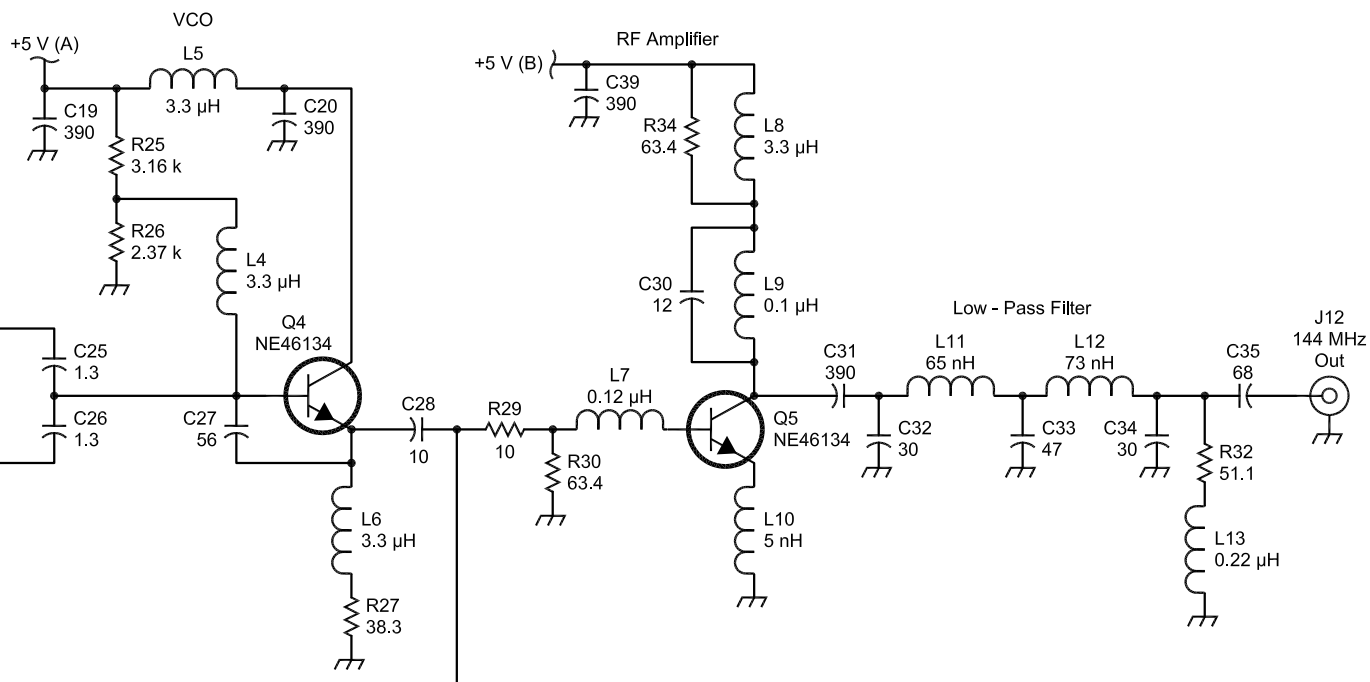
signals. In this design, the phase difference increases to about 54° when the VCO frequency is corrected by 900 kHz. A Type 2 loop, more typically used for PLL applications, has two loop integrations and holds the phase of the signals at the two phase detector inputs exactly equal. We used a Type 1 feedback loop because it is simpler, easier to design and provides more than adequate performance for this application.

The FM sensitivity of the VCO is constant as modulation frequency changes. Therefore the *phase* deviation sensitivity of the VCO (and PLL loop gain) decreases at 6 dB/octive with increasing modulation frequency (remember, phase deviation = frequency deviation divided by modulation frequency), equivalent to a single loop integration. For the chosen dc gain, the loop gain crosses through unity (0 dB) at 33 Hz.

The phase-detector output contains a strong 5-kHz component that must be removed to prevent it from modulating the VCO and generating spurious sidebands at multiples of 5 kHz. The 120 Hz Active LP Filter attenuates this 5 kHz component by about 64 dB. The R-C filter formed by R24 and C23 in parallel with C24 (for signals originating in the active filter, the end of C23 attached to U5b pin 7 is effectively grounded) attenuates the 5-kHz component by another 30 dB. The total attenuation of 94 dB reduces all spurious 5-kHz sidebands to a level that is too low to measure.

Another major consideration in designing the PLL feedback system is phase margin. At the system unity-gain frequency of 33 Hz, the excess phase shift through the active filter is 23°. The R24, C23, C24 circuit adds 13° of phase shift at 33 Hz. The 6dB/octive rolloff in VCO phase deviation sensitivity adds 90° of phase shift. Therefore, the total loop phase shift at 33 Hz is 126°, resulting in good phase margin for the feedback loop.

The final consideration in the feedback system is the method for coupling APRS audio to the VCO. Audio from the TT3 first passes through the high-pass circuit formed by C22, R23 and voltage follower U5b. This circuit boosts the amplitude of the 2200 Hz APRS tone by a factor of 1.6 compared to the 1200 Hz tone, in compliance with FM pre-emphasis standards. C21 bypasses the input of U5b at RF but has negligible effect at AF. C23 couples the voltage follower audio output to Varactor diode pair D9. The PLL feedback system does not affect VCO modulation of the APRS audio tones

because its 33 Hz bandwidth is much less than the lowest tone frequency of 1200 Hz.

The power-supply regulator circuit consists of reverse voltage protection diode D8 and voltage regulator U3. U3 is a low drop-out voltage regulator. It has a maximum drop-out voltage of 0.35 V. This, plus the maximum drop of 0.8 V across diode D8, means the regulator will still provide well regulated 5 V for supply voltages as low as 6.2 V. Supply voltages as high as 16 V can be used while maintaining the regulator junction temperature well below its maximum rating. No external heatsink is required, even for ambient temperatures as high as 150°F.

Power Sequencing

Proper design of the power sequencing circuit was critical for long battery life. When power is applied to the Pocket APRS Transmitter, U3 supplies regulated +5 V at about 4 mA to the TT3 circuitry. This assumes the TT3 LEDs are off. Since each LED consumes about 3 mA, they have a significant impact on power drain and battery life. Therefore, for maximum battery life, install LED jumper J4 only when checking TT3 status, then remove it during normal operation.

At user-defined intervals, the TT3 keys the transmitter to send APRS data. To do this, the TT3 turns on Q1, grounding the gate of Q2, which then supplies +5 V at a total current of about 36 mA to the PIC (U6), PLL IC (U4), active filter/pre-emphasis circuits (U5) and the VCO. After U6 goes through its power-on sequence, which takes about 72 ms, it programs the PLL IC to the correct frequency, taking an additional 20 ms. After another delay of about 40 ms to insure that the VCO frequency has stabilized, pin 6 of U6 goes low, turning on Q3 and supplying +5 V to the RF amplifier. After turning on Q3, U6 goes into sleep mode, drawing only a few microamperes. At this time, APRS data is transmitted, and the total dc supply current increases to about 110 mA. About 440 ms later (typical, assuming that the default TT3 Auto transmit Delay is set), the TT3 turns Q1 off, removing power from everything except the regulator and the TT3.

In summary, here's a power-supply current profile:

When APRS data is not being transmitted = 4 mA (TT3 plus U3 regulator, LED jumper J4 open)

Each time APRS data is transmitted:

Total supply current = 40 mA for 132 ms

Total supply current = 110 mA for 440 ms (typical)

The default TT3 configuration transmits position data once every two minutes, resulting in an average power-supply current of 4.4 mA. With this average current, the Pocket APRS Transmitter can operate from a standard 9 V alkaline battery for about 120 hours . In fact, even if position data is transmitted once per minute, the demonstrated battery life is over 100 hours.

Construction, Packaging and Options

There are several options for constructing the Pocket APRS Transmitter. A complete set of parts including the PC board with all surface-mount parts soldered in place is available at **www.byonics.com/pockettracker**. The bare PC board or the PC assembly with all surface-mount components soldered in place is available by contacting N7MTZ via the link at **www.byonics.com/pockettracker**. (Scroll to the bottom of the Web page.) Complete, step-by-step instructions for constructing the transmitter can be downloaded from **www.byonics. com/pockettracker**.

For our "pocket tracking" application, small size was important, leading us to package the PC board and battery in a 2.4×3.4×0.8-inch breath-mint can. You can use any enclosure or power source suitable for your application. The power source should be between +16 and 6.2 V and capable of supplying at least 120 mA. Make sure your enclosure contains a shielded compartment for the PC board to minimize VCO detuning by changes in the environment.

The set of parts available at **www. byonics.com/pockettracker** supports the basic APRS functions of automatic position transmission and "Smart Beaching". If the additional parts noted on the schematic (Fig 5) are loaded, the TT3 is completely equivalent to a normal Byonics TT3, giving additional functionality. A parts list, parts kit and loading instructions for adding these optional components is available on request by contacting N7MTZ via the link given at **www. byonics.com/pockettracker**.

The Pocket APRS Transmitter can send weather-station data via the APRS weather protocol[8] if you substitute the Byonics WXTrak chip for the TT3 GPS position-encoder chip.

Alignment and Testing

1. Connect the transmitter RF output to a 50 Ω dummy load.

2. Set the transmitter deviation to

≈4 kHz by adjusting R6 for a resistance of 2.8 kΩ as measured from its wiper (test pad marked D at the edge of the board near U1 pin 9) to ground.

3. Connect a 9 V battery to the battery clip. Make sure that jumper J9 is in the "on" position.

4. Configure the TT3 to transmit your callsign each time data is transmitted. To enter your callsign or to modify any of the other TT3 default settings, use the *TinyTrak3Config.exe* program. To get this program, download TINYTRAK3.zip from **www.byonics.com/tinytrak**. Extract all the files from the zip file. One of the extracted files will be the *TinyTrak3 Owner's Manual*. The document contains detailed configuration, adjustment and troubleshooting information. One of the other extracted files will be the *TinyTrak3Config.exe* program. Launch this program and follow the instructions in the *TinyTrak3 Owner's Manual* to configure your call sign or other settings.

5. Make the following adjustments with jumper J13 (at the point marked T on the PC board) in place. This ties the collector of Q1 to ground, thereby applying +5 V continuously to all of the transmitter circuits. Note that the TT3 will periodically transmit APRS data during the following adjustments. In addition, the enclosure lid should be closed for the following adjustments, since it affects VCO tuning.

Put the Frequency Select jumper (J11) on the pair of pins near the number 9 at the 3-pin connector marked FS. This selects 144.39 MHz operation.

Tune a 2-meter receiver to 144.39 MHz. With the lid closed, the tuning slug for L3 can be reached through an access hole in the back of the transmitter. Slowly tune L3 until you can hear a signal in the receiver.

Wait until you hear an unmodu-lated carrier in the 2-meter receiver, then measure the voltage at the VCO Control Test Point, which can be reached from the back of the transmitter through the other access hole described in the assembly instructions. Carefully adjust L3 for a reading of +2.5 ±0.2 V.

6. Move the Frequency Select Jumper (J11) to the pair of pins near the number 4 at the three-pin connector marked FS to select 144.34 MHz operation.

Important: Remove, then reinstall power jumper J9 to reprogram the PLL IC to 144.34 MHz. Remember that the PLL chip is only reprogrammed when the power is cycled.

7. Tune the 2 meter receiver to 144.34 MHz and confirm that the transmitter is now operating on that frequency.

8. If necessary, change the Frequency Select Jumper (J11) to select the desired operating frequency.

9. Remove jumper J13, allowing the TT3 to control the transmitter.

The RF amplifier isolates the VCO from the antenna, minimizing any detuning from changes in antenna impedance. However, if you expect the transmitter to experience extreme changes in temperature (for example, when "Near Space Balloon Tracking"), it may be prudent to maximize the PLL locking range. You can do this by adjusting VCO L3, as described in "Alignment and Testing", with the RF output BNC connected to the same antenna you will use when operating the transmitter.

Summary

Developing the Pocket APRS Transmitter was a fun project. It makes APRS tracking practical for many exciting applications where conventional approaches don't work well because of size, weight, cost or battery constraints. It was not designed to address every APRS application, however.

If the Pocket APRS Transmitter fits your requirements, try it. It can be a refreshing experience, especially if you package it in a breath mint can.

Jim Hall, W4TVI, grew up in Halifax, Virginia, earning his Novice license in 1951 at age 14. He upgraded to General the next year and later to Extra.

Jim received a BSEE from North Carolina State and an MS in physics from Lynchburg College. After college,

he spent 13 years designing communications systems for General Electric. In 1972, he joined Hewlett Packard and designed communications and microwave test equipment. In 1976, Jim became R&D manager for HP's first laser printer. When he retired in 2000, he was responsible for all HP LaserJet printer R&D. Jim now enjoys electronics design, his grandchildren and travel You can contact him at **w4tvi@arrl.net**.

Tony, N7MTZ has been a ham for 15 years and his main interest for the last few years has been APRS. Before the APRS bug bit, he enjoyed building and operating ATV transmitters. Two years ago, one of his winter projects was to build a digipeater that was installed on a nearby mountain top when the snow cleared the following summer. He's an active local ham club member and a long-time supporter of ARES and RACES. He helps out with numerous public-service events, and for the past year he's concentrated on bringing the most valuable technology to Search And Rescue teams. The Pocket APRS Transmitter was conceived during a five-day search for some lost snowmobilers in March of 2003. He likes to participate in "Near Space" balloon missions (Pocket Trackers were developed with this application in mind) and he is very interested in the design, test, and operation of autonomous Unmanned Aerial Vehicles.

Notes
[1]J. Lehman, KD6DHB, "APRS and Search and Rescue," *QST*, Sep 2003, pp 75-77.
[2]L. Verhage, KD4STH, "Ham Radio Ballooning to Near Space," *QST*, Jan 1999, pp 28-32.
[3] 2004 *ARRL Handbook* (Newington, Connecticut: ARRL, 2003), Chapter 15 "Mixers, Modulators and Demodulators."
[4] 2004 *ARRL Handbook,* Chapter 25 "Circuit Construction."
[5] 2004 *ARRL Handbook*, Chapter 14 "AC/RF Sources."
[6] 2004 *ARRL Handbook*, Chapter 8 "Analog Signal Theory and Components."
[7] Firmware listing for the PIC (U6) is available at **www.byonics.com/pockettracker**.
[8] R. Parry, W9IF, "Amateur Radio, Paragliding and an APRS Weather Station," *QST*, Aug 2003, pp 28-33.

Boxkite Yagis—Part 2

---

*Design notes for high-performance
single- and dual-band Boxkite Yagis*

By Brian Cake, KF2YN

Introduction

In the first two articles, I described the basic theory behind Twin Cs and Boxkites, and gave some constructional data on the limited number of prototypes that I had built. At that stage in the development the dual-band Boxkite had different polarization on the two operating frequencies, and I felt that it was worth further effort to investigate the possibility of providing similar polarization sense on both bands. This has indeed proved to be the case, and dual-band Boxkites with the same polarization sense on both bands have been designed for 6 m/2 m, 2 m/70 cm, 70 cm/23 cm, 33 cm/13 cm, 23 cm/9 cm and 6 cm/9 cm. For these bands some interesting antennas have been designed, and practical tests on 6 m/2 m, 70 cm/23 cm and 23 cm/9 cm prototypes show that the model is remarkably accurate both in terms of pattern and SWR predic-

248 Barrataria Drive
St Augustine
Florida 32080
bcake@bellsouth.net

tion. I have also attempted to improve the mechanical design both by moving to a folded dipole feed where appropriate and by simplifying construction, while at the same time providing a much more positive method for preventing rotation of the elements.

The directivity (gain) of the dual-band Boxkites with the same polarization on both bands is remarkably close to that of published data for state of the art long Yagis designed by K1FO and DL6WU. From the published K1FO data[1], the expression that gives the gain of a given boom length Yagi is as follows, and is within 0.3 dB of the published data:

$$G \approx 10\log[9.1(L_\lambda + 0.6)] \text{ for } L_\lambda \geq 1$$

where G is the antenna gain in dBi (same as directivity for zero loss) and L_λ is the Yagi length in wavelengths

Comparison of Boxkite gains with Yagi gains having the same boom length will use the expression above as the reference gain in this article. Also note that all the models used include skin effect losses in the elements, which are 6061-T6 aluminum in every case.

As far as single band Boxkites are concerned (referred to as Boxkite Xs in the second article) I have more data to share with you that shows that they have between 2.2 and 2.6 λ advantage in terms of boom length over contemporary long Yagis having the same gain, and this advantage is to first order independent of length. Naturally this has a more profound effect on boom length on the lower VHF bands, such as 2 meters.

I will discuss how to stack both dual band and single band Boxkites, and in a couple of cases compare Box kite and stacked Boxkite gain with theoretical supergain limits.

I think you will see from the data presented that these antennas are capable of quite remarkable performance, even in the dual-band versions.

Dual-band Boxkites having the same polarization on both operating frequencies

From the theory presented in the second article, remember that the Boxkite driven-element has three useful frequencies, with the lower two, designated f_1 and f_2, being the result
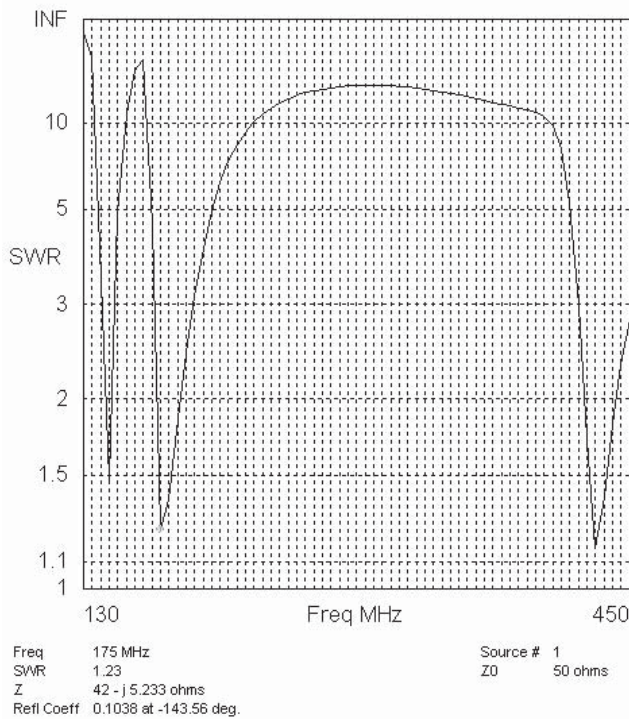
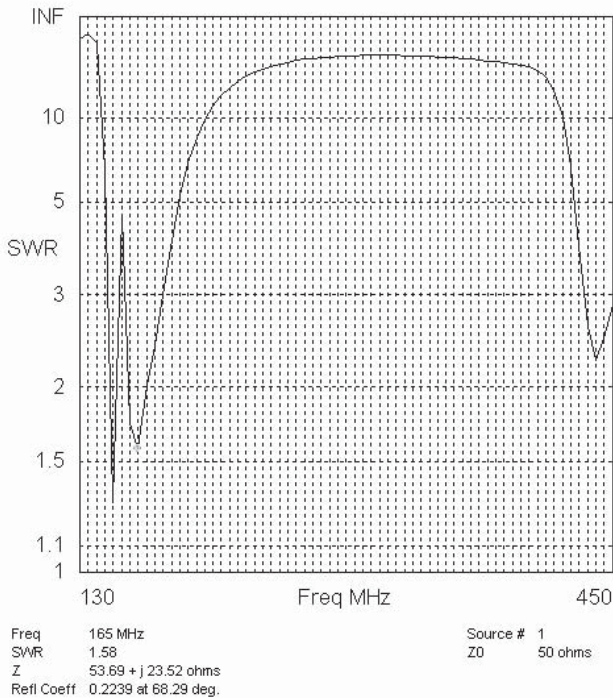**Fig 1—SWR plot for 2-element Boxkite for 2 m and 70 cm with s= 16 mm.**

Fig 3—2-element Boxkite for 2 and 70 cm with s=35 mm.

of over-coupling between the two sub-elements. The upper operating frequency, f_3, is close to three times the self-resonant frequency of one sub-element. Also, remember that the current phases at f_1 are such that the resultant field polarization is vertical; at f_2 the polarization is horizontal, and at f_3 the polarization is again horizontal. Fig 1 shows an SWR plot for a Boxkite 2-element Yagi designed for operation on 2 m and 70 cm, with vertical polarization on 2 m and horizontal on 70 cm. The three resonances can be seen clearly. The first resonance, f_1, at the extreme left of the plot, produces vertical polarization. The second resonance, f_2, produces horizontal polarization, as does the third resonance, f_3, which is at the extreme right of the plot. In this case, f_1 is at 145 MHz; f_2 is at 175 MHz and f_3 is at 432 MHz. Thus the ratio between f_3 and f_2 is about 2.5:1. We now note that there are some microwave bands that have non-integer frequency ratios, for example 9 cm/ 23 cm (3456 MHz and 1296 MHz) where the ratio is 2.67:1;
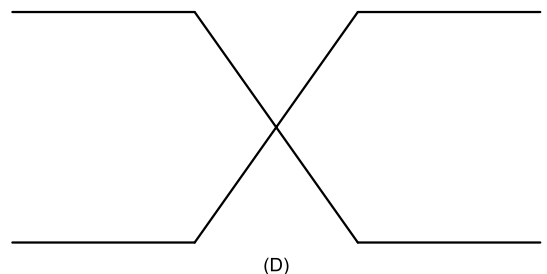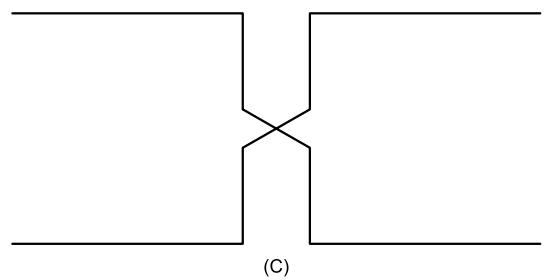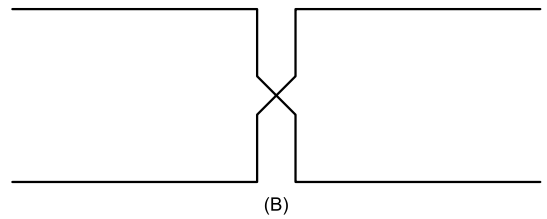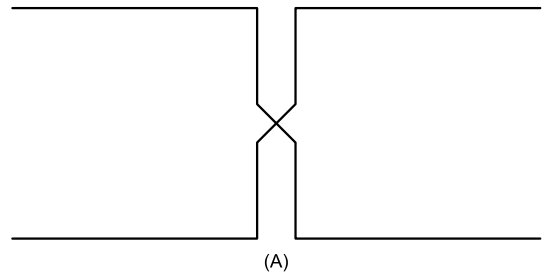

Fig 2A thru 2D—Methods of adjusting the coupling between Boxkite sub-elements.

13 cm/33 cm (2304 MHz and 902 MHz), where the ratio is 2.55; and 6 cm/13 cm (5.7 GHz and 2.304 GHz) where the ratio is 2.49. The first and second resonances, f_1 and f_2, are varied by changing the coupling between the two sub-elements while maintaining the same sub-element total length. If the coupling is reduced, then f_1 and f_2 move closer together. Conversely, increasing the coupling moves f_1 and f_2 further apart. In both cases, f_2 moves relative to f_3 (which stays relatively constant as the coupling is changed), so different ratios between f_3 and f_2 can
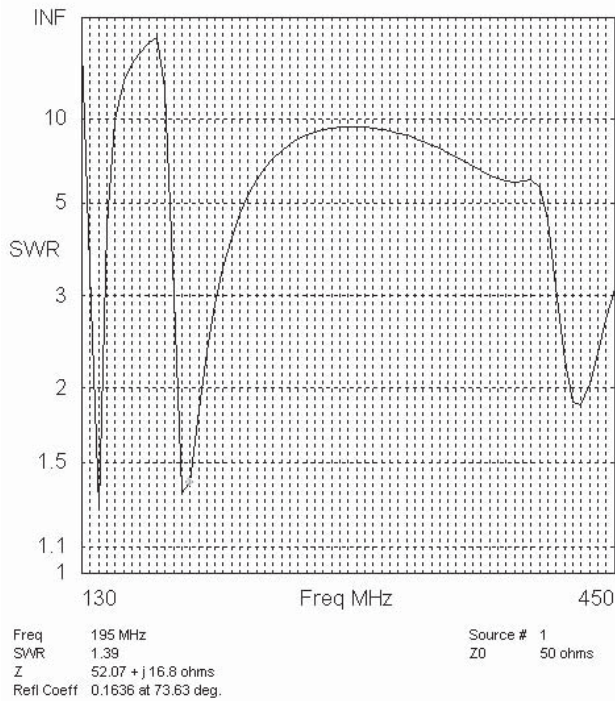

Freq	195 MHz	Source # 1	
SWR	1.39	Z0	50 ohms
Z	52.07 + j 16.8 ohms		
Refl Coeff	0.1636 at 73.63 deg.		

Fig 4—2-element Boxkite for 2 m and 70 cm with s=8 mm.

Freq	160 MHz	Source # 1	
SWR	2.29	Z0	50 ohms
Z	31.51 + j 28.42 ohms		
Refl Coeff	0.3928 at 103.83 deg.		
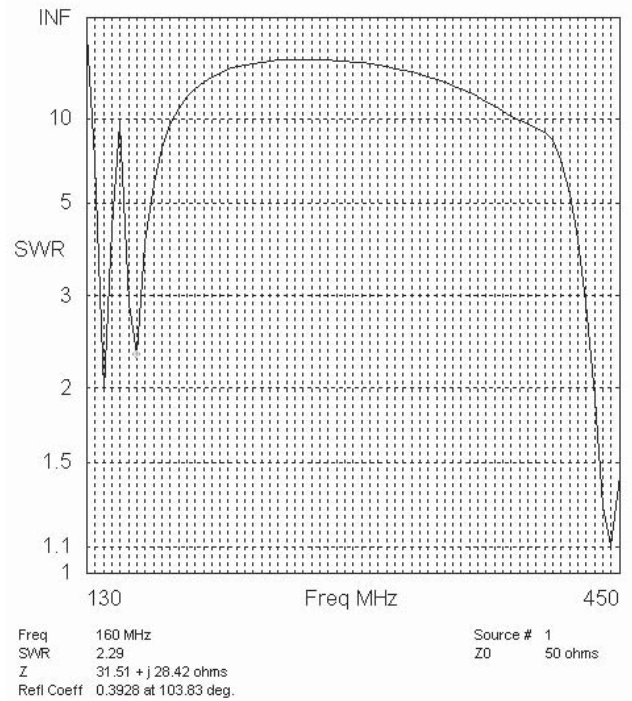
Fig 5—2-element Boxkite for 2 m and 70 cm with s=16 mm and transmission lines = +- 120mm.

Freq	155 MHz	Source # 1	
SWR	2.23	Z0	50 ohms
Z	27.4 + j 20.55 ohms		
Refl Coeff	0.3814 at 122.86 deg.		
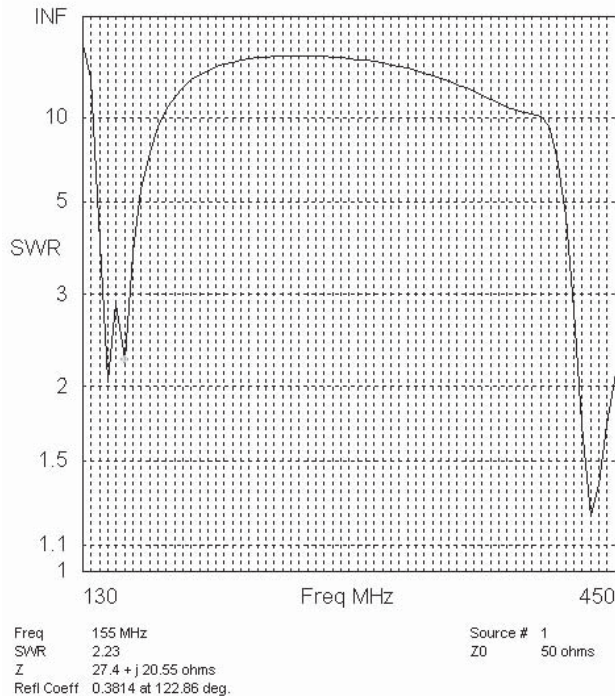
Fig 6—2-element Boxkite for 2 m and 70 cm with s=25 mm and transmission lines = +- 120 mm.

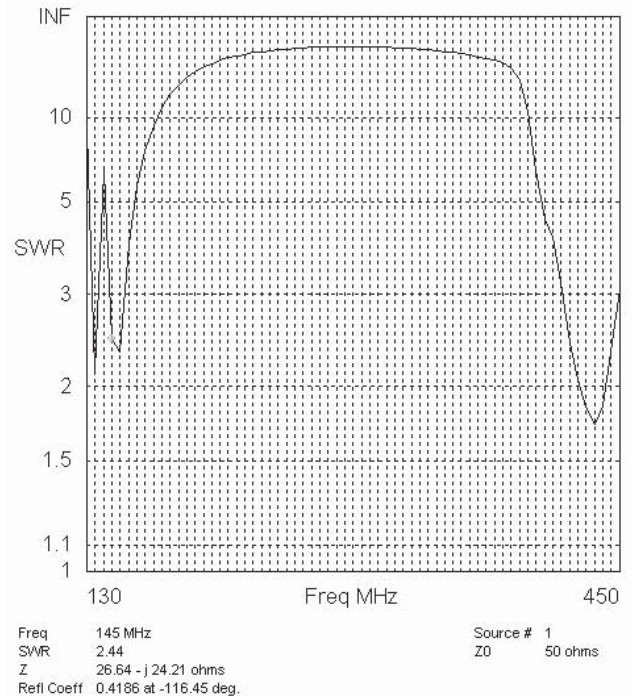| Freq | 145 MHz | Source # 1 | |
SWR	2.44	Z0	50 ohms
Z	26.64 - j 24.21 ohms		
Refl Coeff	0.4186 at -116.45 deg.		

Fig 7—2-element Boxkite for 2 m and 70 cm with s=16 mm and ends of transmission lines spaced by 100 mm.

be achieved simply by changing the coupling between the sub-elements.

There are three methods by which the coupling between the sub-elements may be changed, and these are shown in Fig 2. Note that for clarity I have placed the crossover in the center of the vertical parallel sections. These sections will be referred to as "transmission line" sections because that is their function at f_3. Fig 2A shows the basic Boxkite structure, with the transmission lines a half wavelength long. We can reduce the coupling by reducing the length of the transmission lines, while maintaining resonance by increasing the length of the horizontal sections, as shown in Fig 2B. This also produces higher gain at f_3 but we have to be careful not to overdo it or the sidelobes at f_3 will suf-

fer. We can also reduce the coupling by increasing the spacing between the transmission lines, as shown in Fig 2C. This changes the characteristic impedance of the transmission line so it also changes the drive-point impedance at f_3. Finally, we can separate the ends of the transmission lines as shown in Fig 2D. This increases both the impedance of the transmission line and the spacing of the horizontal sections. In practice some combination of all these methods will produce a practical design, but modeling is currently the only way of ending up with a working design. In practice, for Boxkite Xs, a short vertical section is used at the center of the transmission lines to support the-elements on a square boom.

As examples of these methods of

changing f_2, first we look at increasing the spacing, s, between the transmission lines. The plot in Fig 1 is for s= 16 mm. Fig 3 shows the SWR plot for the same 2-element Boxkite with s= 35 mm. The resonances are now at 150, 162.5 and 440 MHz. As expected, f_2 has shifted downwards. Note also that the SWR at f_3 has increased because of the increase in the characteristic impedance of the transmission lines. Fig 4 shows the result of reducing s to 8 mm in the same 2-element Boxkite. Here the resonances are at 140, 187.5 and 427.5 MHz, and the SWR at f_3 has again risen because of the change in transmission line impedance.

So we can see that f_2 can be changed simply by changing s, although in practice the achievable range for f_2 is rather
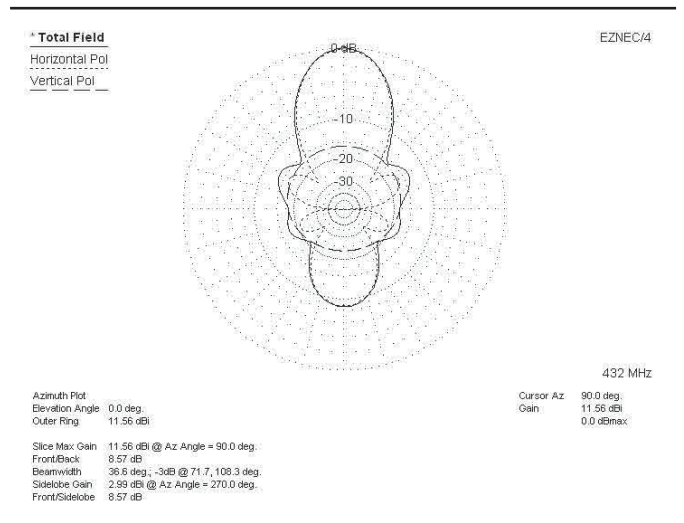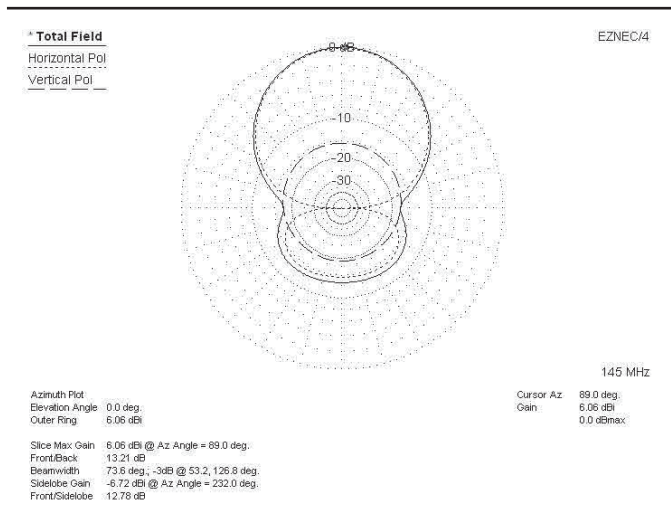

Fig 8—E-plane pattern of 2-element Boxkite for 2 m and 70 cm at 145 MHz s=16 mm and transmission line end spacing = 100 mm.

Fig 9—E-plane pattern of 2-element Boxkite for 2 m and 70 cm at 432 MHz s=16 mm and transmission line end spacing = 100 mm.
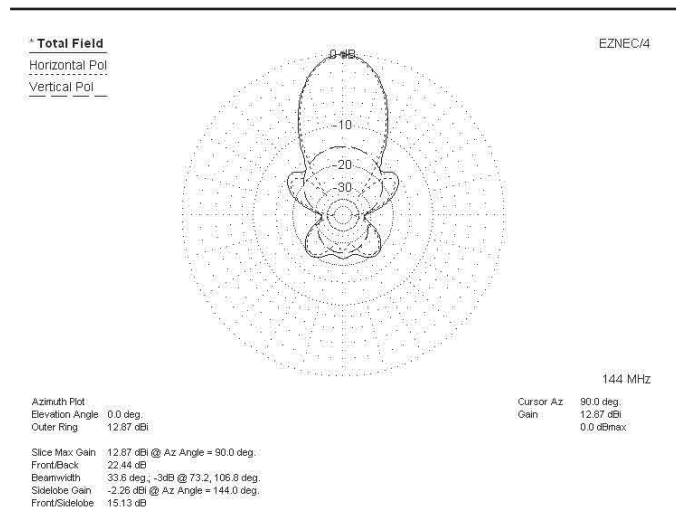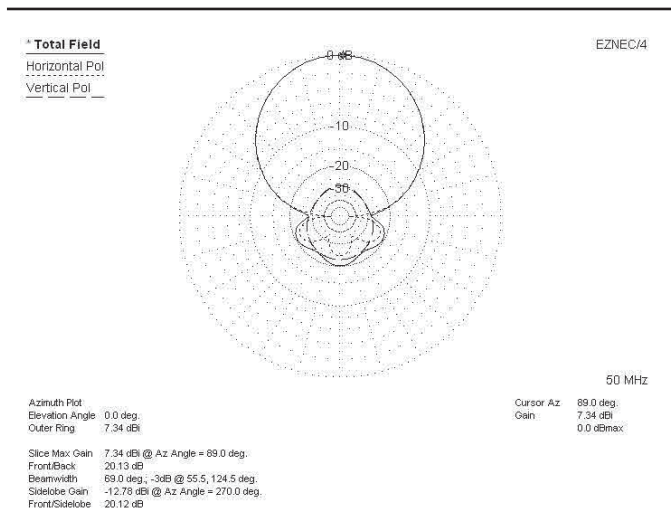

Fig 10—E-plane pattern of a 3-element Boxkite for 6 m and 2 m at 50 MHz.

Fig 11—E-plane pattern of a 3-element Boxkite for 6 m and 2 m at 144 MHz.

restricted because of the need to avoid spacing that is too close for comfort at one extreme and spacing that is too large compared with the operating wavelength at the other. Now we will look at reducing the length of the transmission lines. Fig 5 shows the same 2-element Boxkite with s=16 mm but with the transmission line length reduced from +- 183 mm to +-120 mm, and with the length of the horizontal sections increased to maintain reso-

nance at f_3. The resonances are at 142.5, 157.5 and 445 MHz. By combining the two methods of reducing coupling shown above we can further reduce f_2, as shown in Fig 6. This is a plot for s= 25 mm and transmission line length =+-120 mm. The resonances are at 145, 155 and 437.5 MHz. However, the pattern at f_3 becomes unacceptable because the horizontal sections are now too long. As an example of the third method of reducing the coupling, Fig 7

shows the SWR plot for a 2-element Boxkite with s=16 mm but with "crossed" transmission lines such that the inner ends of the horizontal sections are spaced by 100 mm. Resonances are at 135, 145 and 432.5 MHz, so this is a potential 2 m/70 cm beam, although as can be seen in Figs 8 and 9, the patterns need work! Although these patterns are far from perfect, they were enough to encourage more work. The result, after the burning of
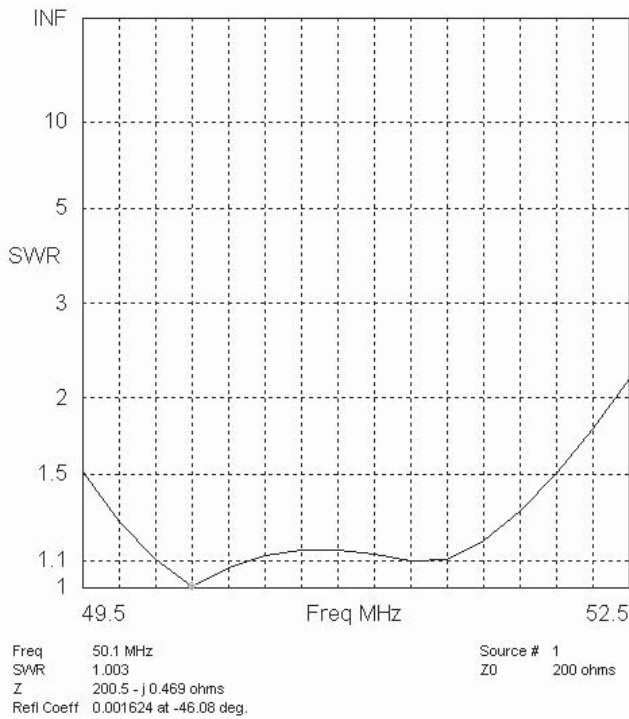

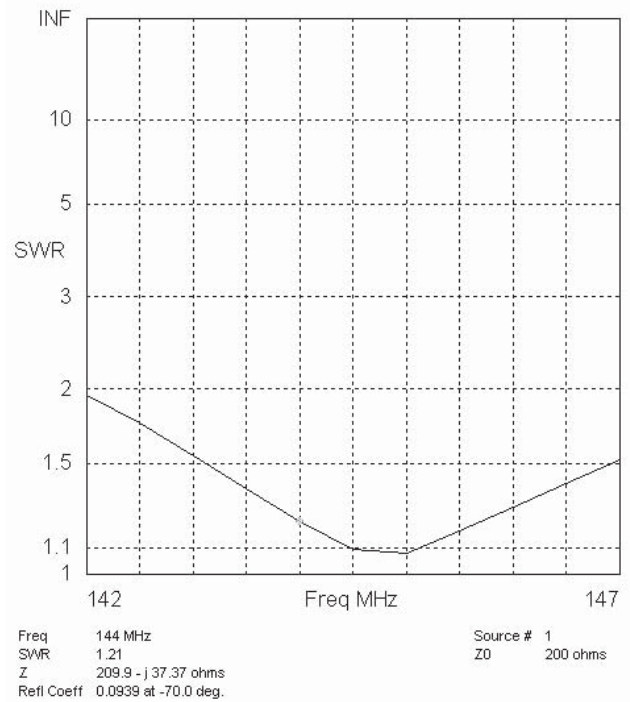**Fig 12—SWR plot for the 3-element Boxkite on the 6 m band.**

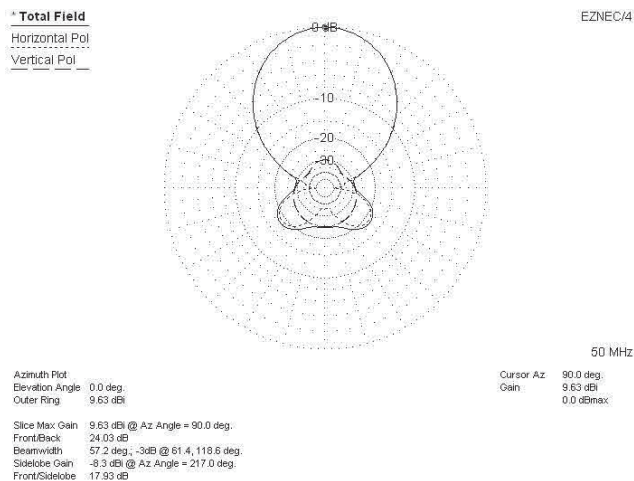**Fig 13—SWR plot of the 3-element Boxkite on the 2 m band.**

Fig 14—E-plane pattern for the 6-element Boxkite for 6 m and 2 m at 50 MHz.
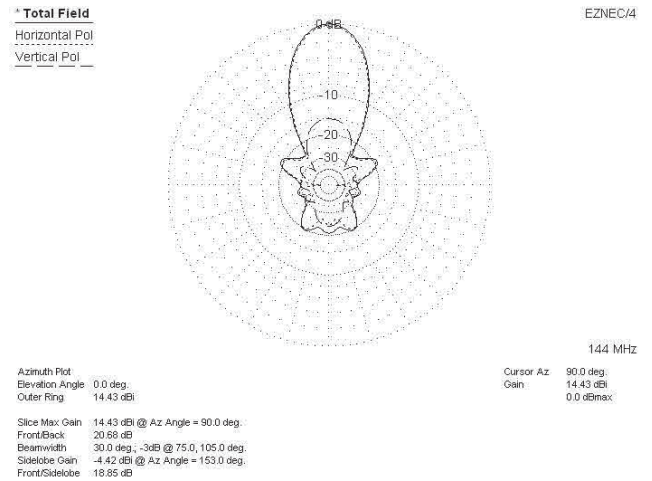

Fig 15—E-plane pattern for the 6-element Boxkite for 6 m and 2 m at 144 MHz.

much midnight oil, and the squirting of much test RF across the Matanzas Inlet, will be shown in the following examples. I will show the modeled results for many antennas first, then I will go on with general comments and some comments on the reasons for the observed behavior of some antennas.

Dual-band Boxkites

Boxkites for 6 m and 2 m

I have fully developed 2 versions of the 6 m and 2 m Boxkites, the first has 3-elements and the second 6-elements. The 3-element version has a boom length of 33 inches and a maximum "wingspan" of 101 inches. The E-plane patterns at 50 MHz and 144 MHz are shown in Figs 10 and 11 respectively. The –1 dB gain-bandwidth is 6 MHz on 6 meters and 10 MHz on 2 meters. As is usual for conventional Yagis, F/B ratio and sidelobe levels deteriorate at the –1 dB band edges. Note that a con-

temporary high performance Yagi would need a boom length of 1.5 λ, or 124 inches, for the same gain on 2 m. The turning radius is not much reduced compared to a conventional Yagi because of the "wingspan". Fig 12 shows the SWR of the Box kite in the 6 meter band. The antenna has a folded dipole feed (the fed sub-element is simply doubled with a horizontal spacing of 1 inch, and the ends connected to form a "bent" folded dipole). Design feed im-
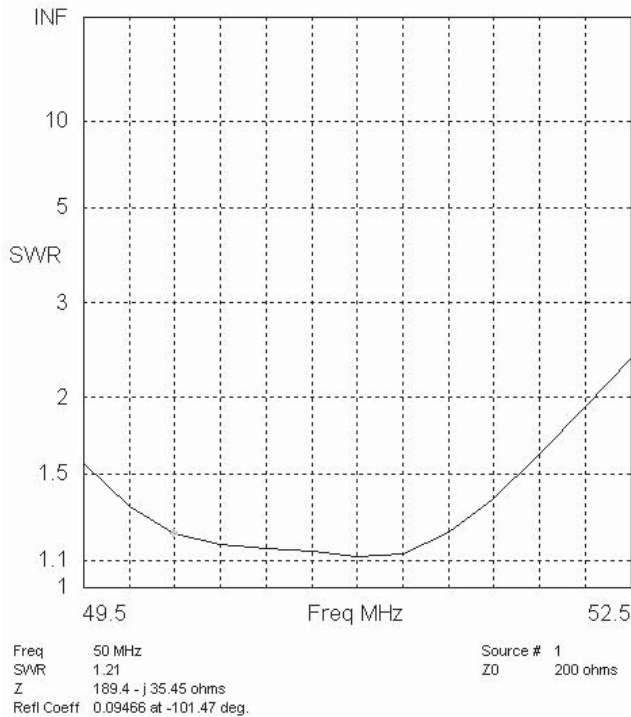

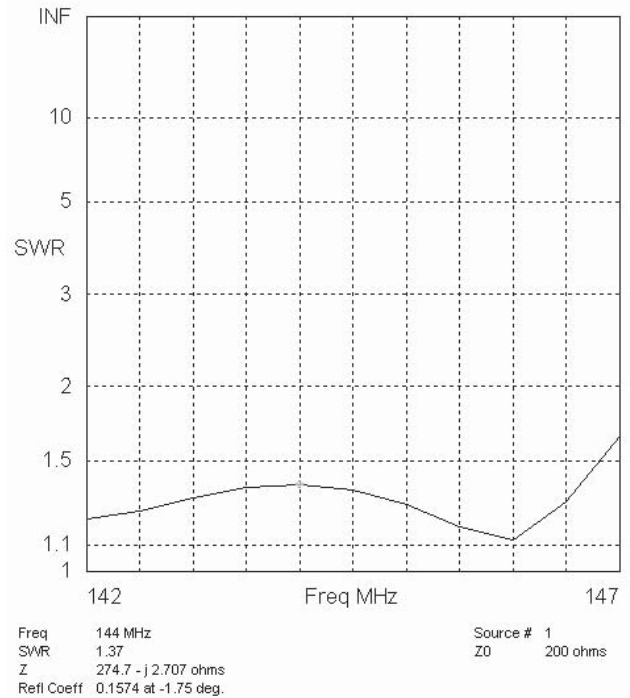Fig 16—SWR plot for the 6-element Boxkite for 6 m and 2 m in the 6 m band.

Fig 17—SWR plot for the 6-element Boxkite for 6 m and 2 m in the 2 m band.
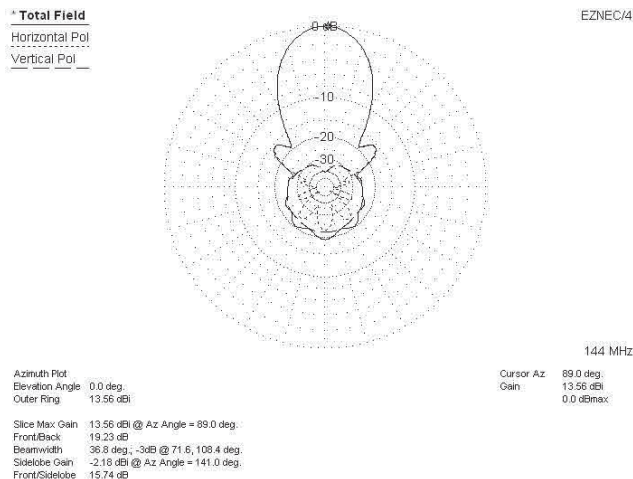

Fig 18—E-plane pattern of the 20-element Boxkite for 2 m and 70 cm at 144 MHz.
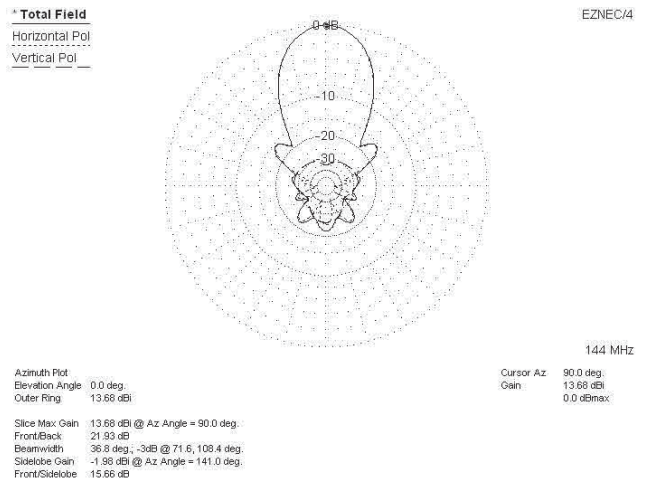

Fig 19—E-plane plot of 21-element Boxkite for 2 m and 70 cm, with third vertical reflector.

pedance is 200 ohms, and the antenna is fed with 50-ohm cable via a simple dual-band 1:4 balun. Fig13 shows the SWR curve on 2 m. It shows an SWR of less than 2:1 from 142 MHz to greater than 147 MHz. I have built a prototype of this antenna, and it is shown in Photo 1. Because of materials that I had to hand, the transmission lines are made of ¹/₂ inch aluminum and the horizontal-elements are of ¹/₄ inch aluminum, although ideally

¹/₂ inch material should be used for both. The SWR curve on both bands is close to the predictions of the model, but I have not yet done a pattern test. On-air tests are notoriously unreliable but the front-to-back ratio and sidelobe levels seem to be good.

Now for the 6-element version. Figs 14 and 15 show the E-plane pattern at 50 MHz and 144 MHz respectively. The boom length on 144 MHz is 1.6 λ, or 11 feet 2 inches, with a "wingspan"

of 8 feet 6 inches. A contemporary high performance Yagi would need a boom length of 2.4 λ, or over 16 feet, for the same gain on 2 m. On 6 m the gain is about what we would expect for the same boom length in a conventional Yagi. SWR plots on 6 m and 2 m are shown in Figs 16 and 17 respectively.

Boxkites for 2 m and 70 cm

Fig 18 shows the E-plane pattern for a 20-element Boxkite at 144 MHz. Note
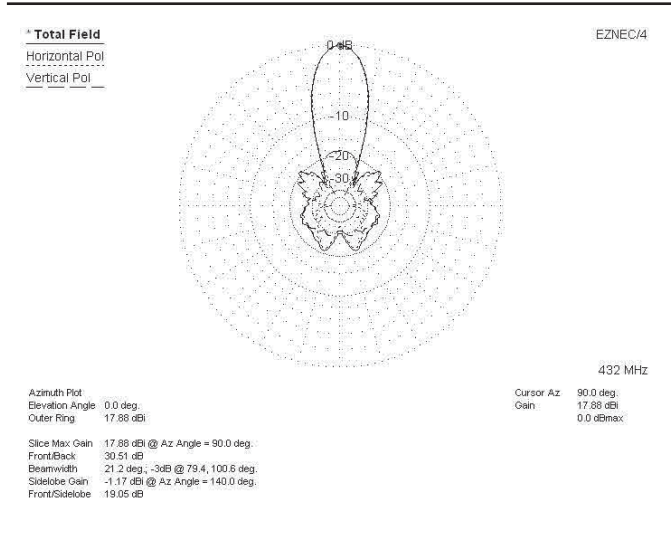

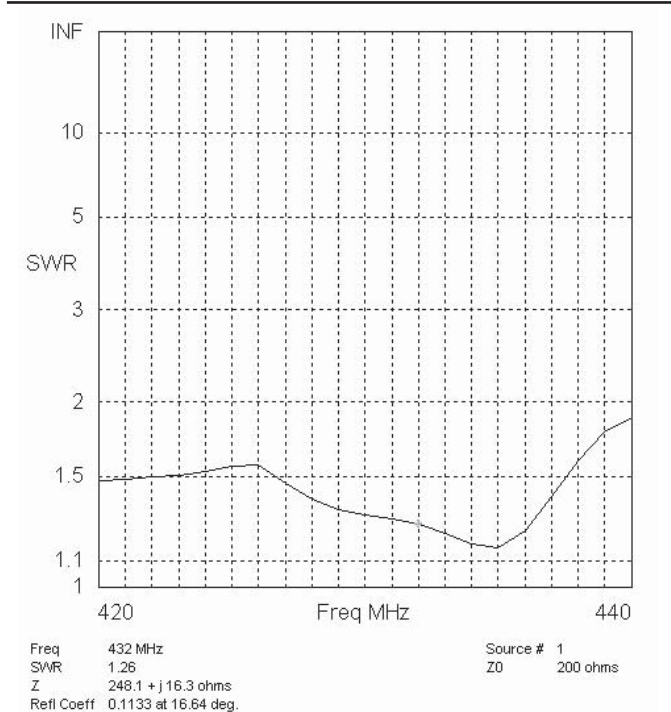Fig 20—E-plane pattern of the 21-element Boxkite for 2 m and 70 cm at 432 MHz.

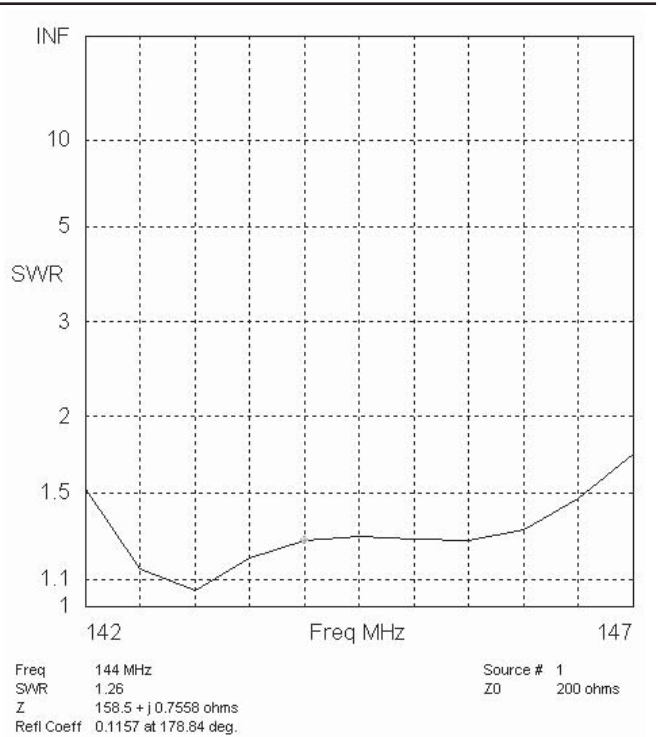Fig 21—SWR plot of the 21-element Boxkite for 2 m and 70 cm in the 2 m band.

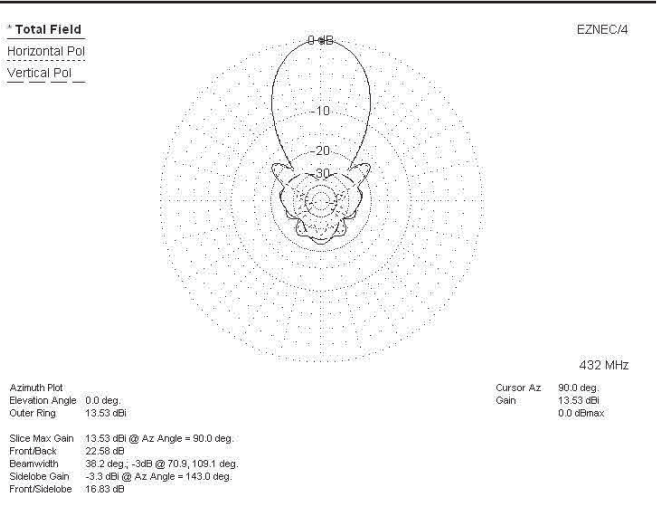Fig 22—SWR plot for the 21-element Boxkite for 2 m and 70 cm in the 70 cm band.

Fig 23—E-plane pattern of the 21-element Boxkite for 70 cm and 23 cm at 432 MHz.

that the most significant rear sidelobes at 144 MHz are vertically polarized. This seems to be a characteristic of Boxkites having an operating frequency ratio of near 3:1, and is caused by unequal currents in the driven-element transmission lines. In order to achieve a frequency ratio of 3:1, the coupling between the driven sub-element and its un-driven parasitic sub-element has to be reduced until the pair is operating in a region where the coupling between

them is relatively weak, so the currents in the transmission lines are not equal, and are not in antiphase. A simple solution to this problem is to add a conventional vertical reflector at about 0.2 λ behind the driven-element. The resulting pattern is shown in Fig 19, and we see a substantial improvement in the rear lobes. Note that this fix is not needed for Boxkites where the frequency ratios are less than 3:1, or for single band Boxkites. The pattern at

432 MHz is shown in Fig 20. The antenna is 13 feet 6 inches long and on both 2 m and 70 cm has approximately the same gain as an equal-boom-length Yagi. SWR plots for 2 m and 70 cm are shown in Figs. 21 and 22 respectively.

Boxkites for 70 cm and 23 cm

Patterns for a 21-element Boxkite for 70 and 23 cm are shown in Figs. 23 and 24. The antenna is 4 feet 6 inches long. The gain on 70 cm is the same as a Yagi
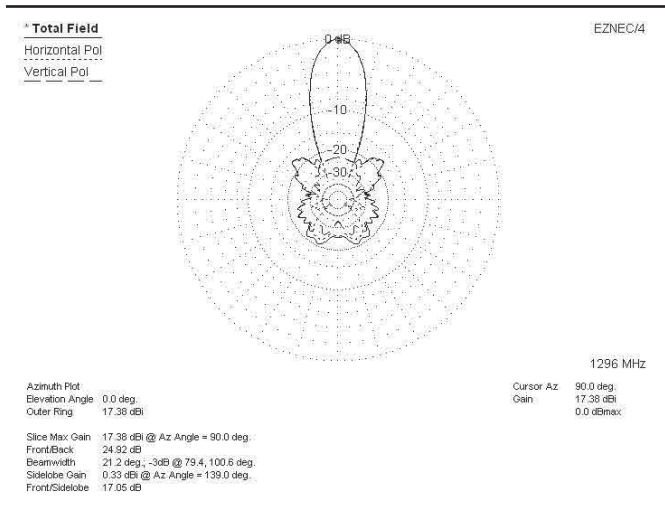

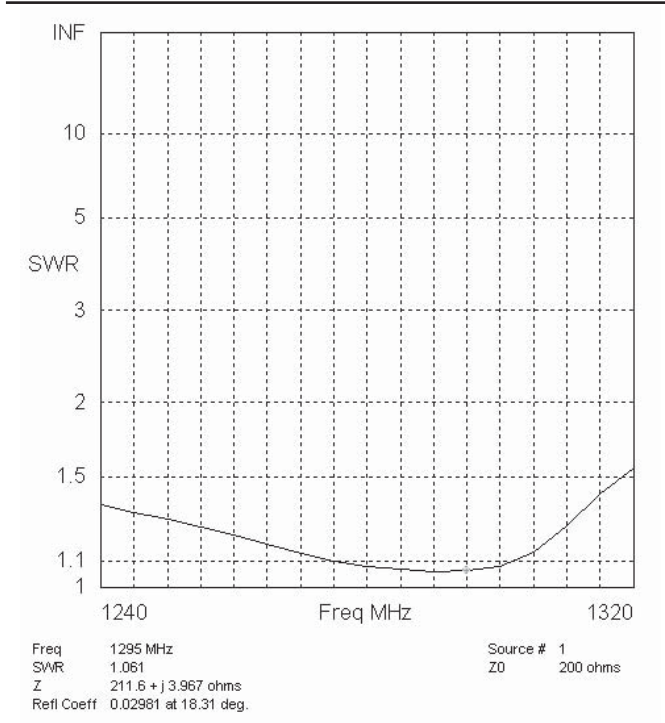Fig 24—E-plane pattern of the 21-element Boxkite for 70 cm and 23 cm at 1296 MHz.

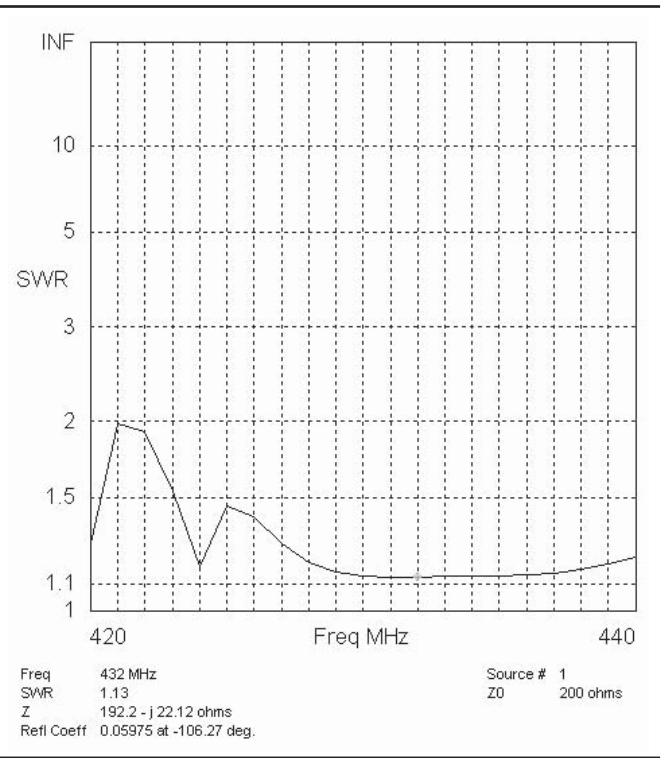Fig 25—SWR plot for the 21-element Boxkite for 70 cm and 23 cm in the 70 cm band.

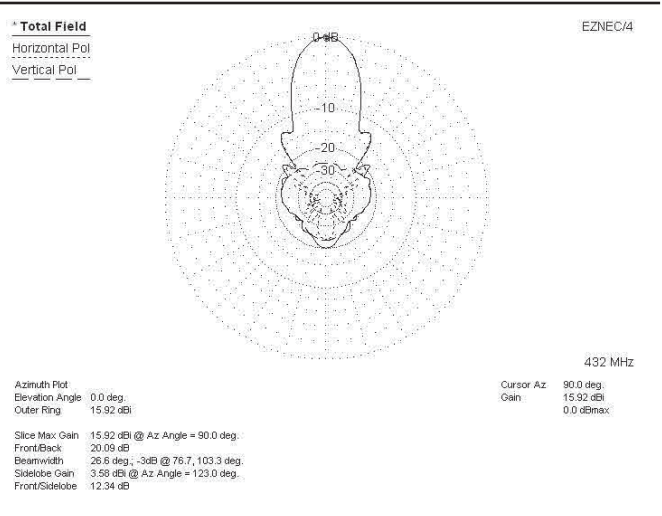Fig 26—SWR plot for the 21-element Boxkite for 70 cm and 23 cm in the 23 cm band.

Fig 27—E-plane pattern of the 39-element Boxkite for 70 cm and 23 cm at 432 MHz.

having the same boom length, and on 23 cm the Boxkite gain is about 1 dB more than that of an equal-length Yagi. The −1 dB gain-bandwidth extends from 1270 MHz to 1325 MHz, and from 423 MHz to 455 MHz. SWR plots are shown in Figs. 25 and 26. I have built and tested two prototypes of the antenna above, but without the third (vertical) reflector. Both of them have performed, both in terms of measured pattern and SWR, very closely to the model

predictions. The first of these used round ³/₁₆ inch diameter aluminum sub-elements mounted via conventional Delryn insulators mounted through a round boom. As expected I had problems with element rotation, although even large element rotation does not appear to impact the performance in a serious way. The second prototype uses square element material mounted to a square boom via custom polycarbonate insulators that lock the elements in place.

This mounting method is very rugged, but requires either machining the mounting blocks, or having them injection molded. I am looking into the latter possibility. The prototype antenna is shown in Photo 2.

Now for a longer 23/70 cm Boxkite. The plots for a 39-element Boxkite are shown in Figs. 27 thru 30. This antenna is 9 feet 6 inches long. The gain on 70 cm is within 0.4 dB of that expected for an equal length Yagi, and
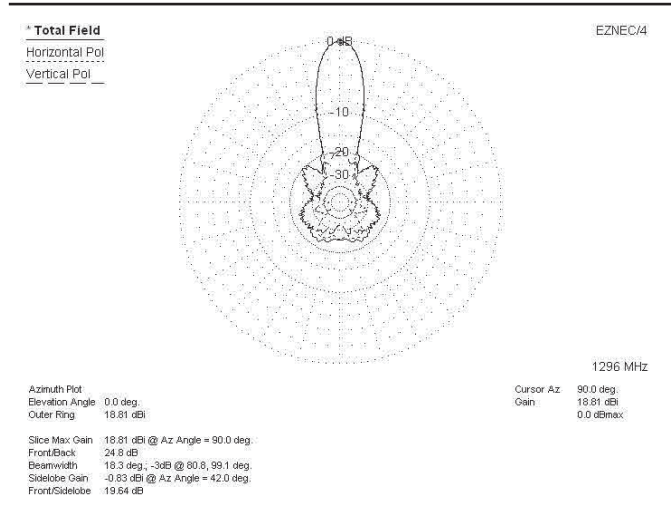

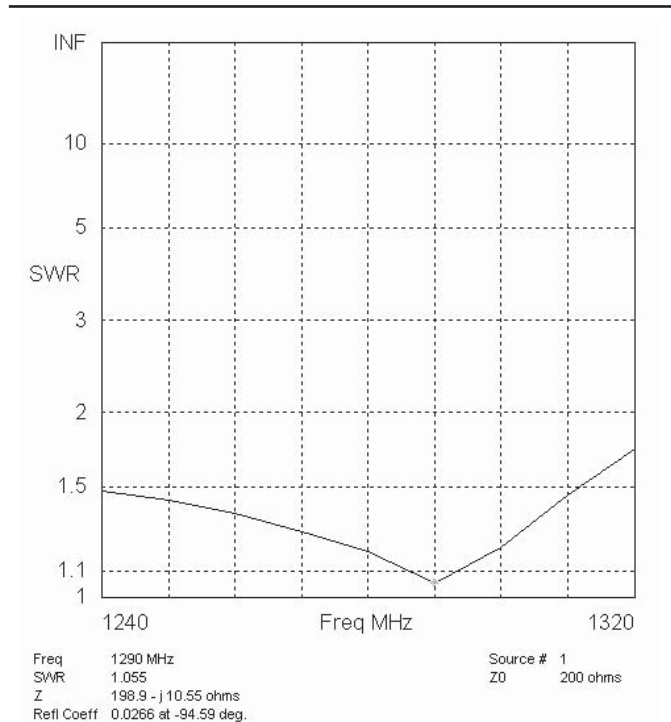**Fig 28—E-plane pattern of the 39-element Boxkite for 70 cm and 23 cm at 1296 MHz.**

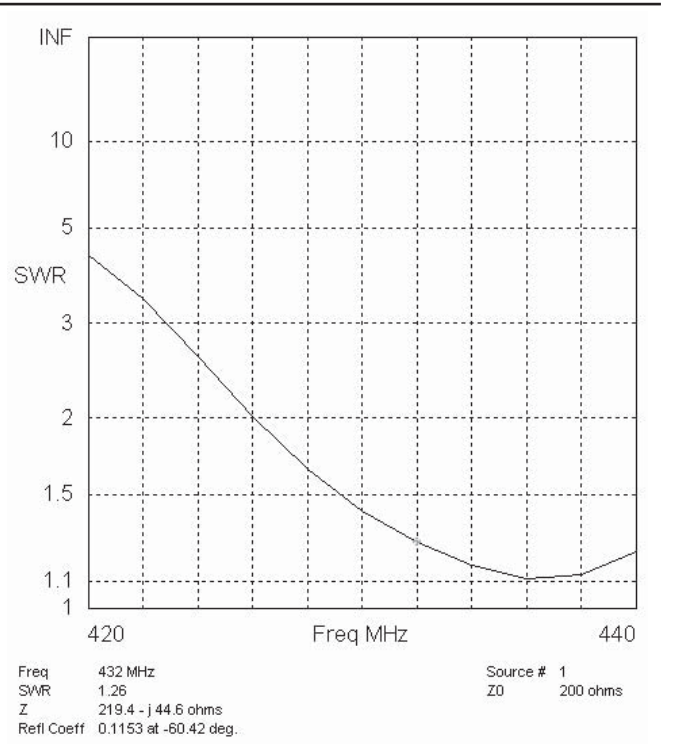**Fig 29—SWR plot of the 39-element Boxkite for 70 cm and 23 cm in the 70 cm band.**

Fig 30—SWR plot for the 39-element Boxkite for 70 cm and 23 cm in the 23 cm band.
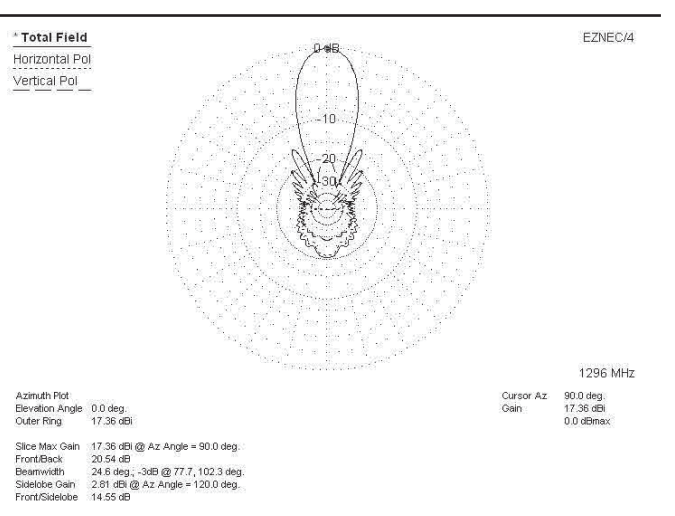

Fig 31—E-plane pattern of the 56-element Boxkite for 23 cm and 9 cm at 1296 MHz.

on 23 cm is about 1.5 dB less than an equal length Yagi. These gains can be improved somewhat by reducing the SWR bandwidth.

Boxkites for 23 and 9 cm

Data for a 56-element Boxkite for 23 and 9 cm are shown in Figs 31 thru 34. The antenna is 5 feet 6 inches long, and uses $1/16$ inch diameter elements. The feed element is not folded, and the nominal feed-point impedance is de-signed to be 50 ohms. Because of the non-harmonic relationship between 3456 MHz and 1296 MHz, the Boxkite uses reduced-length transmission lines to reduce coupling between the sub-elements, and the elements are of the non-X variety. The expected gain for a long Yagi with the same boom length at 3456 MHz is 22.5 dBi, and we are at 21.9 dBi. At 1296 MHz these numbers are 18.5 dBi and 17.4 dBi respectively. See later for some comments on this.

The –1 dB gain-bandwidth is from 3400 to 3550 MHz, and, remarkably, from 1180 to 1390 MHz, or 16% of the center frequency. The reason for this is that, as can be seen from the SWR curve in Fig 33, there are two minima in the SWR plot, one at 1200 MHz and one at 1300 MHz. At 1300 MHz the po-larization is horizontal, and at 1200 MHz it is vertical, with equal vertical and horizontal field magnitude at about 1235 MHz. The gain-bandwidth
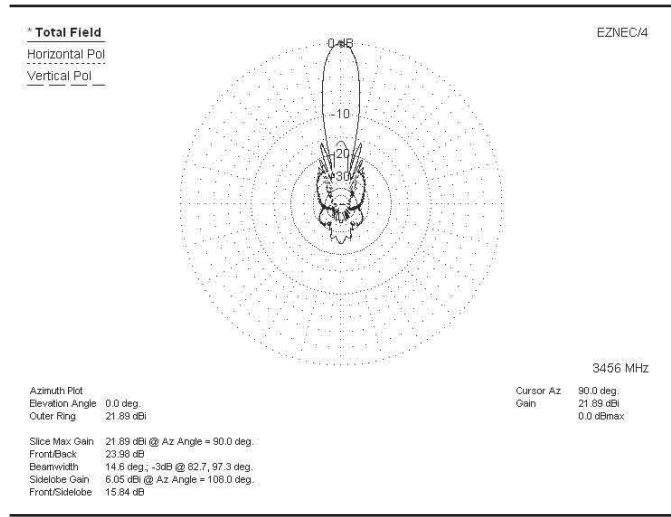

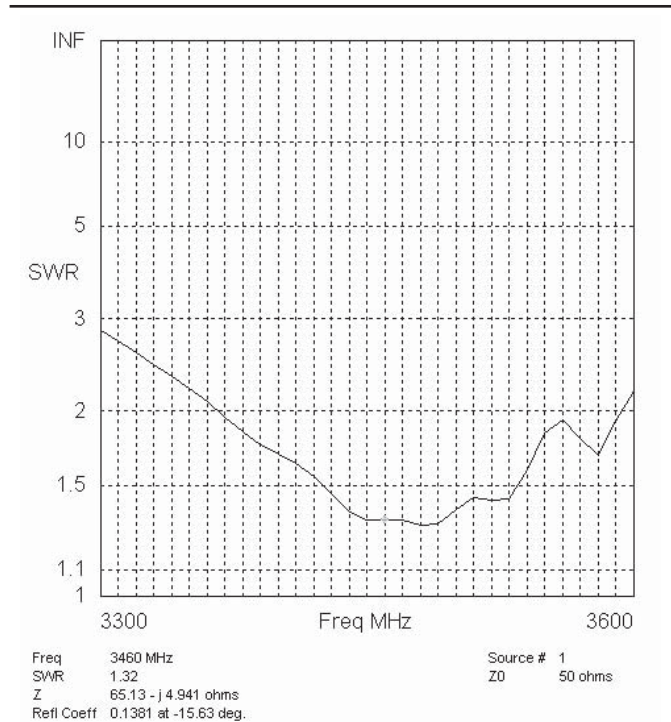Fig 32—E-plane pattern of the 56-element Boxkite for 23 cm and 9 cm at 3456MHz.

Fig 33—SWR of the 56-element Boxkite for 23 cm and 9 cm on 23 cm.

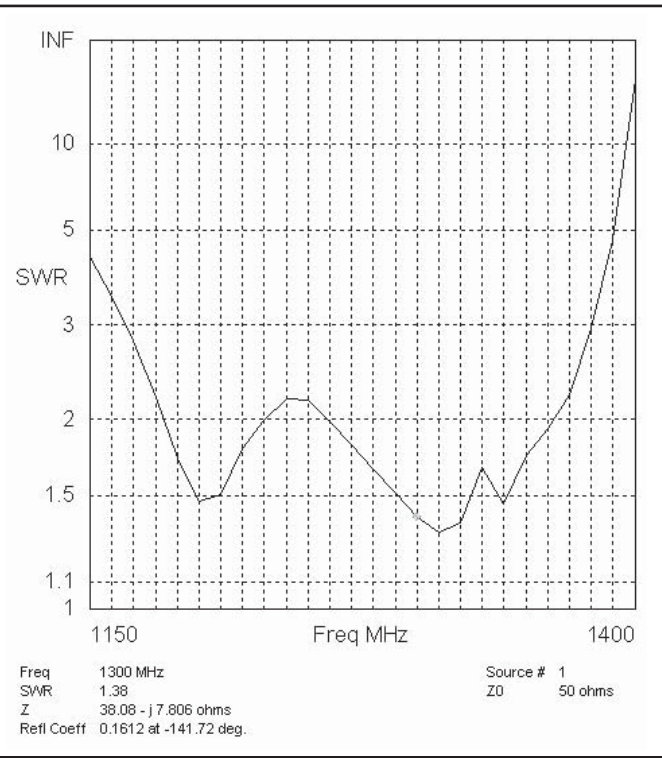
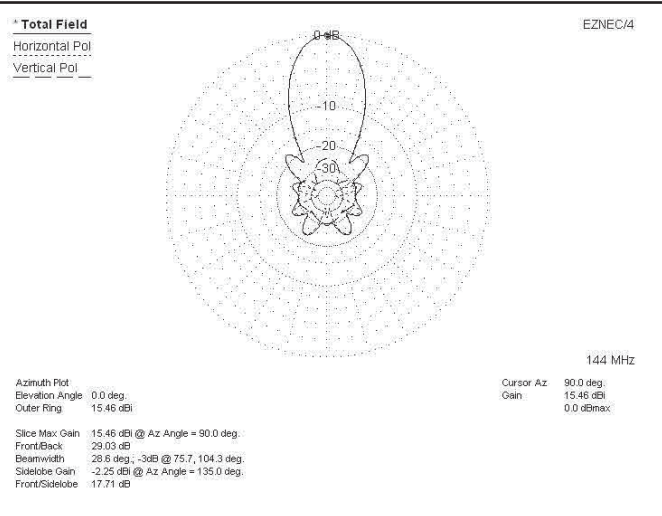Fig 34—SWR of the 56-element Boxkite for 23 cm and 9 cm at 9 cm.

Fig 35—E-plane pattern of the 7-element Boxkite X for 2 m.

noted above is referenced to the sum of the vertical and horizontal fields. However, it is interesting to note that, at the frequency where the horizontal and vertical fields are equal, the antenna is radiating a circularly polarized field. This is because there is zero phase delay between the feed-point and the vertical-elements (the transmission lines) in the transmitting antenna, but approximately 90º phase shift from the feed-point to the horizontal-elements because of the transmission lines. If an identical receiving antenna is used there is zero phase shift from the vertical-elements to the feed-point, and 90º from the horizontal-elements. So the polarization sense is the same in each, and the broadband expectations are met. The polarization sense may be changed by switching the feed-point from one of the driven-element transmission lines to the other. The vertical phase is independent of which transmission line is fed, because the currents in the two transmission lines are in phase, but the horizontal phase changes. I checked this (in the model) by rotating a dipole receiving antenna in the far field, and found that, at 1235 MHz, indeed the received signal is virtually independent of rotation angle. Also, when using identical 56-element Boxkites for transmitting and receiving, the –1 dB gain-bandwidth extends from 1210 to 1380 MHz, if the transmission line phasing is correct as noted above.

Note that the ratio of the two operating frequencies for this antenna is 3456/1296 = 2.67. I have built a prototype 3-element 23/9 cm antenna and it is shown in Photo 3. It performs very closely to the model predictions, even though I did not use a balun. In order to decouple the feed cable outer sheath from the antenna, I believe that a pair of concentric sleeve baluns would probably work just fine, but I have not tried them.

Single-band Boxkites (Boxkite X)

A 7-element Boxkite X for 2 meters

If we restrict operation to f_3, and optimize for that, we end up with the Boxkite X versions. As an example, a 7-element Boxkite X for 2 meters has performance shown in Figs. 35 and 36. The boom length is 8 feet, and the "wing-span" is 8 feet 4 inches. A conventional Yagi would need a boom length of 3.3λ, or 22.5 feet, for the same gain. The relative turning radii are approximately 5.7 feet and 11 feet respectively. The –1 dB gain-bandwidth is 7 MHz, with a gain peak of 15.5 dBi at 147 MHz. It is interesting to note that the supergain limit for this antenna at 144 MHz is 15.9 dBi,
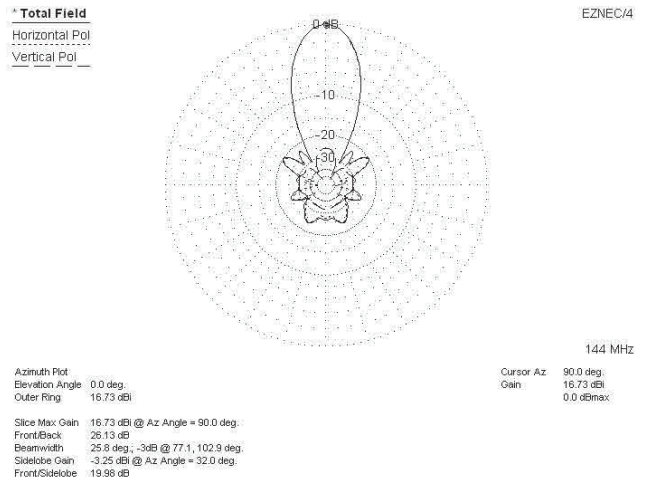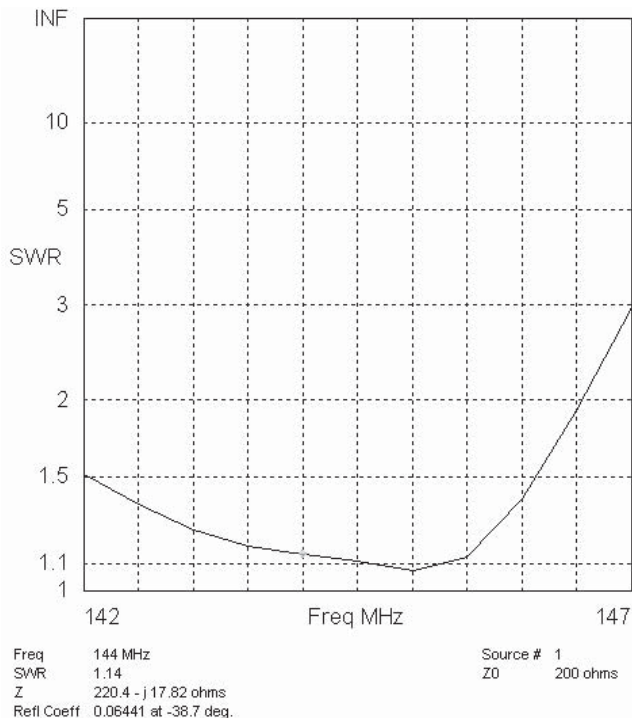
Fig 37—E-plane pattern for 10-element Boxkite X for 2 m.

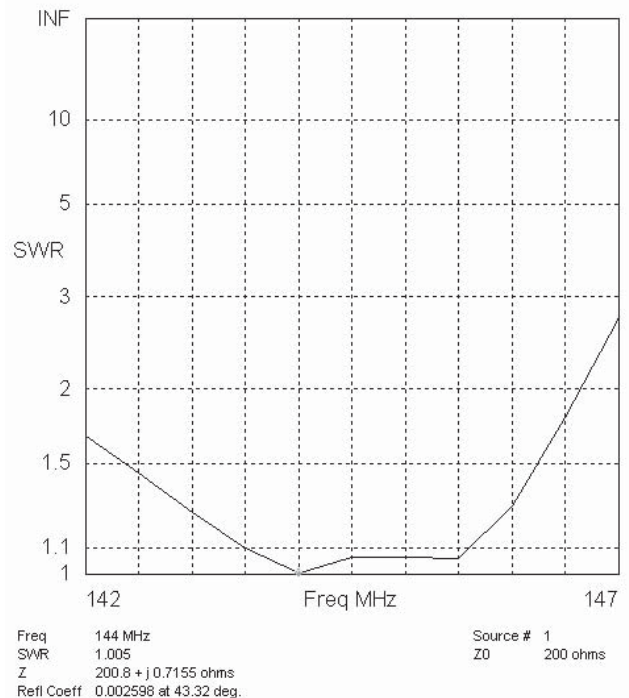Fig 36—SWR plot for the 7-element Boxkite X for 2 m.

Fig 38—SWR of 10-element Boxkite X for 2 m.

so we are within 0.4 dB of this. See under "stacking Box kites" later for notes about supergain.

A 10-element Boxkite X for 2 meters

Fig 37 shows the E-plane pattern for the 10-element version. The SWR plot is shown in Fig 38. The –1 dB gain-bandwidth is over 6 MHz. The boom length is 14 feet (2 λ) and a conventional Yagi would need a boom length of 4.5 λ, or over 30 feet, for the same gain.

The turning radii are approximately 8 feet and 15 feet respectively. A stack of four of these Boxkites, spaced 160 inches in the E-plane and 145 inches in the H-plane, provides 22.4 dBi gain. The Boxkite stack has roughly half the boom length of the Yagi stack for the same gain. It can

Fig 39—E-plane pattern for the 10-element Boxkite for 70 cm at 432 MHz.

Fig 40—SWR of 10-element Boxkite X for 70 cm.

be seen that the Boxkite X design provides a major advantage, in terms of boom length, over a conventional Yagi.

A 10-element Boxkite X for 70 cm

The pattern for this antenna is shown in Fig 39. The antenna is less than 5 feet long and has the same gain as a conventional Yagi that is about 10 feet long. The –1 dB gain-bandwidth is 20 MHz, with a gain peak at 435 MHz. The SWR plot is shown in Fig 40.

20-element Boxkite X for 70 cm

The plots for this antenna are shown in Figs 41 and 42. The antenna is 13 feet long and has the same gain as a 19 foot Yagi.

From the above few examples, it can be seen that the 10-element 70 cm Boxkite X has a boom length advantage over a conventional high performance long Yagi of 5 feet or 2.2 λ, and the 20-element version has a length advantage of 6 feet or 2.6 λ. For the 2 m versions, the boom length advantage is approximately 15 feet or 2.2 λ.

20-element Boxkite X for 23 cm

Box kite Xs for 23 cm still maintain similar boom length advantages, in terms of wavelengths, but of course a 2.5 to 3 λ advantage over a Yagi is only a little over 27 inches, so one can argue that the added complication of the Boxkite X is not worth the effort. However, I have included data for two Boxkites for this band for completeness. For bands above 23 cm, the advantage becomes negligible for any reasonable boom length. Plots for this antenna are shown in Figs. 43 and 44. This antenna is 53 inches long and has the same gain as a Yagi 73 inches long. The boom length advantage over a Yagi is 2.2 λ.

34-element Boxkite X for 23 cm

This antenna is 91 inches, or 10 λ, long and has the gain of a 13.1 λ (119 inches) Yagi. Plots are shown in Figs. 45 and 46.

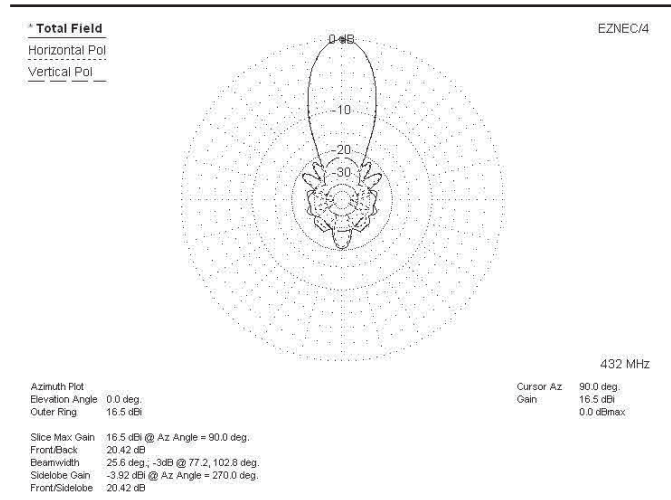**Discussion**

The modeled data for dual-band Boxkites shows that these are perfectly practical, and this is supported by measurements on prototypes. The difficulty with designing
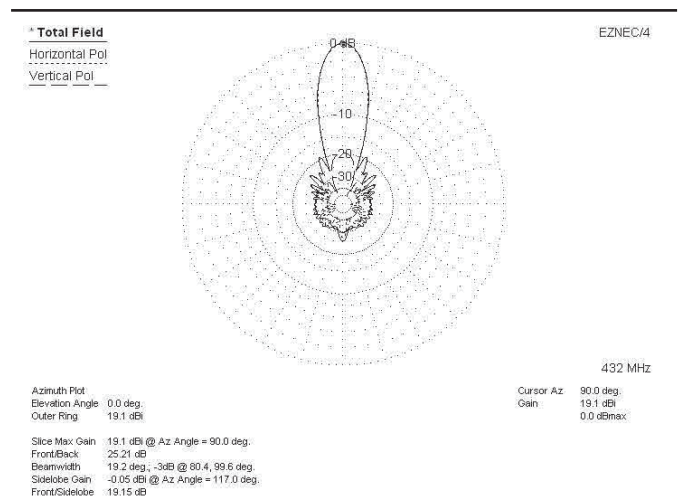

Fig 41—E-plane pattern of the 20-element Boxkite X for 70 cm.

Boxkites, however, is significantly greater than for Yagis because of their three dimensional nature. For a regular contemporary long Yagi for the VHF/UHF/microwave bands, the variables are the element diameter, the element lengths, and the element spacings (ignoring matching problems). These are optimized on one band only. For a dual-band Boxkite, the variables are the element diameter, the sub-element geometry (which is not necessarily the same for all sub-elements), the spacing of the sub-elements, the spacing of the sub-element pairs and the sub-element lengths. These have to be optimized on two bands, and the feed-point impedance has to be the same on both bands if complex matching networks are to be avoided. Although this seems to be a daunting task, the foregoing data shows that the results can be reasonably good, if not perfect.

One of the problems I encountered was that of understanding why it was that the antenna performance at f_2, in terms of pattern and gain, was so good when the geometry seemed to be all wrong. In particular, the director spacing is much smaller than for conventional Yagis, and it appeared that the director lengths were nowhere near optimum. However, I believe I have at least the glimmer of an idea as to why this should be so. I will only consider the horizontal/horizontal polarization case: the vertical/horizontal case is quite different and I think of limited interest.

First we'll consider the director spacing at f_2, which is set by the spacing requirement at f_3. This spacing is about 0.36 λ for the 21-element Boxkites at f_3 for directors far from the feed-point, so for dual-band Boxkites where f_3 is 3 times f_2, the spacing at f_2 is 0.12 λ. Although this is very close spacing, it turns out that it is not a problem. An excellent article by Emerson[2] points out that the more (correctly phased) directors that a Yagi has, the better. To check this, I took the 21-element 23 cm/70 cm Boxkite, left the first five directors in place, and removed every other di-

rector. The gain on 70 cm dropped by 0.1 dB with virtually no change in the pattern, and, remarkably, the SWR curve remained very good. Then I removed two out of three directors, while retaining the first five directors, and the gain on 70 cm dropped by 0.9 dB compared to the original, again with a very good SWR curve and unchanged pattern. In both cases of course the performance on 23 cm was strongly affected. So it seems that the close spacing on 70 cm really is not important either from the standpoint of gain or feed-point impedance. Now let's consider the geometric differences between the elements on the two bands. Consider Fig 47, which shows a director sub-element pair. Note that, at both f_2 and f_3, there is a voltage node at the center of the
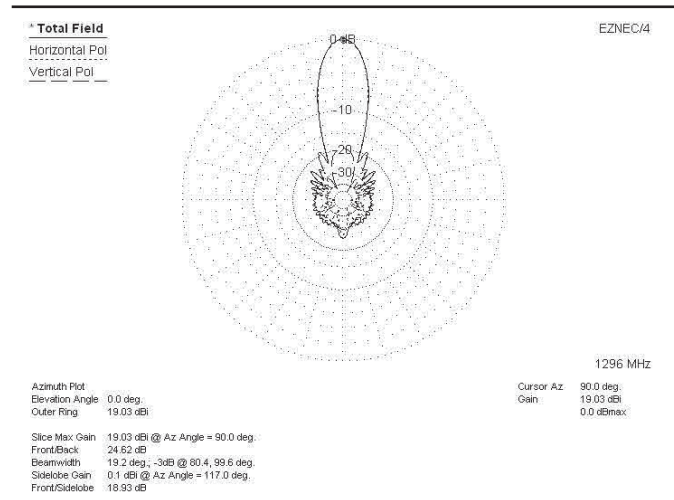

Fig 43—E-plane pattern of the 20-element Boxkite X for 23 cm.
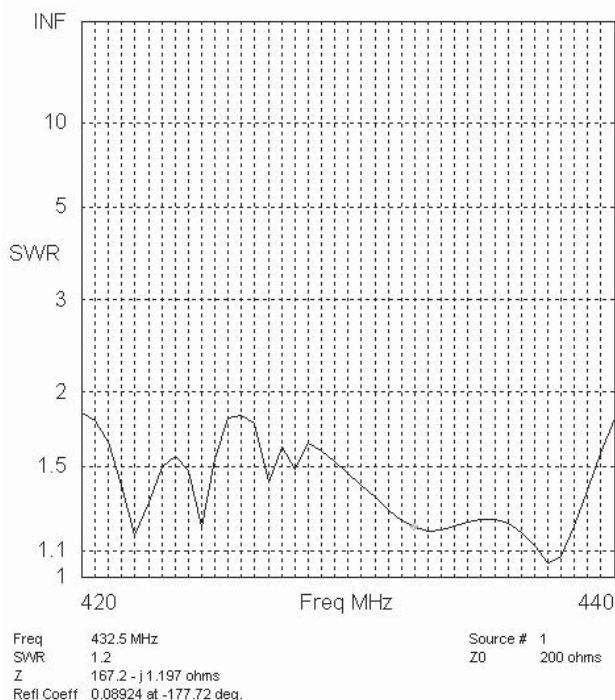

Fig 42—SWR of 20-element Boxkite X for 70 cm.

Fig 44—SWR of the 20-element Boxkite X for 23 cm.

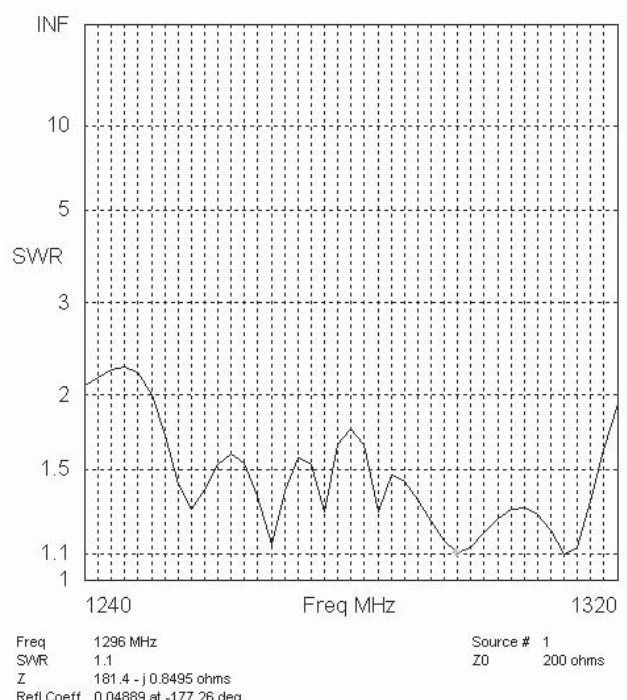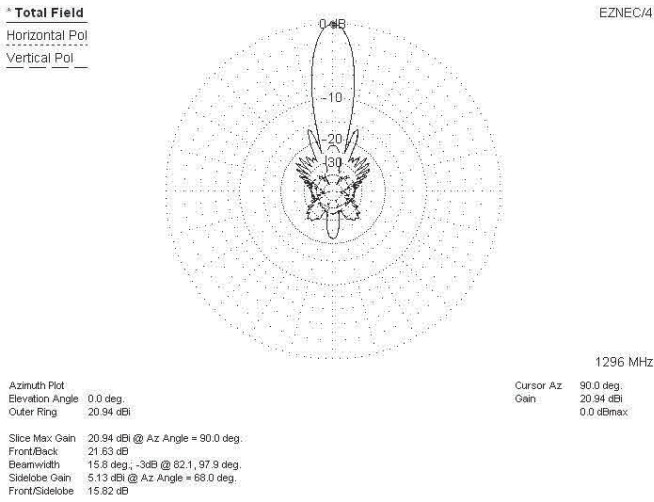**Fig 45—E-plane pattern of the 34-element Boxkite X for 23 cm.**

Fig 46—SWR of the 34-element Boxkite X for 23 cm.

Fig 47—Geometry of a Boxkite director.
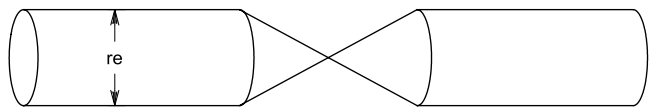
Fig 48—Equivalent Boxkite director.
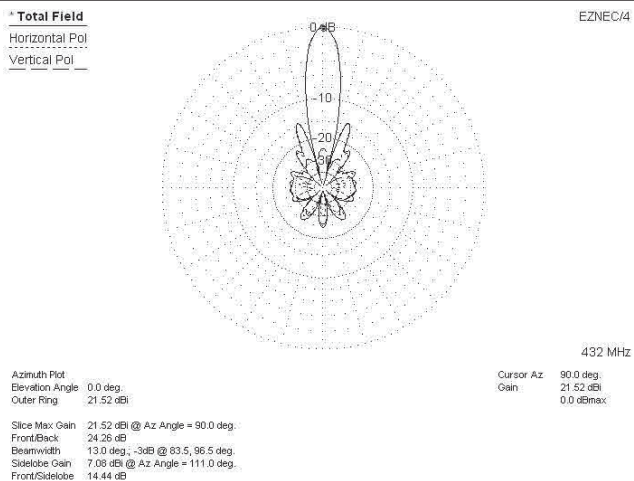
Fig 49—E-plane pattern of a 4 stack of 10-element Boxkite Xs for 70 cm.
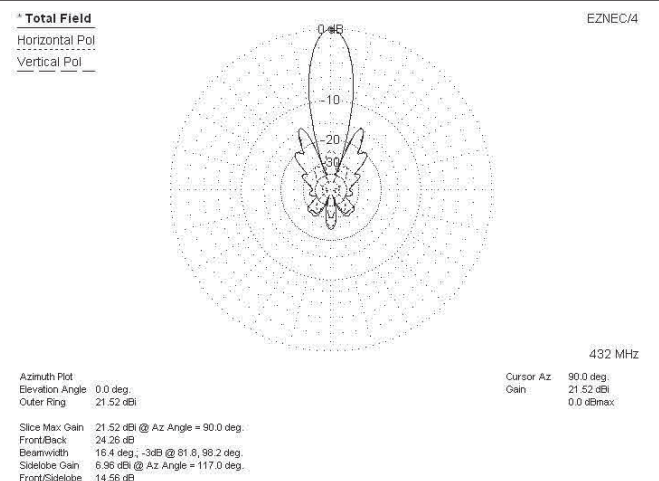
Fig 50—H-plane pattern of 4 stack of 10-element Boxkite Xs for 70 cm.
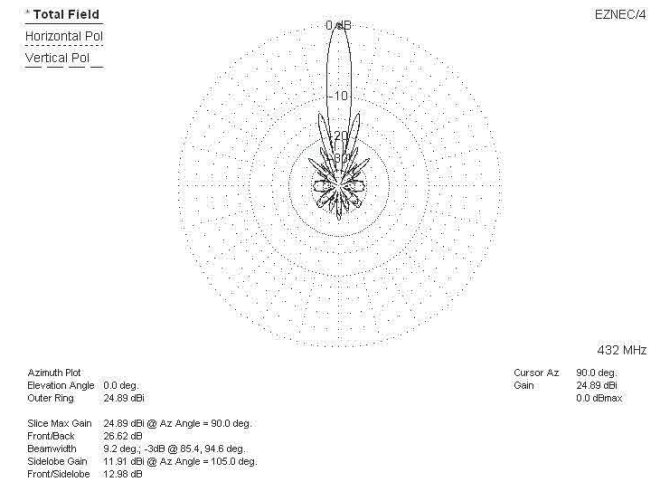
Fig 51—E-plane pattern of 4 20-element Boxkite Xs.
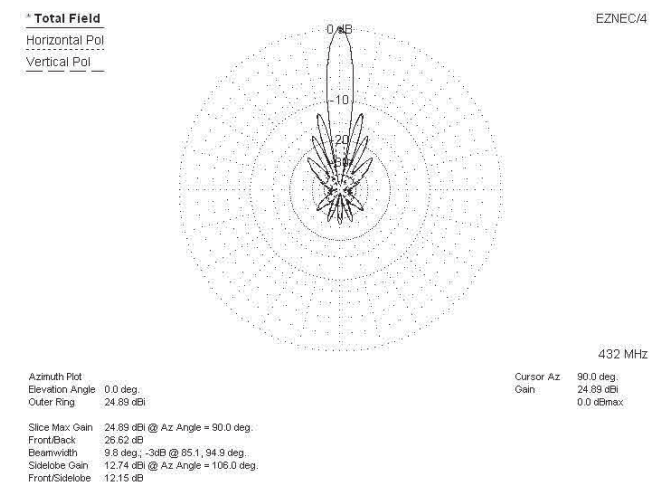
Fig 52—H-plane plot of 4 20-element Boxkite Xs for 70 cm.

Fig 53—E-plane pattern of a 5 stack of 21-element Boxkites for 2 m and 70 cm at 432 MHz.

Fig 54—H-plane plot of 5 stack of 21-element Boxkites for 2 m and 70 cm at 432 MHz.

Fig 55—E-plane pattern of 5 stack of 21-element Boxkites for 2 m and 73 cm at 144 MHz.

Fig 56—H-plane pattern of 5 stack of 21-element Boxkites for 2 m and 70 cm at 144 MHz.

transmission lines, so we can consider them to be connected together at this point. At f_3, as explained earlier, the element behaves as a stacked quad of approximately $\lambda/2$ di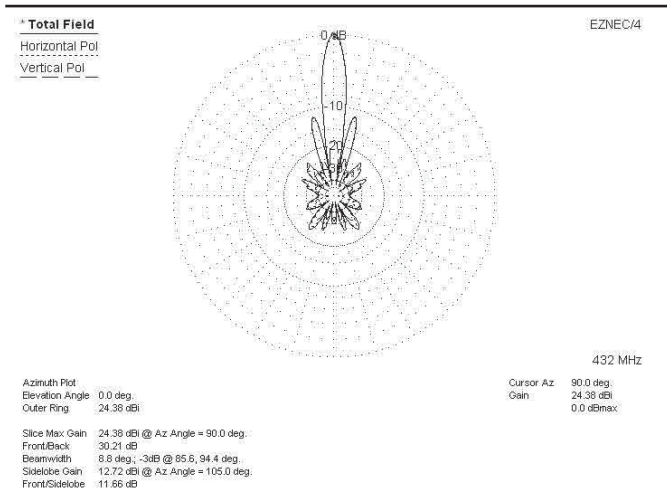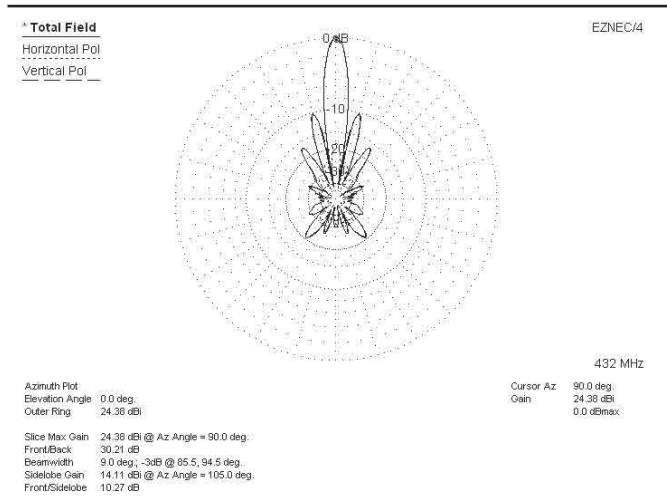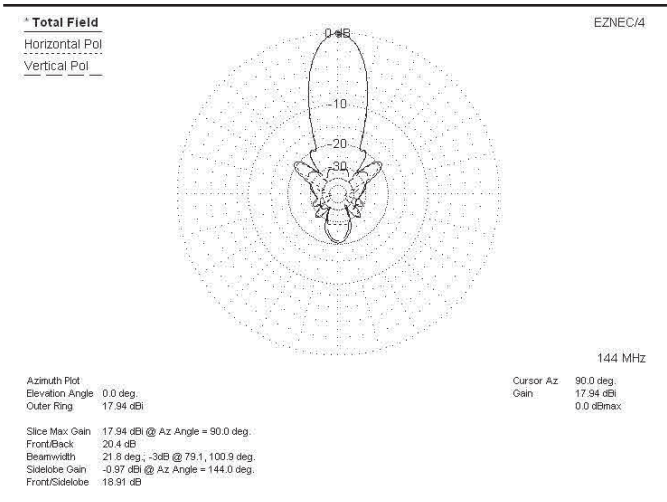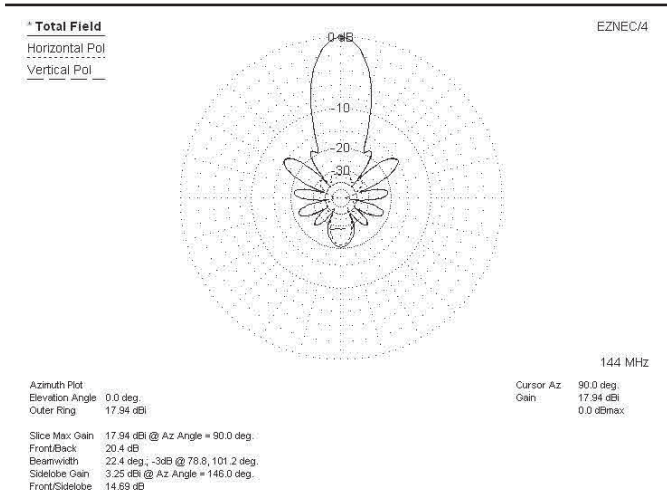poles insulated from each other by $\lambda/4$ shorted stubs. At f_2 the currents in the horizontal sections of the elements are in phase, so the sub-elements can be replaced by a single element having a radius equivalent to that of the spaced elements. See Fig 48. (The transition at the center is almost certainly a lot more complex than illustrated, but I hope you will get the point).

In order to achieve the maximum gain for a surface-wave antenna, which a Boxkite is when the length is several wavelengths or more, it is necessary to optimize the phase delay along the antenna. This is determined by the spacing and diameter of the equivalent directors. The equivalent radius of two identical parallel wires is given by[3]

$$r_e \approx \sqrt{rd} \qquad \text{Eq 1}$$

where r_e is the equivalent radius of the two sub-elements, r is the radius of the sub-elements and d is the center-to-center spacing of the sub-elements

For the 21-element Boxkite for 23 and 70 cm, d is approximately $\lambda/6$ on 70 cm (4.6 inches) and is set by the requirement that it be roughly $\lambda/2$ on 23 cm. The diameter of the elements is set by mechanical considerations, and in the example antenna is the equivalent diameter of 0.1875 inches square extrusion, which is 0.22 inches. On 23 cm, the element diameter to wavelength ratio, d_e/λ, is 0.024, so from available charts[4] relating-element length to d_e/λ, the length of the directors needs to be somewhere in the region of 0.41 λ for

the first director and 0.35 λ for the final director, the latter being dependent on the antenna length. The spacing between the fanned out upper and lower ends of the transmission lines on the 20-element Box kite for 23 and 70 cm is 1.4 inches (0.15 λ at 23 cm) so the total antenna width is twice the director length plus 0.15 λ, or 1.05 λ for the first director and 0.89 λ for the final director, in terms of λ on 23 cm. On 70 cm this translates to .35 λ and .3 λ respectively. For a relatively thin element diameter this would be far too short to provide effective director action. However, on 70 cm the effective diameter of the element is much greater than it is on 23 cm. From (1), r_e=0.7 inches, or d_e/λ =.05. If we now look at design curves[3] relating antenna length to the phase shift along the antenna needed for maximum gain, we find that, again for the 21-element Boxkites, the boom length at f_2 is

$$L \approx 2\lambda \qquad \text{Eq 2}$$

For a boom length of 2 λ, then for maximum gain

$$\frac{\lambda}{\lambda_z} \approx 1.13 \qquad \text{Eq 3}$$

where λ is the free space wavelength and λ_z is the wavelength along the antenna surface

The surface wavelength is determined by the spacing of the directors and by their reactance, which is determined by their diameter and length. Curves relating these parameters are given in ref. 3, and show that, for d_e/λ= .05, and s/λ = .12 (where s is the director spacing), the director length required to achieve the necessary surface wave velocity is 0.32 λ. This is close to that determined above from consider-

ations of the required dimensions at f_3, given that the data for surface wave antennas assumes that the all the directors are equally spaced and of equal diameter (note however that I have ignored the effect of the conical center sections of the equivalent director). This is why the performance on the two bands is better than might have been expected. Despite this, I have not found it possible to maintain the high gain of a single band Box kite at f_3 while maintaining good pattern and gain at f_2. From the modeled results, it seems that the best that can be done is to produce directivity on each of the two bands that is close to that of a contemporary long Yagi having the same boom length. The "fat" elements at f_2 help to produce high gain-bandwidth and SWR bandwidth at that frequency.

Stacking Boxkites

Like Yagis, Boxkites can be stacked horizontally and/or vertically to give increased gain. For single band Boxkites, there are no more difficulties than there are with stacking Yagis. Depending on the application, we can stack for maximum gain or for moderate gain with low sidelobes. As an example, Figs 49 and 50 show the E-plane and H-plane patterns respectively for a stack of 4 10-element Boxkite Xs for 70 cm. The individual Yagi gain is 16.4 dBi, and it can be seen that the total gain of the stack is 21.8 dBi, which is close to the maximum that can be achieved with reasonably low sidelobes. Stacking distance is 53 inches by 46 inches. This is not necessarily optimum, but illustrates what can be achieved. The array is contained in a cube that is approximately 70 inches wide by 60 inches tall by 58 inches long.

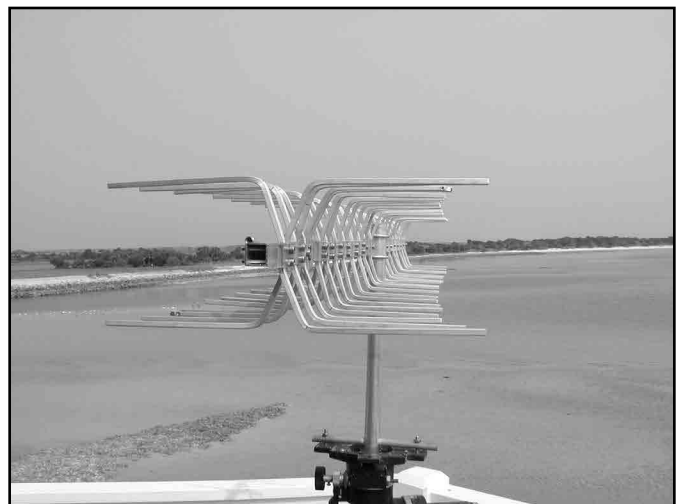**Photo 1—Prototype 3-element Boxkite for 6 m and 2 m.**

Photo 2—Prototype 20-element Boxkite for 70 cm and 23 cm.

It is interesting to note how close this comes to the supergain limit. An antenna possesses supergain when its directivity is higher than a fundamental limit imposed by the dimensions of its enclosing sphere[5]. If the antenna is in the supergain region, all sorts of woes occur, such as high losses from very high antenna currents, and high Q resulting in narrow bandwidths. The supergain limit is given by

$$G_{\max} \leq \left(\frac{2\pi A}{\lambda}\right)^2 + \frac{4\pi A}{\lambda} \qquad \text{Eq 4}$$

where A is the radius of the enclosing sphere and $G_{\max}$ is the maximum allowable gain without entering the supergain region

For our stacked 10-element 70 cm Boxkite Xs, the radius of the enclosing sphere is 53 inches, or 1.9 λ, from which $G_{\max}$ is 22.4 dBi. Our stacked gain is 21.8 dBi, so we are in the interesting situation where the stacked Boxkite X produces almost the maximum gain achievable for its enclosed volume without entering the supergain region.

Figs 51 and 52 show the results of stacking four 20-element 70 cm Boxkite Xs. The stacking distances are 75 inches (1.9 m) in the E-plane and 72 inches (1.8 m) in the H-plane. This antenna provides sufficient gain for serious moon bounce work[6]. Its dimensions are roughly 6 feet by 6 feet by 13 feet long.

Stacking dual-band Box kites is not quite so simple. The optimum stacking distance for Yagis is:

$$D_{opt} = \frac{\lambda}{2\sin\dfrac{\varphi}{2}} \qquad \text{Eq 5}$$

where φ is the half-power beamwidth, and for long Yagis

$$D_{opt} \approx \frac{57\lambda}{\varphi} \qquad \text{Eq 6}$$

Also, for long Yagis, the E and H-plane beamwidths are virtually equal. The gain is given approximately by:

$$G \approx \frac{42,000}{\varphi_E \varphi_H} \approx \frac{42000}{\varphi^2} \qquad \text{Eq 7}$$

The gain is also proportional to the length, L, of the Yagi:

$$G \approx \frac{10L}{\lambda} \qquad \text{Eq 8}$$

The above expression is approximately true for dual-band Boxkites so

$$D_{opt} \approx 0.9\sqrt{L\lambda}$$

For a given length, the optimum spacing is proportional to the square root of the wavelength. For two operating frequencies that are a factor three apart, this means that the optimum spacing is root three different for the two frequencies. However, setting the stacking distance to give maximum gain at f_3 will not produce the maximum stacking gain achievable at f_2. Conversely, setting the stacking distance at f_2 for maximum gain will produce an over stacked condition at f_3, with consequent very large sidelobes. With a rectangular stack of four Boxkites this is indeed true. However, if we slightly under stack at f_2, then put a fifth Boxkite right in the middle of the array, we can overcome this problem. Figs. 53 thru 56 show the patterns for a stack of five 21-element Box kites for 2 m and 70 cm, with the four outer antennas spaced 90 inches apart both vertically and horizontally, and the fifth antenna centered in the square. These patterns are very reasonable on both bands, and are almost certainly not optimized. There are other geometries that provide good performance, for example a triangular arrangement of three Boxkites with a fourth set in the center of the triangle also gives a good pattern and gain.

For the *big guns*, a stack of four of the above antennas, spaced 160 inches in both E and H-planes provides the very high directivity required for moonbounce work. The gain at 432 MHz is 30 dBi with a beamwidth of

4.2º, and on 144 MHz the gain is 23 dBi with a beamwidth of 12º. For the 2 m/70 cm and 70 cm/23 cm Boxkites, where the frequency ratio is three, the individual Box kites may be driven by a conventional power splitter that is a quarter wavelength long at f_2, and this will also work at f_3. Although it is quite unlikely that such a dual-band stacked array gives the ultimate in performance on both bands, especially in terms of G/T, it is nevertheless intriguing to be able to consider a dual-band Yagi-based moonbounce antenna.

Summary

I hope I have shown that Boxkites have some unique advantages over conventional Yagis on the VHF, UHF and microwave bands. The ability to use one antenna on two bands, which do not have to be harmonically related, with virtually no compromise in performance, has the advantage that only a single feeder is necessary. The single band Boxkites have a length advantage over conventional Yagis that is, to first order, independent of length. On 2 meters a single band Boxkite has the same gain as a regular Yagi that is approximately 15 feet longer. Although not as easy to construct as regular Yagis, all the antennas described are not difficult to make, and I hope to have kits of parts available in the near future.

In the next article I will provide detailed constructional data for some of the Boxkite Yagis, along with mea-
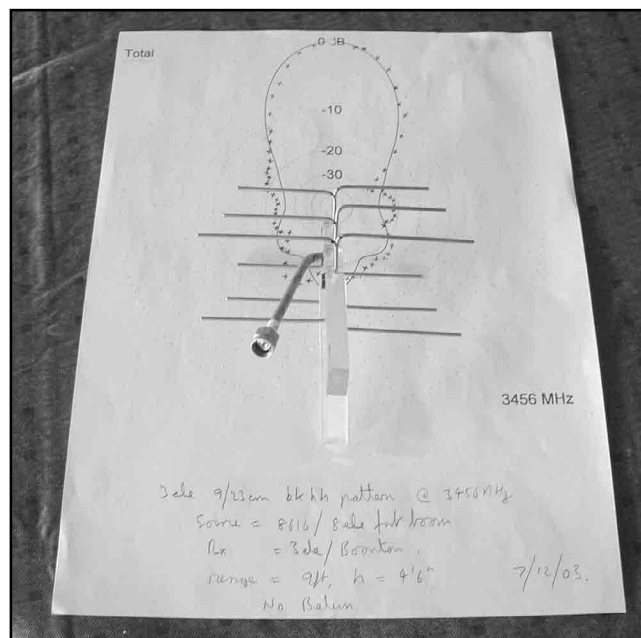
Photo 3—Prototype 3-element Boxkite for 23 cm and 9 cm, along with modeled and measured pattern at 3456 MHz.

surements of SWR and pattern made on the prototypes.

I must confess that the most important lesson I have learned from the endeavor that produced the Boxkite designs, and others as yet unpublished, is that even with technology that is over a hundred years old, there is still plenty of room for innovation.

It is also an awful lot of fun!

Notes
[1]S. Powlishen, K1FO, *The ARRL Handbook for Radio Amateurs*, 76th edition, ARRL, 1999.
[2]D. Emerson, AA7FV, "The Gain of an Endfire Array". *ARRL Antenna Compendium*, Volume 5, ARRL 1996.
[3]R. Johnson. *Antenna Engineering Handbook*, 3rd edition, McGraw-Hill Inc, 1961.
[4]G. Hoch, DL6WU, "Yagi antennas for UHF/VHF", *UHF/Microwave Handbook*, ARRL, 1990.
[5]R. Haviland, W4MB, "Supergain Antennas", *Communications Quarterly*, Summer 1992.
[6]R. Turrin, W2IMU, and A. Katz, K2UYH, "Earth-Moon-Earth (EME) Communications", *ARRL UHF/Microwave Handbook*, ARRL, 1990. □□

Build A Super Transceiver— Software for Software Controllable Radios

Homebrew software can enhance the performance of a PC controllable radio.

By Steve Gradijan, WB5KIA

Not satisfied with your present radio or are you craving features available only on the newest radios? You can spend a lot of money on hardware or, if you already have a personal computer in your radio shack, you can significantly transform the capabilities of your existing equipment for less than $100, possibly for free. Home-brew software can transform your existing transceiver into a near state of the art communications machine, or add features the manufacturer forgot to provide.

Software Processing Augmentation of Communications Equipment (SPACE) is the process of substituting

1902 Middle Glen Dr
Carrollton, TX 75007
wb5kia@arrl.net

software for hardware to enhance under-performing hardware. SPACE can work when implemented with slower personal computers and even if the radio you want to improve was not designed with software control in mind.

The techniques described here showcase improvements to a Kenwood TS-2000. This radio is already pretty hot with lots of bells and whistles. However, even the TS-2000 can be made better and more user friendly. If you have another brand or model of a radio that has serial (RS-232) terminal communication capabilities, that radio can be smartened-up too. The performance of transceivers lacking serial communications ports can also be improved by processing the received audio using a PC's soundcard for various purposes or using the PC's serial port as a switch.

Why the TS-2000?

PC controllable radios that have significant potential for relatively easy software augmentation include: Kenwood's TS-2000, TS-870 and TS-570; Yaesu's FT-1000; Ten-Tec's Pegasus, Jupiter and Orion; and certainly others I am not familiar with. I started with the TS-2000 because I have one. It wasn't very convenient to use its manual controls with my trifocals and large fingers, and the computer control commands provided by Kenwood make it easy to program compared to other brands.

What Can You Expect?

A program that demonstrates the types of improvements that are possible for the TS-2000 is free from my Web site at **www.qsl.net/wb5kia**. *ARCS-Lite* is a functional rig control

program that will give, at least TS-2000 owners, a chance to play with the toys available through software radio enhancement and control (see Figure 1). Try it safely, you can uninstall the application by deleting the entire folder it came in, since nothing is written to the Window's Registry if it isn't what you expected.

Considerable improvements can be made to your transceiver if it has a serial communications capability and a built-in keyer. Software can provide your transceiver with features such as:
- Band limits monitoring (stay within your license limits).
- A wide range frequency spectrum scanner showing current band activity using serial communication.
- A Morse keyboard and/or memory keyer (the easy way using a TS-2000 or similar radio with a built in CW keyer).
- A Morse keyboard and/or memory keyer (the more difficult way, as described on the WB5KIA Web site).
- An enhanced DX Cluster monitor for the TS-2000.
- Most of the Amateur Radio control program features available on commercial ARCP software.

TS-2000 owners can duplicate all the features and conveniences described above. Most of the enhancements can be replicated using other manufacturers' equipment. You can use your radio to do things that it was never designed to do if you are willing to learn to program virtually any of the high level programming languages.

You don't have a compiler and probably never will? You can still play although you will miss out on some of the fun. The free transceiver enhancement programs available on my Web site and those programmed by others may change your mind. A *Delphi Standard, Visual Basic Learning Edition* or "professional" compiler programmer can use the critical code snippets described to start making his or her transceiver "super". The entry-level compilers retail at around $100. This represents the "total cost of enhancements" excluding your time and a serial cable ($2.95 at a local parts supplier). Source code and helpful code snippets for related projects are available on the Web site. Be aware that the coding projects may be beyond the capabilities of novice programmers if the code needs to be adapted to other radios.

How It Can Work

The ability to communicate with your radio using a simple terminal program and/or an average quality PC soundcard, opens the possibility for sig-nificant software modifications to your radio to increase its utility. Software can establish communication with your transceiver rather easily if the transceiver has PC control capabilities and a serial interface. A simple terminal program with pre-programmed instructions can command virtually all of your transceiver's functions. Even if a transceiver lacks a serial port, software is able to "talk" to your transceiver with a connection between the transceiver's audio and your soundcard. Also the software can turn relays on and off to control older rigs using simple hardware. If the transceiver audio is used with a soundcard, remember to use an interface to avoid damaging your soundcard. Your radio has software upgrade potential even if it isn't PC enabled, although the possibilities for upgrade are greater if it has serial communication capabilities.

Most of the example code here, which can be used to enhance your transceiver, is written in *Delphi*. A few *Visual Basic* code snippets examples are given to help port the code to *Visual Basic,* if required. If you decided to program, you will need a free *Delphi* COM port control like *ComPort* by Dejan Crnila or *Async Pro* to establish the software communication link to your transceiver in addition to the compiler. A third-party COM control or *Mscom32* for *Visual Basic* works fine. *Learning Edition* users will need a free third-party control (there are several on the Internet). The provided example code assumes either *ComPort* or *Mscomm32* is used. If you have another COM control, you'll have to adapt the example code.

You may need a serial cable between your transceiver and PC, a cable from your transceiver's audio line to soundcard, and/or a cable from the serial or parallel port of your PC to the key jack on your radio, depending on the improvements you make and your rig's capabilities. You need a serial cable to use *ARCS-Lite*.

The Toys—

It would take a book to describe what can be done to improve your transceiver's operation using software. The possibilities are almost limitless. The code snippets to get you started using SPACE to design several relatively easy to program features are described here. The *ARCS-Lite* program includes the following "toys' and more.

DXCluster

The TS-2000 has a feature called *P.C.T.* (Packet Cluster Tuning). The radio's built-in TNC lets you access your local DXCluster node to receive DX spots on your TS-2000. Use SPACE to display all the DX spots you receive (instead of the hardware limited 10). Your radio can jump directly to a particular DX spot, if you write the program so that a double-click on a listing will take
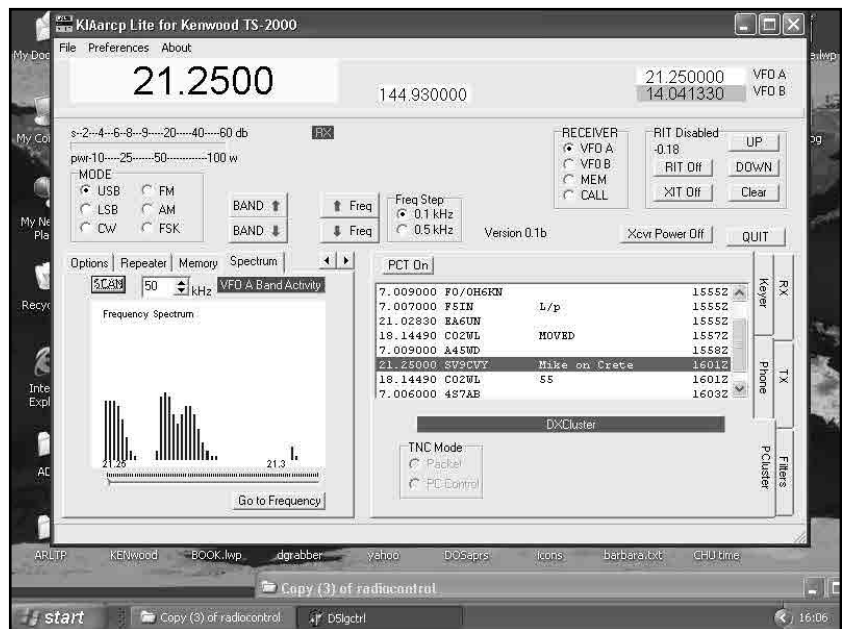

Figure 1—The *ARCS-Lite* application is a many featured TS-2000 rig control program. The featured spectrum display is on the left panel, the DXCluster is on the right panel. A similar program for other radios can be written with entry level, high level computer languages.

you directly to the DX station's frequency. Listing 1 shows how to get started. Your DXCluster display could look like the panel shown in Figure 1.

If you don't have a TS-2000, the DXCluster functionality can be achieved in several ways. Have a TNC? You might write a specialized terminal program for your TNC. If you don't have a TNC, download SV2AGW's *Soundcard Packet Terminal Engine* and interface to it with a homemade terminal program. Example code on SV2AGW's Web site (**www.elcom.gr/sv2agw/agwsc.htm**) and Yahoo forum show several ways to implement the *no TNC* case using *Delphi* and *VB* code.

Memory Keyer/Morse Keyboard

A software memory keyer or Morse keyboard can key your rig using the PC's serial or parallel ports or command a built-in keyer in your radio, if it is programmable. Commanding the built-in keyer in the TS-2000 is fairly easy and only takes a few lines of code using *Delphi* or *VB*. Listing 2 describes *Delphi* and *Visual Basic* algorithms for a single memory keyer function. The rig's key jack is not switched on/off as in a conventional keyer program so it is not necessary to provide a keying line. The serial cable you might already use with a logging program allows you to command the keyer. This technique might also be possible with other radios if they permit programming messages to a built-in keyer. Alternative example code and links having example code for those whose radio's do not have a built-in keyer are on the WB5KIA Web site. The example *ARCS-Lite* application implements a Morse keyboard feature and the memory keyer as shown in Figure 2.

Spectrum Scan

A spectrum scan is not very difficult to implement once you have written a basic radio control program. Poll a set frequency range within a loop and provide a simple plotting interface to record apparent S-meter readings. The spectrum shown in Figure 1 is simply generated and it is possible to jump to the frequency of any of the signals displayed by using the slide control.

Band Limits

The algorithm described in Listing 3 can monitor the transceiver's frequency to determine if you are operating your rig within predetermined frequency ranges. Relatively simple code helps you or your guest operator stay within the limits of license privileges during contest or at other times when the excitement of a special con-tact might let you forget your frequency limitations.

Commanding Kenwood and Other Radios

Commands for Kenwood radios are of three types: *Set, Read* and *Answer*. It is actually possible to command your radio using the general purpose terminal program that comes with *Windows*, however, you'll want to write a specialized terminal program. The *Delphi* and *Visual Basic* COM controls make this simple. The command to set VFO A to 14.195 MHz is **FA00014195000;**. The terminal program sends the command as a string. You can request the receiver to report its present frequency using **FA;** and it will respond by sending a text string that looks like **FA00014195000** to be read by the terminal program. I code everything manually but the *Delphi* control written by Marinus, ZS6MAW, may facilitate coding for some programmers (**www.qsl.net/zs6maw**). He also has written a free ARCP for the Kenwood TS-570 and TS-870 available at his Web site.

A *Delphi* command to instruct the transceiver to go to a specific frequency using the *ComPort* control looks like this:

```
Comport.writestr('FA00014195000;');
Sleep(25);
```

The commands to use with *Mscomm32* and *Visual Basic* to go to the same frequency looks like this:

```
MSComm1.InBufferCount = 0
MSComm1.Output
    = ("FA00014195000;")
```

and need to be followed by a few additional lines of code shown in Listing 2.

Yaesu or Ten-Tec commands look a little different. Not only are their command sets unique, these manufacturers read the comparable frequency information in binary data code. The article in February 2002 *QST* by Brian Wood for Yaesu (B.Wood, WØDZ, "The Return of the Slide Rule Dial," *QST*, Feb 2002, pp 33-35) or the Sept/Oct 2002 *QEX* article by Mark Erbaugh, N8HE, for Ten-Tec ("Customize the Ten-Tec Pegasus—Without Soldering"), help make the Yaesu or Ten-Tec commands to decode frequency information understandable.

ICOM also uses different instructions and approaches to command their radios as discussed below.

Programming Other Radios

Yaesu

Brian Wood demonstrated how to extract the Yaesu FT-1000 frequency, band and mode information in his article "The Return of the Slide Rule Dial" using *Visual Basic*. The routines used with the FT-1000 to convert the binary frequency data returned by the FT-1000 into useful values are calculated as follows:

```
'Calc new freq
    Freq = x(1) * 256 + x(2)
    Freq = Freq * 256 + x(3)
    Freq = Freq * 256 + x(4)
    Freq = Freq / 16
    Freq = Freq / 10 ^ 6
```

The *Delphi* code would look something like:

```
//Calc new freq
begin
    Freq := x(1) * 256 + x(2);
    Freq := Freq * 256 + x(3);
    Freq := Freq * 256 + x(4);
```
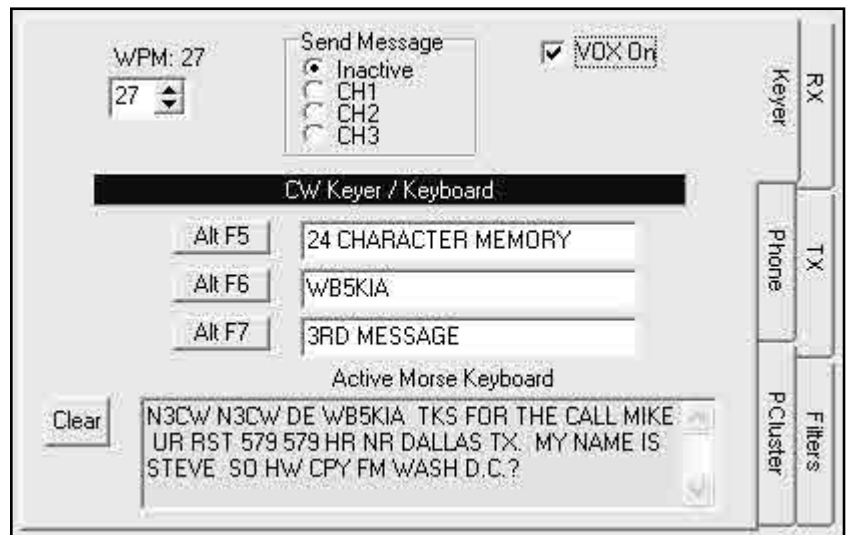

Figure 2—Software controls the built-in keyer. You have a choice of the existing built-in memory messages, as many external memories as you want or the ability to use a keyboard for real-time sending.

```
    Freq := Freq / 16;
    Freq := Freq / 10 ^ 6;
  End;
```

The *Delphi* code snippet has not been tested with a Yaesu radio so some experimentation might be necessary if you attempt to use it in your project. As with the Kenwood radios, most Yaesu computer control functions appear relatively simple to implement.

Ten-Tec

Ten-Tec radios have a RS-232 COM port for PC control. Information for developers who wish to interface their programs with Ten-Tec's products is available on the Ten-Tec Web site. A code listing there shows how to use their proprietary command set to control the Pegasus and Jupiter transceivers using C++. The commands can be adapted to *Visual Basic* or *Delphi*. N8ME's *Delphi* control (0209ERBAUGH.ZIP) to command a Pegasus can be downloaded from the ARRL Web at **www.arrl.org/qexfiles**.

ICOM

ICOM radios use TTL logic to command functions. This can be converted to and from RS-232 as described below.

DF4OR has collected most of the control signal information Icom users need to control their rigs using the CI-V interface or its home-brew equivalents. The CI-V control information is currently available at his Web site at **www.plicht.de/ekki/**. Also visit **www.ambersoft.com/Amateur_Radio/index.htm/**. The *ICOM Receiver Page* at **uk.geocities.com/blakkekatt/software.html** has information about interfacing to ICOM radios including several *Visual Basic 6* code snippets and links to a small *Visual Basic 6* control program with source code.

Construction plans for interfaces to mimic ICOM's commercial CI-V interface can be found in several Amateur Radio journals if you need to build the additional hardware needed for PC frequency and function control with some ICOM radios.

To Do List

Here are some ideas about what to code. Some of these projects may be described in a future article or discussed at **www.qsl.net/wb5kia**.
- Code to transform your radio into a CW beacon for 10 or 6 meters (add a timer control to the memory keyer code snippet and write code to provide frequency and power output control).
- Code to transform your radio into an APRS weather station using limited hardware (thermistor, diode, capacitor) to report temperature. A digital 'thermometer' is described by Natan Osterman at **http://users.auth.gr/~mixos/projects/nopcb/pc/006**. Download the *Delphi* code at **http://users.auth.gr~mixos/projects/nopcb/pc/006/tempmeter.zip**. You will need to code the packet part of the project to transmit the temperature data.
- Code to transform your radio into an APRS beacon.
- Off the air voice recorder with playback using a soundcard.
- DXCluster monitor (more difficult approach for all 2 m capable radios).
- Display received audio spectrum.
- Display received audio sinusoidal curve [described on the WB5KIA Web site].
- Short range frequency spectrum scanner using receiver audio.
- Store favorite frequencies or channels in a database file.

Sure, you can program your transceiver manually. If you were lucky, the manufacturer also provided you with a free (?) program to administer the memory channels. You can do better storing the frequency information in a file on your PC!
- Store SWL frequency lists in files and use the lists to control your short wave listening selections.
- Add DSP audio filtering.
- Store power, mike, speech processor,

Listing 1. *Delphi* Algorithm to Implement DXCluster

```
Requires a ListBox, Button and the ComPort control.
procedure TMainForm.Button11Click(Sender: TObject);
var
  ctr,found:integer;
  Packt,memo,PFreq,PCall,PComment,PTime:string;
  PFreqR:real;
begin
  Try
    comport.writestr('AI3;');
    Sleep(25);  // give the radio time to respond. Values valid at 38400bps
    Comport.writestr('PK;');  //command to query the radio's P.C.T. function
    Sleep(20);
    ComPort.ReadStr(Packt,65);   //read more than we need
    sleep(20);
    Packt:=copy(Packt,pos('PK',packt)+3,51); // read exactly what is needed
    Pfreq:=copy(Packt,1,10);
    PfreqR:=strtofloat(Pfreq);
    PfreqR:=PfreqR*0.000001;
    Pfreq:=trim(floattostr(PfreqR));
    while length(Pfreq)<8 do
     begin
       Pfreq:= Pfreq+'0';
     end;
    PCall:=copy(Packt,11,12);
    PComment:=copy(Packt,23,20);
    PTime:=copy(Packt,43,5);
    // depending on whether the DX Spot has been received previously
    // add it to the list box or reject it
    for ctr := 0 to (ListBox4.items.Count -1) do
      if  trim(listbox4.Items[ctr])= trim(Pfreq+' '+PCall+' '+Pcomment+' '+PTime)
then
        begin
          Found :=  1;
        end;
      if (Found <>1) then
        begin
          listbox4.Items.Add(trim(Pfreq+' '+PCall+' '+Pcomment+' '+PTime));
        end;
        Found:= 0;
     end;
end;
```

Listing 2. Algorithm for A Simple Memory Keyer Bank

Using Delphi (Requires a Button and Label.)

```
procedure TMainForm.Button21Click(Sender: TObject);
var
CWmsg,S:string;
begin
  CWmsg:=edit4.text;
  if length( CWmsg )<=24 then
   begin
    S:= StringofChar(' ',24 - length(cwmsg)); // message
     //must not exceed 24 characters
    CWmsg := Cwmsg + S;
   end
  else
  edit4. color:= clRed; //turn edit red if exceed 24 character
     //limit

  comport.writestr('KY '+CWmsg+';'); // send the command
     //to the built-in keyer and give it time to execute
  Sleep(25);
  comport.connected:=false; //to avoid program hang-up
    using ComPort
  Sleep(10);
  comport.connected:=true;
end;
```

Using Visual Basic (A Text box and Command button are needed. Mscom32 is used.)

```
Private Sub Command3_Click()
Timer1.Enabled = False 'don't run freq scan while doing
     'this
CWmsg = UCase(Text4.Text)
If Len(CWmsg) <= 24 Then message must not exceed 24
     'characters
 S = Space(24 - Len(CWmsg))
  CWmsg = CWmsg + S
   Text4.BackColor = QBColor(7)
Else
  Text4.BackColor = QBColor(12) 'turn box red if exceed 24
     'character limit
End If
MSComm1.InBufferCount = 0
MSComm1.Output = ("KY " + CWmsg + ";") 'command the
     'TS-2000
Counter = 0
 Do
  Counter = Counter + 1
 Loop Until MSComm1.InBufferCount > 25 Or Counter >
  2000
 If Counter >= 20000 Then
  GoTo skip2  'to avoid possibility of endless loop
 End If
skip2:
MSComm1.RTSEnable = False
Timer1.Enabled = True 'ok to run freq scan now
End Sub
```

Listing 3. Partial Algorithm for Determining Out of Band Limits

Requires a Label. The two Radiogroup controls provide current operating mode information. A second case statement is required to handle the CW mode completely.

```
procedure TMainForm.Button2Click(Sender: TObject);
var
limitsi:integer;
begin
 //out of band module  General Class example
 limitsi:=trunc(strtoint(gfreq)*0.01); //link to the xcvr freq
 if RadioGroup1.Itemindex in[0,1,4] then begin //if
 //USB,LSB,AM
  case limitsi of
 18000..20000:  label42.visible:= false;// caption of this
  //label is 'OUT of BAND' 38500..40000:
 label42.visible:= false;
    72250..73000:  label42.visible:= false;
    142250..143500:  label42.visible:= false;
    213000..214500:  label42.visible:= false;
    249300..249900:  label42.visible:= false;
    283000..297000:  label42.visible:= false;
    501001..540000: label42.visible:=false;
  else
   begin  // CW
    if RadioGroup10.itemindex in[3] then // if CW
     begin label42.visible:= true;
     label42.caption:= ' Out of Phone Band ';
     end;
   end;
  end;//case
 end;//if
```

and VOX settings for PSK, SSB etc. for easy recall.

Settings stored in a file will save you time when going back and forth from PSK and SSB activities and may save your transceiver amplifier transistors from burn out.

Since this article was written, I discovered the excellent, free, COM control "Omni-Rig" by Alex, VE3NEA. The control simplifies writing code for rig control programs with either *Delphi* or *Visual Basic*. See **www.dxatlas.com/omnirig/** or the WB5KIA Web site for more information.

I described ways for beginners to start programming and suitable compilers for the implementation of these projects in the February, March and April 2003 issues of *QST*. Supplementary information may be available on the WB5KIA Web site.

Acknowledgments

Networks for 8-Direction 4-Square Arrays

By Al Christman, K3LC

After writing an article describing a 4-square array that could fire in 8 directions,[1] I thought it might be helpful to review the steps involved in designing the passive networks that are required to make the array work properly.

This article shows how to measure the self-impedances of the elements and utilize this data to calculate the corresponding values for the mutual and driving-point impedances. Transmission-line equations are then used to transform the relevant parameters from the antenna feed-points to the input ends of the quarter-wave phasing lines. Next, W7EL-style[2] networks are designed which provide the necessary excitation voltages, along with impedance-matching networks to allow low-SWR operation from a 50-Ω source.

Element Description

The analysis begins with a simple computer model for a four-square array, with the side-length of the square fixed at 0.25 wavelength. A frequency of 3.79 MHz in the 80-meter band was selected for the simulation, which was performed using *EZNEC*.[3] Full-size quarter-wave vertical elements made from # 12 AWG copper wire were placed over "average" soil with a conductivity of 5 milliSiemens per meter and a dielectric constant of 13. *MiniNEC*-style ground was utilized to minimize computation time.

It is very important that all four elements of the array be as similar as possible in terms of their input impedance, so the performance of the array will be identical in all directions of fire. This is easy to do on the computer, but more difficult in real life. By adjusting the length (height) of each monopole, the same value of input reactance can be achieved for all four of the elements, at some particular frequency. Usually, the goal is to achieve resonance (zero reactance) at the desired center frequency within the operating band. Equalizing the input resistances are accomplished by adding more radials to the ground system of those elements whose driving-point resistances are larger than the others. I made the height of each monopole slightly different (63.05,
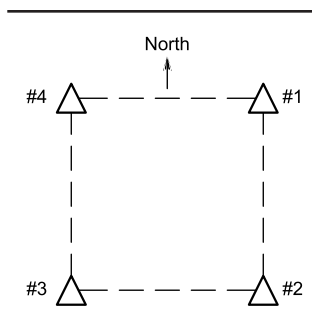
[1]Notes appear on page 48.

Grove City College
100 Campus Drive
Grove City, PA 16127-2104

63.15, 63.25, and 63.35 feet) in my *EZNEC* model, so the resulting impedances would more-closely resemble data gleaned from an actual antenna system.

Measuring the Self-Impedances

The first step in the design process is measuring the self-impedance of each element, under a variety of conditions. Figure 1 shows a plan view of the array, with the elements numbered consecutively, beginning with the northeast monopole. It is helpful to have an assistant available for this series of measurements, but they can be made by a lone individual, if necessary. Initially the base (feed-point) of each element is open-circuited, which virtually removes those elements from the picture, electrically speaking. Using an impedance bridge or similar instrument, the impedance seen at the base of element #1 (at the frequency of interest) is measured and recorded as Z_{11}; this value is the "self impedance" of element #1. Next the feed-point of element #2 is temporarily short-circuited, perhaps by using a small jumper-wire with alligator clips at both ends. (In other words, the base of element #2 is connected directly to its ground screen.) The impedance at the base of element #1 is measured again, but this time the numerical value is recorded as $Z_{1(2)}$. Now the short-circuit jumper is moved to the base of element #3, and the corresponding input impedance seen at the base of element #1 is measured yet again, with the value recorded as $Z_{1(3)}$. The short-circuit jumper is then moved to the base of element #4, and the corresponding input impedance seen at the base of element #1 is measured one last time, the value here being recorded as $Z_{1(4)}$. We now have four impedance measurements listed on our data-sheet, all of them having been made at the feed-point of element #1.

The entire process described above is then repeated, but

Figure 1—Plan view of 4-square array. Each side has a length of 0.25-WL at f = 3.79 MHz, which is approximately 64.88 feet.

Table 1

"Measured" Impedance Data for the Four-Square Array discussed in the text. The tallest monopole (#1) has a height of 63.35 feet, while the shortest (#4) is 63.05 feet tall. The frequency is 3.79 MHz.

Element #1	Element #2
Z_{11} = 36.44 + j 2.137 Ω	Z_{22} = 36.28 + j 0.766 Ω
$Z_{1(2)}$ = 32.84 + j 17.92 Ω	$Z_{2(1)}$ = 33.29 + j 16.58 Ω
$Z_{1(3)}$ = 45.28 + j 9.507 Ω	$Z_{2(3)}$ = 32.11 + j 16.34 Ω
$Z_{1(4)}$ = 31.66 + j 17.59 Ω	$Z_{2(4)}$ = 44.78 + j 8.429 Ω

Element #3	Element #4
Z_{33} = 36.13 - j 0.602 Ω	Z_{44} = 35.97 - j 1.977 Ω
$Z_{3(1)}$ = 45.39 + j 6.015 Ω	$Z_{4(1)}$ = 33.01 + j 13.70 Ω
$Z_{3(2)}$ = 32.56 + j 15.05 Ω	$Z_{4(2)}$ = 44.96 + j 4.967 Ω
$Z_{3(4)}$ = 31.39 + j 14.72 Ω	$Z_{4(3)}$ = 31.83 + j 13.47 Ω

the impedance bridge is now placed at the feed-point of element #2 for this sequence. For the first measurement, the remaining three elements are left open-circuited at their input terminals (which yields Z_{22}) but then each of the other three monopoles is short-circuited, one at a time, so the remaining three measurements can be taken, giving us values for $Z_{2(1)}$, $Z_{2(3)}$, and $Z_{2(4)}$.

As before, the complete four-measurement process is then performed again at the base of element #3, and finally at the base of element #4. When completed, you will have 16 impedance values written on your data-sheet. Table 1 lists the values I obtained from my "computer array." To simulate an open-circuit, I placed a 0-ampere current source at the feed-point, while a short-circuit was modeled by a 0-volt voltage source. In Table 1, notice that all four self-*resistances* are very similar, with a value close to 36 Ω, while the self-*reactances* span the range from roughly +2 to -2 Ω. A height difference of just 0.3 foot (from 63.35' to 63.05') yielded a reactance difference of around 4 Ω, while the corresponding resistances varied by only about 0.5 Ω. The tallest element has the most-positive value of reactance, and also the largest resistance.

Looking at the data for element #1, we can see that $Z_{1(2)}$ is similar to $Z_{1(4)}$, which makes sense because elements 2 and 4 are both spaced a quarter-wavelength away from element #1. However, $Z_{1(3)}$ is noticeably different from the other two values, because element #3 is spaced farther away from element #1.

Calculating the Mutual Impedances

As the name implies, mutual impedance is the impedance which exists "between" any pair of elements. I will carry out one of these calculations in detail, to show how it is done, and then just list the formulas which are used for the others. In general, the mutual impedance between any two elements ("i" and "j") is given as: $Z_{ij} = $ sqrt $\{Z_{jj}[Z_{ii} - Z_{i(j)}]\}$

This expression is correct for base-fed quarter-wave vertical elements spaced from 0.15 to 0.4 wavelengths apart. Therefore, the mutual impedance between elements 1 and 2, which is calculated by using the data gathered when element #1 was the reference, is: $Z_{12} = $ sqrt $\{Z_{22}[Z_{11} - Z_{1(2)}]\}$

We must convert Z_{22} from rectangular to polar form, so that $Z_{22} = 36.28 + j\ 0.766\ \Omega = 36.288 < 1.2095º\ \Omega$. Most calculators have built-in functions to perform this conversion. $Z_{12} = $ sqrt $\{36.288 < 1.2095º[(36.44 + j\ 2.137) - (32.84 + j\ 17.92)]\} = $ sqrt $\{36.288 < 1.2095º[3.60 - j\ 15.783]\}$

Now we must convert $(3.60 - j\ 15.783\ \Omega)$ from rectangular form back to polar form, yielding $16.188 < -77.151º\ \Omega$. $Z_{12} = $ sqrt $\{36.288 < 1.2095º[16.188 < -77.151º]\}$

To obtain the product, we multiply the magnitudes and add the angles, to get: $Z_{12} = $ sqrt $\{587.4433 < -75.9415º\}$

To find the square root of this expression, we take the square root of the magnitude, and divide the phase-angle by two, which gives us: $Z_{12} = 24.237 < -37.971º\ \Omega$, or $Z_{12} = 19.11 - j\ 14.91\ \Omega$, in rectangular form.

The formulas for calculating the other 11 mutual impedances are:

$Z_{13} = $ sqrt $\{Z_{33}[Z_{11} - Z_{1(3)}]\}$

$Z_{14} = $ sqrt $\{Z_{44}[Z_{11} - Z_{1(4)}]\}$

$Z_{21} = $ sqrt $\{Z_{11}[Z_{22} - Z_{2(1)}]\}$

$Z_{23} = $ sqrt $\{Z_{33}[Z_{22} - Z_{2(3)}]\}$

$Z_{24} = $ sqrt $\{Z_{44}[Z_{22} - Z_{2(4)}]\}$

$Z_{31} = $ sqrt $\{Z_{11}[Z_{33} - Z_{3(1)}]\}$

$Z_{32} = $ sqrt $\{Z_{22}[Z_{33} - Z_{3(2)}]\}$

$Z_{34} = $ sqrt $\{Z_{44}[Z_{33} - Z_{3(4)}]\}$

$Z_{41} = $ sqrt $\{Z_{11}[Z_{44} - Z_{4(1)}]\}$

$Z_{42} = $ sqrt $\{Z_{22}[Z_{44} - Z_{4(2)}]\}$

$Z_{43} = $ sqrt $\{Z_{33}[Z_{44} - Z_{4(3)}]\}$

All of the resulting mutual impedances are listed in Table 2, along with the four self-impedances, which are repeated for completeness. Be very careful while performing these mutual-impedance calculations, because it's easy to make a mistake. While reviewing the Table, note that, in every case, Z_{ij} is virtually identical to Z_{ji}, which is a good check to verify that you carried out the mathematics correctly.

Table 2

Self- and Mutual-Impedance Data for the 4-Square Array discussed in the text. The frequency is 3.79 MHz.

Element #1	Element #2
$Z_{11} = 36.44 + j\ 2.137\ \Omega$	$Z_{22} = 36.28 + j\ 0.766\ \Omega$
$Z_{12} = 19.11 - j\ 14.91\ \Omega$	$Z_{21} = 19.11 - j\ 14.91\ \Omega$
$Z_{13} = 6.785 - j\ 19.23\ \Omega$	$Z_{23} = 19.02 - j\ 14.85\ \Omega$
$Z_{14} = 19.03 - j\ 14.85\ \Omega$	$Z_{24} = 6.759 - j\ 19.15\ \Omega$

Element #3	Element #4
$Z_{33} = 36.13 - j\ 0.602\ \Omega$	$Z_{44} = 35.97 - j\ 1.977\ \Omega$
$Z_{31} = 6.788 - j\ 19.22\ \Omega$	$Z_{41} = 19.02 - j\ 14.85\ \Omega$
$Z_{32} = 19.03 - j\ 14.85\ \Omega$	$Z_{42} = 6.759 - j\ 19.14\ \Omega$
$Z_{34} = 18.95 - j\ 14.79\ \Omega$	$Z_{43} = 18.95 - j\ 14.79\ \Omega$

Corner-Fire: Calculating the Driving-Point Impedances

The driving-point impedance is the value of impedance (the ratio of voltage to current) that exists at the feed-point of an element while it is operating as a part of the array, with power flowing. This impedance cannot be directly measured using an ordinary antenna bridge. However, a specialized (and relatively expensive) instrument, often called an "operating impedance bridge," is designed specifically for this type of application. Nevertheless, we now have all the impedance data that is needed to *calculate* the driving-point impedances, provided that we know the desired base current for each element of the array.

I will give the equations for all four elements, but will carry out a detailed analysis for only the first one. Let's assume that we want the array to fire through the corners of the square (along the diagonals), in typical 4-square fashion. Again referring to Figure 1, if we want the array to fire toward the northeast, then the requisite feed-point currents will have relative magnitudes and phase-angles as follows:

$I_1 = 1 < -180º\ = -1 + j\ 0\ A$ (front element)

$I_2 = I_4 = 1 < -90º\ = 0 - j\ 1\ A$ (side elements)

$I_3 = 1 < 0º\ = 1 + j\ 0\ A$ (back element)

If these relative currents (the actual current magnitudes depend upon the output power of the transmitter) are flowing into the feed-points of the four vertical monopoles, then the driving-point impedance of element #1 is:

$Z_1 = Z_{11} + (I_2/I_1)Z_{12} + (I_3/I_1)Z_{13} + (I_4/I_1)Z_{14}$
  $= (36.44 + j\ 2.137) + (-j1/-1)(19.11 - j\ 14.91) + (1/-1)$
  $(6.785 - j\ 19.23) + (-j1/-1)(19.03 - j\ 14.85)$
  $= (36.44 + j\ 2.137) + (j)(19.11 - j\ 14.91) + (-1)$
  $(6.785 - j\ 19.23) + (j)(19.03 - j\ 14.85)$
  $= (36.44 + j\ 2.137) + (j\ 19.11 + 14.91) + (-6.785 + j\ 19.23)$

+ (j 19.03 + 14.85)
= (36.44 + 14.91 - 6.785 + 14.85) + j(2.137 + 19.11 + 19.23 + 19.03)

$Z_1 = 59.42 + j\,59.51\ \Omega = 84.091{<}45.044°\ \Omega$

The formulas and calculated results for the other three elements are:

$Z_2 = Z_{22} + (I_1/I_2)Z_{21} + (I_3/I_2)Z_{23} + (I_4/I_2)Z_{24}$

$Z_2 = 42.98 - j\,18.47 = 46.781{<}{-}23.260°\ \Omega$

$Z_3 = Z_{33} + (I_1/I_3)Z_{31} + (I_2/I_3)Z_{32} + (I_4/I_3)Z_{34}$

$Z_3 = -0.298 - j\,19.36 = 19.362{<}{-}90.882°\ \Omega$

$Z_4 = Z_{44} + (I_1/I_4)Z_{41} + (I_2/I_4)Z_{42} + (I_3/I_4)Z_{43}$

$Z_4 = 42.67 - j\,21.19 = 47.640{<}{-}26.406°\ \Omega$

Notice that in all four of the self-impedance equations the currents always appear as *ratios*. For this reason, we don't need to know the *absolute* magnitudes of the currents; we only need to know their *relative* magnitudes. The driving-point impedances Z_2 and Z_4, for the two "side" elements, are very similar to each other, which is what we expected. Also, the driving-point *resistance* of the "back" element (#3) is slightly negative, which means this element is not receiving power from the transmitter, but is actually sending a small amount of power back toward the source.

For comparison, if I simply insert the desired currents into my *EZNEC* model, the computer predicts the following driving-point impedances:

$Z_1 = 59.42 + j\,59.50\ \Omega$

$Z_2 = 42.98 - j\,18.46\ \Omega$

$Z_3 = -0.302 - j\,19.35\ \Omega$

$Z_4 = 42.67 - j\,21.20\ \Omega$

All of these values are extremely close to the ones we calculated, which makes sense, because we based our calculations on impedance "measurements" that we derived from the computer program itself.

Current Forcing

Roy Lewallen, W7EL, has shown that low-loss quarter-wave sections of transmission line have an interesting feature: "The magnitude of the current out of a ¹/₄-WL transmission line is equal to the input voltage divided by the characteristic impedance of the line, independent of the load impedance. In addition, the phase of the output cur-rent lags the phase of the input voltage by 90°, also independent of the load impedance." He further states: "The properties of ¹/₂-WL lines are also useful. Since the current out of a ¹/₂-WL line equals the input current shifted 180°, regardless of the load impedance, any number of half wavelengths of line may be added to the basic ¹/₄-WL, and the current and phase 'forcing' property will be preserved."[4] It is important to remember that this "current forcing" technique works best when the losses in the transmission lines are as low as possible.

Thus, if we feed each element of our four-square array through a 0.25-WL section of low-loss coax, then the magnitude of the current at the output end (the antenna feedpoint) is equal to the magnitude of the voltage at the input end, divided by the characteristic impedance of the line. Also, the phase-angle of the current at the output end lags the phase-angle of the input voltage by 90°, which is the electrical length of the cable.

In our case, we have decided to drive the four elements in the array with equal-magnitude currents, using progressive 90° phase-shifts. What we need, then, is a network that will generate two voltages that are equal in magnitude, but separated by 90° in phase angle. The *leading* voltage from this network can be used to drive the ¹/₄-WL phasing-line connected to the back element of the array, since this element has the *leading* current phase-angle. And, this same voltage can also drive the front element of the array (whose current lags that of the back element by 180°) by connecting an extra ¹/₂-WL of coax in series with the ¹/₄-WL phasing-line that extends to the front element. The *lagging* voltage from our network can be used to drive the ¹/₄-WL phasing-lines connected to the two side elements of the array, since their currents *lag* that of the back element by 90°. Figure 2 illustrates the concept.

Because the quarter-wave phasing lines are assumed to be lossless, we can use a few basic transmission-line equations to calculate the impedance, voltage, and current that will be present at the input ends of these lines:

$Z_{in} = Z_o{}^2/Z_a$

$V_{in} = jI_aZ_o$

$I_{in} = jV_a/Z_o = jI_aZ_a/Z_o$

where Z_o is the characteristic impedance of the ¹/₄-WL phasing lines and Z_a, I_a, & V_a are the impedance, current, and voltage at the output end of the line (at the antenna

$I_2 = I_4 = \dfrac{V_1}{Z_0}\ \underline{/{-}90°}$

$I_3 = \dfrac{V_1}{Z_0}\ \underline{/0°}$ } Element Currents at Antenna Input Terminals

$I_1 = \dfrac{V_1}{Z_0}\ \underline{/{-}180°}$
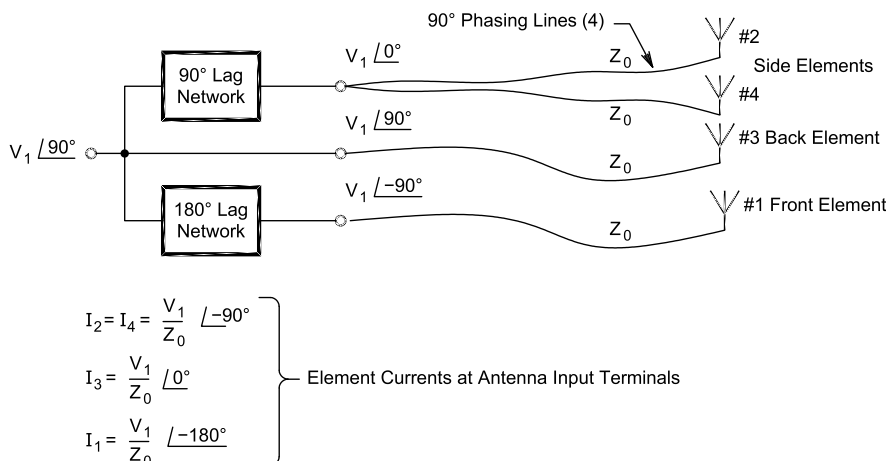
Figure 2—A block diagram of the circuit which will be designed to enable the array to fire through the corners of the 4-square.

feed-point). If we utilize 75-Ω CATV hard-line for the quarter-wave phasing lines, then:

$$Z_{in} = Z_o^2/Z_a = (75)^2/Z_a = 5625/Z_a \ \Omega$$

$$V_{in} = j\,I_a Z_o = j\,I_a(75) \ V$$

$$I_{in} = j\,V_a/Z_o = j\,I_a Z_a/Z_o = j\,I_a Z_a/(75) \ A$$

We will utilize the currents specified previously:

$I_1 = 1<\text{-}180^o = \text{-}1 + j\,0 \ A$		(front element)
$I_2 = I_4 = 1<\text{-}90^o = 0 - j\,1 \ A$		(side elements)
$I_3 = 1<0^o = 1 + j\,0 \ A$		(back element)

and the driving-point impedances calculated earlier:

$$Z_1 = 59.42 + j\,59.51 = 84.091<45.044^o \ \Omega$$

$$Z_2 = 42.98 - j\,18.47 = 46.781<\text{-}23.260^o \ \Omega$$

$$Z_3 = \text{-}0.298 - j\,19.36 = 19.362<\text{-}90.882^o \ \Omega$$

$$Z_4 = 42.67 - j\,21.19 = 47.640<\text{-}26.406^o \ \Omega$$

We can now calculate the parameters at the input ends of the four phasing lines. I will do the math for phasing-line #1, and will use the "prime" symbol (') to differentiate these parameters from those measured at the output ends of the lines:

$$Z_1' = 5625/Z_a = 5625/Z_1 = 5625/(84.091<45.044^o)$$
$$= 66.892<\text{-}45.044^o$$

$$Z_1' = 47.26 - j\,47.34 \ \Omega$$

$$V_1' = j\,I_a(75) = j\,I_1(75) = (1<90^o)(1<\text{-}180^o)(75) = 75<\text{-}90^o \ V$$

$$V_1' = 0 - j\,75 \ V$$

$$I_1' = j\,I_a Z_a/(75) = j\,I_1 Z_1/(75) = (1<90^o)(1<\text{-}180^o)$$
$$(84.091<45.044^o)/(75)$$

$$I_1' = 1.121<\text{-}44.956^o = 0.793 - j\,0.792 \ A$$

To check our work, we can use Ohm's Law. Since V = IZ, we should get the same answer for V_1' (as shown above) when we multiply I_1' by Z_1'. It works!

Table 3 lists all the results for the four 75-Ω ¹/₄-wave phasing lines. There are several important points to note here:

(1) All of the input voltages have the same magnitude, 75.0 V, although the phase-angles are different.

(2) The voltages (V_2' and V_4') at the input ends of the phasing lines leading to the two "side" elements both have the same phase-angle, so these two points can safely be connected together, in parallel, without upsetting circuit operation.

(3) The voltage (V_3') at the input end of the phasing line leading to the "back" element *leads* both V_2' and V_4' by 90°.

(4) The voltage (V_1') at the input end of the phasing line leading to the "front" element *lags* V_3' by 180°.

(5) All of the input voltages lead their corresponding output (antenna feed-point) currents by 90°.

A word of caution must be expressed at this point. The input parameters discussed here, and displayed in Table 3, are really correct only when the array is firing northeast. Because none of the four vertical monopoles are exactly identical, the driving-point impedances seen at the terminals of the "front," "back," and "side" elements will vary slightly as the direction of fire is changed. Table 4 shows the *EZNEC*-predicted results for all four cases,

when the array is firing through the corners of the square.

The Table also includes the average impedance value for each direction of fire. Notice that the average value is identical for both of the "side" elements, even though none of the eight values are exactly the same. If we want to favor one particular direction of fire, we can choose to use the driving-point impedances for that specific direction when designing the phase-shifting and impedance-matching networks. Or, we can decide to use the average values, to achieve balanced performance in all four directions of fire.

Designing the Phase-shift Network

As mentioned before, we need a network that will generate two voltages that are equal in magnitude but 90° apart in phase-angle. We also need a device that will

---

Table 3

Impedance, Voltage, and Current at the input ends of the four 0.25-WL loss-less 75-Ω phasing lines, when the array is firing through the corners of the square.

Element #1 phasing line

$Z_1' = 47.26 - j\,47.34 \ \Omega$
$Z_1' = 66.892<\text{-}45.044^o \ \Omega$
$V_1' = 75.0<\text{-}90^o \ V$
$I_1' = 0.793 - j\,0.792 \ A$

Element #2 phasing line

$Z_2' = 110.47 + j\,47.48 \ \Omega$
$Z_2' = 120.241<23.26^o \ \Omega$
$V_2' = 75.0<0^o \ V$
$I_2' = 0.573 - j\,0.246 \ A$

Element #3 phasing line

$Z_3' = \text{-}4.47 + j\,290.48 \ \Omega$
$Z_3' = 290.518<90.882^o \ \Omega$
$V_3' = 75.0<90^o \ V$
$I_3' = 0.258 - j\,0.00397 \ A$

Element #4 phasing line

$Z_4' = 105.75 + j\,52.51 \ \Omega$
$Z_4' = 118.073<26.406^o \ \Omega$
$V_4' = 75.0<0^o \ V$
$I_4' = 0.569 - j\,0.2825 \ A$

Table 4

Driving-point Impedances for the 4-Square Array, as a function of the direction of fire, when beaming through the corners of the square.

	Driving-point Impedance (Ω)			
Direction of Fire	Front Element	Back Element	Left-side Element	Right-Side Element
Northeast	59.42 +j 59.50	-0.302 -j 19.35	42.67 -j 21.20	42.98 -j 18.46
Southeast	59.29 +j 58.04	-0.434 -j 20.80	43.17 -j 17.17	42.85 -j 19.91
Southwest	58.98 +j 56.59	-0.109 -j 16.77	43.10 -j 18.30	42.79 -j 21.04
Northwest	58.85 +j 55.14	-0.242 -j 18.22	42.97 -j 19.75	43.29 -j 17.01
Average	59.14 +j 57.32	-0.272 -j 18.78	42.98 -j 19.10	42.98 -j 19.10
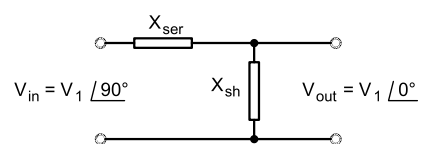
Figure 3—A series-input L-network which produces two voltages that are equal in magnitude but separated by 90° in phase-angle. This is the "90° lag network."

produce a 180º phase-lag. (Refer again to the block diagram shown in Figure 2.)

We have several options when it comes to implementing the 180º phase-lag "network." As described earlier, we can simply insert a half-wave section of low-loss coaxial cable. Or, we can build a 1:1 "un-un" transformer whose primary and secondary windings are connected out-of-phase.

For the 90º phase-lag network, we turn to the fine work of W7EL.[2] A series-input L-network, as drawn in Figure 3, will perform admirably. The component values are derived from these equations:

$X_{ser} = Z_o^2/(R_c + R_d)$

$X_{sh} = Z_o^2/[(X_c + X_d) - (R_c + R_d)]$

where R_c, R_d, X_c, and X_d are the *driving-point* resistances and reactances of the two elements whose phasing lines are connected to the output of the 90º phase-lag network. In this case, these are the two "side" elements, #2 and #4, so the equations become:

$X_{ser} = Z_o^2/(R_2 + R_4)$

$X_{sh} = Z_o^2/[(X_2 + X_4) - (R_2 + R_4)]$

Let's assume that we want to optimize the performance of the 4-square when it is firing northeast, so we will use the "northeast" driving-point impedance data from Table 4 to compute the component values.

$X_{ser} = Z_o^2/(R_2 + R_4) = (75)^2/(42.67 + 42.98) = 5625/85.65$

$X_{ser} = 65.67 \ \Omega$

At f=3.79 MHz, this positive reactance corresponds to an inductance of 2.76 µH.

$X_{sh} = Z_o^2/[(X_2 + X_4) - (R_2 + R_4)]$

$X_{sh} = (75)^2/[(-21.20 -18.46) - (42.67 + 42.98)] = 5625/(-125.31)$

$X_{sh} = -44.89 \ \Omega$

At f=3.79 MHz, this negative reactance corresponds to a capacitance of 936 pF.

Our next task is to determine the voltage and the impedance at the *input* end of the 90º phase-lag network (see Figure 4). The impedance at the output end, looking toward the load, is the parallel combination of Z_2' and Z_4' (the impedances at the input ends of the two quarter-wave phasing lines which lead to the "side" elements). This impedance (Z_{ss}) is determined by using the parallel-resistor rule (result = product/sum):

$Z_{ss} = (Z_2')ll(Z_4') = [(Z_2')(Z_4')]/(Z_2' + Z_4')$

The product is: $[(Z_2')(Z_4')] =$
$(120.241{<}23.26º)(118.073{<}26.406º) = 14,197.21{<}49.666º$

The sum is: $(Z_2' + Z_4') = (110.47 + j\ 47.48) + (105.75 + j\ 52.51) = 216.22 + j\ 99.99 = 238.221{<}24.818º$

So, $Z_{ss} = (Z_2')ll(Z_4') = [(Z_2')(Z_4')]/(Z_2' + Z_4') = (14,197.21{<}49.666º)/(238.221{<}24.818º)$

$Z_{ss} = 59.597{<}24.848º = 54.08 + j\ 25.04 \ \Omega$

The current (I_{ss}) flowing out of the network into the quarter-wave phasing lines to the two "side" elements is:

$I_{ss} = I_2' + I_4' = (0.573 - j\ 0.246) + (0.569 - j\ 0.2825)$

$I_{ss} = 1.142 - j\ 0.5285 = 1.258{<}-24.834º \ A$

Next, we can see that the voltage (V_{ss}) across the output terminals of the network is the same as the voltage at the input ends of the two quarter-wave phasing lines that lead to the "side" elements:

$V_{ss} = V_2' = V_4' = 75{<}0º = 75 + j\ 0 \ V$

This same voltage, V_{ss}, also appears across the shunt capacitor, which has a reactance $X_{sh} = 44.89 \ \Omega$, so that its impedance is $Z_{sh} = -jX_{sh}$. Thus, the current through the shunt capacitor is found using Ohm's Law:

$I_{sh} = V_{ss}/Z_{sh} = V_{ss}/(-jX_{sh}) = (75{<}0º)/(44.89{<}-90º) = 1.671{<}90º$

$I_{sh} = 0 + j\ 1.671 \ A$

$I_{ss} = I_2' + I_4' = 1.142 - j\ 0.5285$ A.

$Z_{ss} = Z_2' \| Z_4' = 54.08 + j\ 25.04 \ \Omega$

$V_{ss} = V_2' = V_4' = 75 \underline{/0º}$ V.

$I_{sh} = 0 + j\ 1.671$ A.

$I_{ser} = 1.616 \underline{/45.025º}$ A.

$Z_p = Z_{sh} \| Z_{ss} = 32.84 - j\ 32.836 \ \Omega$

$Z_{ss}' = Z_{ser} + Z_p = 32.84 + j\ 32.83 \ \Omega$

$Z_{ser} = 65.67 \underline{/90º} \ \Omega$

$Z_{sh} = 44.89 \underline{/-90º} \ \Omega$

$V_{ser} = -75.073 + j\ 75.007$ V.

$V_{sh} = V_{ss} = 75 \underline{/0º}$ V.

Figure 4—Circuit parameters within a 90º lag sub-network that is designed to enable the array to fire through the corners of the 4-square.
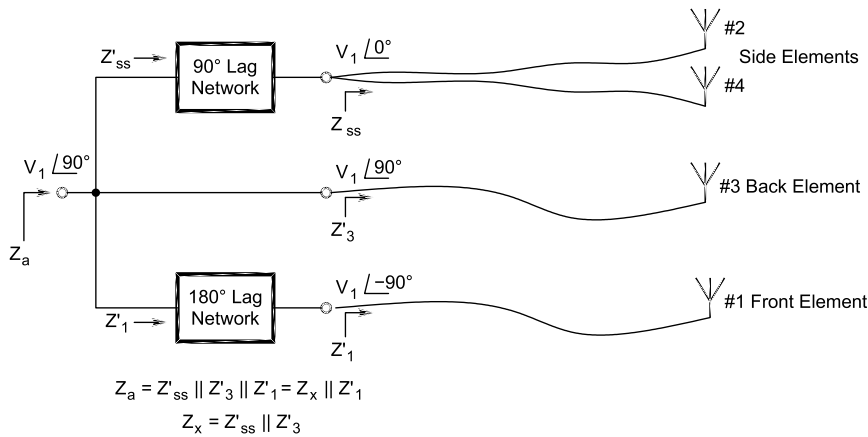
Figure 5—The block diagram of Figure 2, with impedance data added.

$Z_a = Z'_{ss} \| Z'_3 \| Z'_1 = Z_x \| Z'_1$

$Z_x = Z'_{ss} \| Z'_3$

The current (I_{ser}) flowing through the series inductor is the sum of the current flowing into the shunt capacitor and the current flowing into the two 90° phasing lines:

$I_{ser} = I_{sh} + I_{ss} = (0 + j\,1.671) + (1.142 - j\,0.5285)$

$I_{ser} = 1.142 + j\,1.143 = 1.616{<}45.025° \text{ A}$

The voltage (V_{ser}) across the series inductor is found from Ohm's Law:

$V_{ser} = I_{ser}(Z_{ser}) = I_{ser}(jX_{ser}) = 1.616{<}45.025°(65.67{<}90°)$

$V_{ser} = 106.123{<}135.025° = -75.073 + j\,75.007 \text{ V}$

The voltage (V_{ss}') across the input terminals of the 90° phase-lag network is the sum of the voltage across the series inductor and the voltage across the shunt capacitor. Also, it is apparent that the capacitor voltage $V_{sh} = V_{ss}$.

$V_{ss}' = V_{ser} + V_{sh} = V_{ser} + V_{ss} = (-75.073 + j\,75.007) + (75 + j\,0)$

$V_{ss}' = -0.073 + j\,75.007 = 75.007{<}90.056° \text{ V}$

Remember that our goal for this network was for it to produce two voltages that were equal in magnitude but 90° apart in phase-angle. The "perfect" value for V_{ss}' would be 75.0<90.0° V, so our answer is extremely close to the desired result; the difference is probably due to round-off errors.

We have already determined that the impedance at the output terminals of the network, looking toward the load, is Z_{ss}. The shunt capacitor is directly in parallel with Z_{ss}, so their parallel combination is:

$Z_p = (Z_{sh})\text{ll}(Z_{ss}) = [(Z_{sh})(Z_{ss})]/(Z_{sh} + Z_{ss})$

$\quad = [(44.89{<}{-}90°)(59.597{<}24.848°)]/[({-}j\,44.89) + (54.08 + j\,25.04)]$

$\quad = (2,675.309{<}{-}65.152°)/(54.08 - j\,19.85)$

$\quad = (2,675.309{<}{-}65.152°)/(57.608{<}{-}20.156°)$

$Z_p = 46.440{<}{-}44.996° = 32.84 - j\,32.836 \ \Omega$

The impedance (Z_{ss}') looking into the input terminals of the network is the combination of Z_{ser} in series with Z_p:

$Z_{ss}' = Z_{ser} + Z_p = (j\,65.67) + (32.84 - j\,32.836)$

$Z_{ss}' = 32.84 + j\,32.83 = 46.44{<}44.995° \ \Omega$

Figure 5 is similar to Figure 2, but emphasizes the impedances and voltages which exist within the networks that
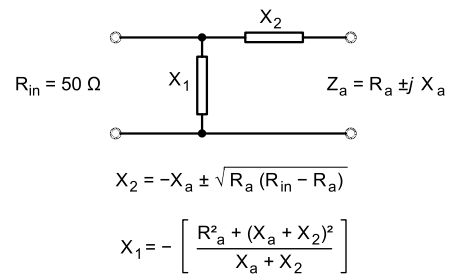
Figure 6—A shunt-input L-network used for impedance-matching. X_2 must be calculated first.

are used to allow the array to fire through the corners of the square. We can see that the input impedance Z_a is actually the parallel combination of three impedances. We already know the value of Z_{ss}' and the value of Z_3' so we combine them using the parallel-resistor formula (I will omit the math since we've done this before) to find:

$Z_x = (Z_{ss}')\text{ll}(Z_3') = (46.44{<}44.995°)\text{ll}(290.518{<}90.882°)$

$Z_x = 41.564{<}50.888° = 26.22 + j\,32.25 \ \Omega$

The 180° lag network simply "repeats" the impedance seen at its output, so the impedance at its input is still Z_1'. This impedance is in parallel with the impedance Z_x listed above, giving us the following expression for Z_a:

$Z_a = (Z_x)\text{ll}(Z_1') = (41.564{<}50.888°)\text{ll}(66.892{<}{-}45.044°)$

$Z_a = 37.064{<}17.443° = 35.36 + j\,11.11 \ \Omega$

This Z_a is the impedance which we would like to match to 50 Ω, so we can operate with a low SWR on the main transmission line that extends from our outdoor "phase/match box" back to the radio room.

Designing the Impedance-matching Network

A shunt-input L-network can be utilized to transform Z_a to a pure resistance of 50 Ω, as shown in Figure 6. The series reactance X_2 must be determined first, as follows:[5]

$X_2 = - X_a +/-$ sqrt $[R_a(R_{in} - R_a)]$ where R_{in} is the desired input resistance (50 Ω), and R_a & X_a are the resistance and reactance appearing at the load end. Plugging in the appropriate values, we get:

$X_2 = -\,11.11 +/-$ sqrt $[35.36(50 - 35.36)]$
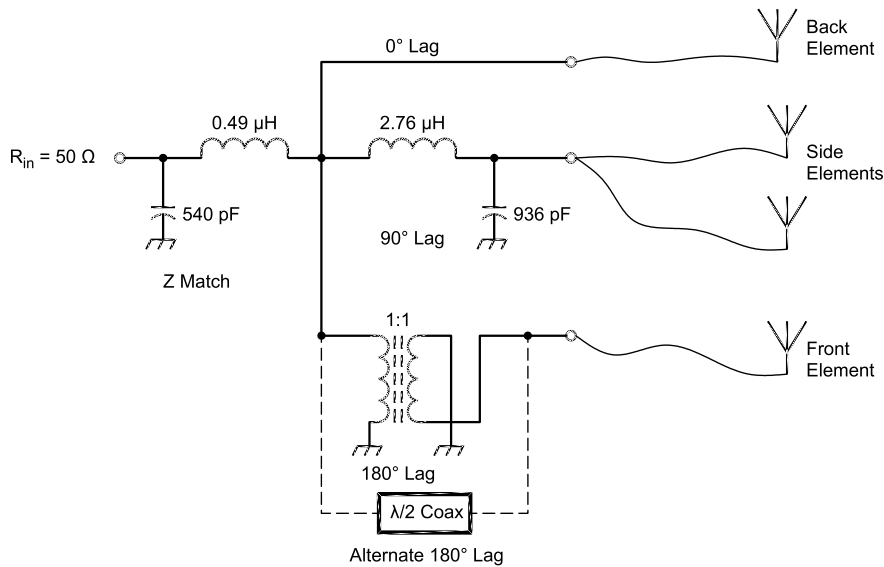
Figure 7—The complete circuit which enables the array to fire through the corners of the 4-square (direction-switching relays are not shown).

=- 11.11 +/- sqrt [35.36(14.64)] = - 11.11 +/- sqrt [517.67]

X_2 =- 11.11 +/- 22.75 = *either* - 33.86 Ω *or* + 11.64 Ω

Now we have a choice of using either a capacitor (reactance = - 33.86 Ω) or an inductor (reactance = + 11.64 Ω) for X_2. I prefer to use low-pass networks whenever possible (series inductors and shunt capacitors) so I will select X_2 = + 11.64 Ω. At a frequency of 3.79 MHz, this positive reactance corresponds to an inductance of 0.49 μH.

To calculate the shunt reactance, we use this equation:

X_1 = - {[$(R_a)^2$ + $(X_a + X_2)^2$]/$(X_a + X_2)$} so that X_1 = - {[$(35.36)^2$ + $(11.11 + 11.64)^2$]/$(11.11 + 11.64)$} = - {[(1250.33) + $(22.75)^2$]/(22.75)} = - {[(1250.33) + (517.56)]/(22.75)} = - (1767.89)/(22.75)

X_1 = - 77.71 Ω

At a frequency of 3.79 MHz, this negative reactance corresponds to a capacitance of 540 pF.

Figure 7 shows the completed circuit, excluding the relays that are needed to change the direction of fire. This information will be provided later.

Side-Fire: Calculating the Driving-Point Impedances

Now let's assume that we want the array to beam through the sides of the square, to give us an additional 4 directions of fire. Referring to Figure 1, if we want the array to beam toward the east, then the requisite feed-point currents will have relative magnitudes and phase-angles as follows:

$I_1 = I_2$ = 1<-90° = 0 - j 1 A   (front elements)

$I_3 = I_4$ = 1<0° = 1 + j 0 A   (back elements)

We can use all of the same values for the self-impedances and mutual-impedances from before, as displayed in Table 2. If the currents listed above flow into the feed-points of the four vertical monopoles, then the driving-point impedance of element #1 is:

$Z_1 = Z_{11} + (I_2/I_1)Z_{12} + (I_3/I_1)Z_{13} + (I_4/I_1)Z_{14}$

Table 5
Driving-point Impedances for the 4-Square Array, as a function of the direction of fire, when beaming through the sides of the square.

Direction of Fire	Driving-point Impedance (Ω)			
	Front Right Element	Front Left Element	Back Right Element	Back Left Element
North	89.61 +j 13.18	88.93 +j 8.875	21.25 -j 39.95	21.14 -j 41.18
South	89.17 +j 10.28	89.37 +j 11.78	21.06 -j 42.53	21.33 -j 38.61
East	89.39 +j 11.64	89.63 +j 13.04	20.99 -j 41.20	20.92 -j 42.55
West	88.91 +j 9.017	89.15 +j 10.42	21.47 -j 38.59	21.39 -j 39.93
Average	89.27 +j 11.03	89.27 +j 11.03	21.19 -j 40.57	21.20 -j 40.57

= (36.44 + j 2.137) + (-j1/-j1)(19.11 - j 14.91) + (1/-j1)(6.785 - j 19.23) + (1/-j1)(19.03 - j 14.85)

= (36.44 + j 2.137) + (1)(19.11 - j 14.91) + (j)(6.785 - j 19.23) + (j)(19.03 - j 14.85)

= (36.44 + j 2.137) + (19.11 - j 14.91) + (j 6.785 + 19.23) + (j 19.03 + 14.85)

= (36.44 + 19.11 + 19.23 + 14.85) + j(2.137 - 14.91 + 6.785 + 19.03)

Z_1 = 89.63 + j 13.04 Ω = 90.574<8.279° Ω

The formulas and calculated results for the other three elements are:

$Z_2 = Z_{22} + (I_1/I_2)Z_{21} + (I_3/I_2)Z_{23} + (I_4/I_2)Z_{24}$

Z_2 = 89.39 + j 11.64 = 90.144<7.416° Ω

$Z_3 = Z_{33} + (I_1/I_3)Z_{31} + (I_2/I_3)Z_{32} + (I_4/I_3)Z_{34}$

Z_3 = 21.01 - j 41.21 = 46.257<-62.986° Ω

$Z_4 = Z_{44} + (I_1/I_4)Z_{41} + (I_2/I_4)Z_{42} + (I_3/I_4)Z_{43}$

$Z_4 = 20.93 - j\ 42.55 = 47.415 < -63.806° \ \Omega$

Notice that the driving-point impedances Z_1 and Z_2, for the two "front" elements, are very similar to each other, as are the impedances Z_3 and Z_4, for the two "back" elements. Because none of the four vertical monopoles have the same exact height, the driving-point impedances will be slightly different when the array fires through the other three sides. All of these results are shown in Table 5, along with the average values. Notice that both "front" elements have exactly the same average impedance, while the values for the two "back" elements are almost identical.

For this section, let's utilize the average impedance values from Table 5, since I have no preferred direction of fire in this situation.

Current Forcing

We have already decided to use loss-less 75-Ω coax for the quarter-wave phasing lines, so we can now calculate the impedance, voltage, and current at the input ends of these four lines. First, the driving-point currents and impedances are summarized below.

$I_1 = I_2 = 1 < -90°\ = 0 - j\ 1$ A   (front elements)

$I_3 = I_4 = 1 < 0°\ = 1 + j\ 0$ A   (back elements)

$Z_1 = Z_2 = 89.27 + j\ 11.03 = 89.949 < 7.044° \ \Omega$

$Z_3 = Z_4 = 21.195 - j\ 40.57 = 45.773 < -62.416° \ \Omega$

Using the equations developed earlier, the circuit parameters at the input ends of the quarter-wave phasing lines are:

$Z_1' = Z_2' = 5625/Z_1 = 5625/(89.949 < 7.044°) = 62.535 < -7.044°$

$Z_1' = Z_2' = 62.06 - j\ 7.669\ \Omega$

$V_1' = V_2' = jI_1(75) = (1 < 90°)(1 < -90°)(75) = 75 < 0°\ = 75 + j\ 0$ V

$I_1' = I_2' = jI_1 Z_1/(75) = (1 < 90°)(1 < -90°)(89.949 < 7.044°)/(75)$

$I_1' = I_2' = 1.199 < 7.044° = 1.19 + j\ 0.147$ A

$Z_3' = Z_4' = 5625/Z_3 = 5625/(45.773 < -62.416°)$
$\quad\quad = 122.889 < 62.416°$

$Z_3' = Z_4' = 56.90 + j\ 108.92\ \Omega$

$V_3' = V_4' = jI_3(75) = (1 < 90°)(1 < 0°)(75) = 75 < 90°\ = 0 + j\ 75$ V

$I_3' = I_4' = jI_3 Z_3/(75) = (1 < 90°)(1 < 0°)(45.773 < -62.416°)/(75)$

$I_3' = I_4' = 0.610 < 27.584° = 0.541 + j\ 0.283$ A

Designing the Phase-shift Network

Again we need a network that will generate two voltages that are equal in magnitude but 90° apart in phase-angle. Figure 8 shows the block diagram of the required circuitry, including important currents and voltages.

For the 90° phase-lag network, we will use once more the series-input L-network of Figure 3, along with these equations:

$X_{ser} = Z_o^2/(R_c + R_d)$

$X_{sh} = Z_o^2/[(X_c + X_d) - (R_c + R_d)]$

where R_c, R_d, X_c, and X_d are the *driving-point* resistances and reactances of those elements whose phasing lines are connected to the output of the 90° phase-lag network. Here, these are the two "front" elements, #1 and #2, so the equations become:
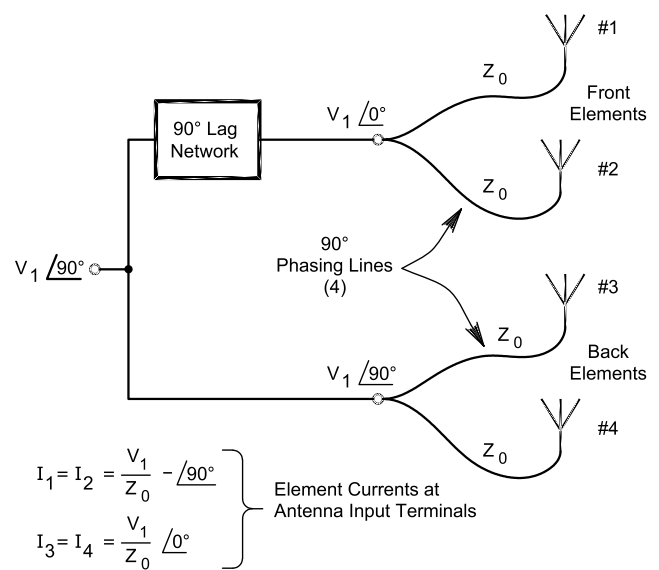
Figure 8—A block diagram of the circuit which will be designed to enable the array to fire through the sides of the 4-square.
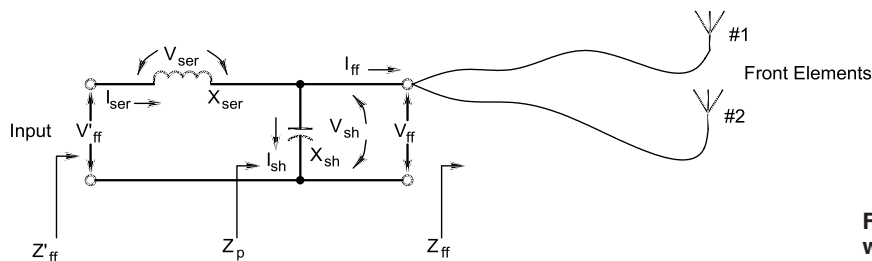
$I_{ff} = I'_1 + I'_2 = 2\ I'_1 \ \ = 2.38 + j\ 0.294$ A.

$Z_{ff} = Z'_1 \parallel Z'_2 = \frac{1}{2}\ Z'_1 = 31.03 - j\ 3.83\ \Omega$

$V_{ff} = V'_1 = V'_2 = 75 \underline{/0°}$ V.

$I_{sh} = 0 + j\ 2.86$ A.

$I_{ser} = 3.366 \underline{/45.0°}$ A.

$Z_p = Z_{sh} \parallel Z_{ff} = 15.76 - j\ 15.75\ \Omega$

$Z'_{ff} = Z_{ser} + Z_p = 15.76 + j\ 15.756\ \Omega$

$Z_{ser} = 31.506 \underline{/90°}\ \Omega$

$Z_{sh} = 35.947 \underline{/-90°}\ \Omega$

$V_{ser} = -74.984 + j\ 74.984$ V

$V_{sh} = V_{ff} = 75 \underline{/0°}$ V

Figure 9—Circuit parameters within a 90° lag sub-network that is designed to enable the array to fire through the sides of the 4-square.

$X_{ser} = Z_o{}^2/(R_1 + R_2)$

$X_{sh} = Z_o{}^2/[(X_1 + X_2) - (R_1 + R_2)]$

For this part of the design exercise, we decided to use the "average" driving-point impedance data from Table 5, in order to compute the component values of the L-network. This strategy should provide us with equal performance from the array when it is firing through any of the four sides of the square. Since we are using "average" values, we realize that $R_1 = R_2$ and $X_1 = X_2$, so the equations for X_{ser} and X_{sh} can be simplified a bit:

$X_{ser} = Z_o{}^2/(R_1 + R_2) = Z_o{}^2/(2R_1) = (75)^2/[2(89.27)] = 5625/178.54$

$X_{ser} = 31.506\ \Omega$

At f=3.79 MHz, this reactance corresponds to an inductance of 1.32 μH.

$X_{sh} = Z_o{}^2/[(X_1 + X_2) - (R_1 + R_2)] = Z_o{}^2/[2(X_1 - R_1)]$

$X_{sh} = (75)^2/[2(11.03 - 89.27)] = 5625/[2(-78.24)]$
  $= 5625/(-156.48)$

$X_{sh} = -35.947\ \Omega$

At f=3.79 MHz, this negative reactance corresponds to a capacitance of 1168 pF.

Now we need to determine the voltage and the impedance at the *input* end of the 90º phase-lag network (see Figure 9). The impedance at the output end, looking toward the load, is the parallel combination of $Z_1{}'$ and $Z_2{}'$ (the impedances at the input ends of the two quarter-wave phasing lines which lead to the "front" elements). Since these two impedances are identical, their parallel combination is simply one-half the value of either alone, so that:

$Z_{ff} = (Z_1{}')ll(Z_2{}') = 0.5(Z_1{}') = 0.5(62.535<-7.044º)$

$Z_{ff} = 31.268<-7.044º) = 31.03 - j\ 3.83\ \Omega$

The current (I_{ff}) flowing out of the network into the two "front" quarter-wave phasing lines is:

$I_{ff} = I_1{}' + I_2{}' = 2I_1{}' = 2(1.19 + j\ 0.147) = 2.38 + j\ 0.294$

$I_{ff} = 2.398<7.042º\ A$

Next, we can see that the voltage (V_{ff}) across the output terminals of the network is the same as the voltage at the input ends of the two quarter-wave phasing lines:

$V_{ff} = V_1{}' = V_2{}' = 75<0º = 75 + j\ 0\ V$

This same voltage, V_{ff}, also appears across the shunt capacitor, which has a reactance $X_{sh} = 35.95\ \Omega$, or an impedance of $Z_{sh} = -jX_{sh}$. Thus, the current through the shunt capacitor is:

$I_{sh} = V_{ff}/Z_{sh} = V_{ff}/(-jX_{sh}) = (75<0º)/(35.95<-90º) = 2.086<90º$

$I_{sh} = 0 + j\ 2.086\ A$

The current (I_{ser}) flowing through the series inductor is the sum of the current flowing into the shunt capacitor and the current flowing into the two 90º phasing lines:

$I_{ser} = I_{sh} + I_{ff} = (0 + j\ 2.086) + (2.38 + j\ 0.294)$

$I_{ser} = 2.38 + j\ 2.38 = 3.366<45.0º\ A$

The voltage (V_{ser}) across the series inductor is found from Ohm's Law:

$V_{ser} = I_{ser}(Z_{ser}) = I_{ser}(jX_{ser}) = 3.366<45.0º(31.506<90º)$

$V_{ser} = 106.044<135.0º = -74.984 + j\ 74.984\ V$

The voltage ($V_{ff}{}'$) across the input terminals of the 90º

phase-lag network is the sum of the voltage across the series inductor and the voltage across the shunt capacitor (again noting that the capacitor voltage $V_{sh} = V_{ff}$).

$V_{ff}{}' = V_{ser} + V_{sh} = V_{ser} + V_{ff} = (-74.984 + j\ 74.984) + (75 + j\ 0)$

$V_{ff}{}' = 0.016 + j\ 74.984 = 74.984<89.988º\ V$

Remember that our goal for this network was to produce two voltages that were equal in magnitude but 90º apart in phase-angle. The "perfect" value for $V_{ff}{}'$ would be $75.0<90.0º\ V$, and our answer is very close to this.

We have already determined that the impedance at the output terminals, looking toward the load, is Z_{ff}. The shunt capacitor is directly in parallel with Z_{ff}, so their parallel combination is:

$Z_p = (Z_{sh})ll(Z_{ff}) = [(Z_{sh})(Z_{ff})]/(Z_{sh} + Z_{ff})$

  $= [(35.95<-90º)(31.265<-7.036º)]/[(-j\ 35.95) + (31.03 - j\ 3.83)]$

  $= (1,123.97<-97.036º)/(31.03 - j\ 39.78)$

  $= (1,123.97<-97.036º)/(50.45<-52.044º)$

$Z_p = 22.279<-44.992º = 15.76 - j\ 15.75\ \Omega$

The impedance ($Z_{ff}{}'$) looking into the input terminals of the network is the combination of Z_{ser} in series with Z_p:

$Z_{ff}{}' = Z_{ser} + Z_p = (j\ 31.506) + (15.76 - j\ 15.75)$

$Z_{ff}{}' = 15.76 + j\ 15.756 = 22.285<44.993º\ \Omega$

Figure 10 is similar to Figure 8, but emphasizes the impedances and voltages that exist within the circuitry that is used to allow the array to fire through the sides of the square. We can see that the input impedance Z_a is the parallel combination of $Z_{ff}{}'$ and Z_{bb}.

Z_{bb} itself is the parallel combination of $Z_3{}'$ and $Z_4{}'$ (the impedances at the input ends of the two quarter-wave phasing lines which lead to the "back" elements). Since these two impedances are identical, their parallel combination is simply one-half the value of either alone. Thus:

$Z_{bb} = (Z_3{}')ll(Z_4{}') = 0.5(Z_3{}') = 0.5(122.889<62.416º)$

$Z_{bb} = 61.444<62.416º) = 28.45 + j\ 54.46\ \Omega$

Now that Z_{bb} has been found, we place it in parallel with
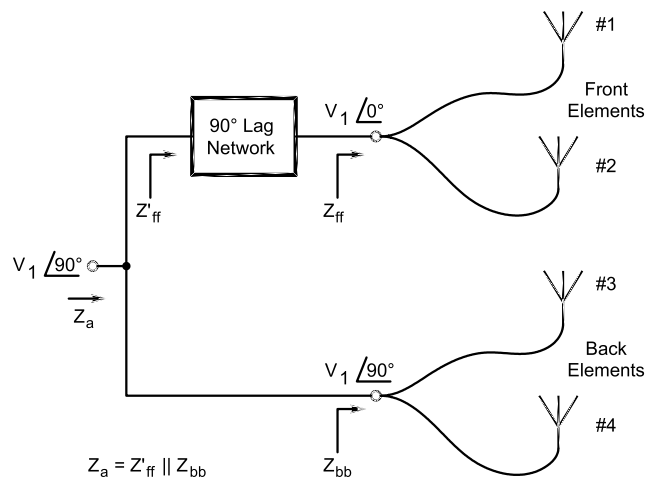
Figure 10—The block diagram of Figure 8, with impedance data added.

Z_{ff}' and use the parallel-resistor formula to calculate Z_a:

$Z_a = (Z_{bb})\text{ll}(Z_{ff}') = (61.444{<}62.416^o)\text{ll}(22.285{<}44.993^o)$

$Z_a = (16.50{<}49.62^o) = 10.69 + j\ 12.57\ \Omega$

This Z_a is the impedance that we would like to match to our main 50-Ω feeder.

Designing the Impedance-matching Network

Again we can use a shunt-input L-network (see Figure 6) to transform Z_a to a pure resistance of 50 Ω. The series reactance X_2 is found from:

$X_2 = - X_a +/- \text{sqrt}\ [R_a(R_{in} - R_a)]$

where R_{in} is the desired input resistance (50 Ω), and R_a & X_a are the resistance and reactance appearing at the load end. Plugging in the appropriate values, we get:

$X_2 = - 12.57 +/- \text{sqrt}\ [10.69(50 - 10.69)]$

$\quad = - 12.57 +/- \text{sqrt}\ [10.69(39.31)] = - 12.57 +/- \text{sqrt}\ [420.22]$

$X_2 = - 12.57 +/- 20.50 = \underline{\text{either}}\ - 33.07\ \Omega\ \underline{\text{or}} + 7.93\ \Omega$

Once again, I will select the positive value $X_2 = + 7.93\ \Omega$, because I like to utilize low-pass networks. At a frequency of 3.79 MHz, this positive reactance corresponds to an inductance of 0.33 µH.

To calculate the shunt reactance, we use:

$X_1 = - \{[(R_a)^2 + (X_a + X_2)^2]/(X_a + X_2)\}$ which gives us:

$X_1 = - \{[(10.69)^2 + (12.57 + 7.93)^2]/(12.57 + 7.93)\}$
$\quad = - \{[(114.276) + (20.5)^2]/(20.5)\}$
$\quad = - \{[(114.276) + (420.25)]/(20.5)\} = - (534.526)/(20.5)$
$X_1 = - 26.07\ \Omega$

At a frequency of 3.79 MHz, this negative reactance corresponds to a capacitance of 1611 pF.

Figure 11 shows the completed circuit, excluding the relays that are needed to change the direction of fire.

Omni-directional Pattern

We can easily obtain a circular (omni-directional) radiation pattern from this array, simply by driving all four elements with equal currents ($I_1 = I_2 = I_3 = I_4 = 1{<}0^o$ A). Ideally, all four of the driving-point impedances will be exactly the same, but that may not happen here, because the height of each vertical monopole is slightly different. Let's do the math:

$Z_1 = Z_{11} + (I_2/I_1)Z_{12} + (I_3/I_1)Z_{13} + (I_4/I_1)Z_{14}$

Since all the currents are the same, each of the current ratios simplifies to 1, and our formula becomes:

$Z_1 = Z_{11} + Z_{12} + Z_{13} + Z_{14}$

Using the self- and mutual-impedance data from Table 2, we find:

$Z_1 = (36.44 + j\ 2.137) + (19.11 - j\ 14.91) + (6.785 - j\ 19.23) + (19.03 - j\ 14.85)$

$Z_1 = 81.36 - j\ 46.85 = 93.885{<}-29.935^o\ \Omega$

The other driving-point impedances are found in a similar fashion:

$Z_2 = Z_{22} + Z_{21} + Z_{23} + Z_{24}$

$Z_2 = 81.17 - j\ 48.14 = 94.372{<}-30.671^o\ \Omega$

$Z_3 = Z_{33} + Z_{31} + Z_{32} + Z_{34}$

$Z_3 = 80.90 - j\ 49.46 = 94.821{<}-31.440^o\ \Omega$

$Z_4 = Z_{44} + Z_{41} + Z_{42} + Z_{43}$

$Z_4 = 80.70 - j\ 50.76 = 95.337{<}-32.170^o\ \Omega$

Although these four impedances aren't identical, they are in close agreement with one another.

If the quarter-wave 75-Ω phasing lines are loss-less, then the impedances seen at the input ends of these lines can easily be calculated:

$Z_1' = 5625/Z_1 = 5625/(93.885{<}-29.935^o) = 59.914{<}29.935^o$

$Z_1' = 51.92 + j\ 29.90\ \Omega$

$Z_2' = 5625/Z_2 = 59.605{<}30.671^o = 51.27 + j\ 30.40\ \Omega$

$Z_3' = 5625/Z_3 = 59.322{<}31.440^o = 50.61 + j\ 30.94\ \Omega$

$Z_4' = 5625/Z_4 = 59.001{<}32.170^o = 49.94 + j\ 31.41\ \Omega$

We don't need to calculate the voltages and currents, because no phase-shift networks are needed. All four of our 0.25-ΩL phasing lines will have their input ends connected together in parallel, so V_{in} is the same for all four.

Table 6

Relay-control Arrangement for the Block Diagram shown in Figure 13. In the event that control power is lost, the array will not function.

Direction of Fire	Energized Relays
NE	K3, K6, K12
E	K9, K10, K13
SE	K4, K5, K12
S	K7, K10, K13
SW	K1, K6, K12
W	K7, K8, K13
NW	K2, K5, K12
N	K8, K9, K13
Omni	K11, K14
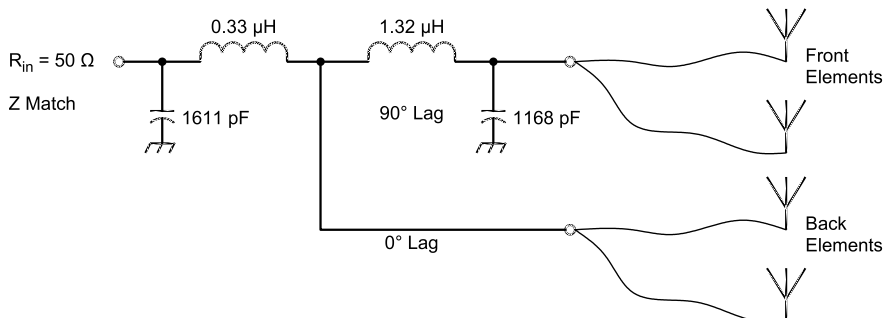
Figure 11—The complete circuit which enables the array to fire through the sides of the 4-square (direction-switching relays are not shown).

We simply design an L-network to transform the resulting impedance to 50 Ω. Repeated applications of the parallel-resistor formula yield:

$Z_a = (Z_1')ll(Z_2')ll(Z_3')ll(Z_4') = 12.73 + j\ 7.67$ Ω, which is the impedance which must be converted into a pure resistance of 50 Ω. As usual we will employ a shunt-input L-network:

$X_2 = -X_a +/- sqrt\ [R_a(R_{in} - R_a)]$ where $R_{in} = 50$ Ω, $R_a = 12.73$ Ω, and $X_a = 7.67$ Ω.

Using the positive result after taking the square root, we find:

$X_2 = 14.11$ Ω

This corresponds to an inductance of 0.59 µH at 3.79 MHz.

Next we calculate the shunt reactance:

$X_1 = -\{[(R_a)^2 + (X_a + X_2)^2]/(X_a + X_2)\} = -29.22$ Ω
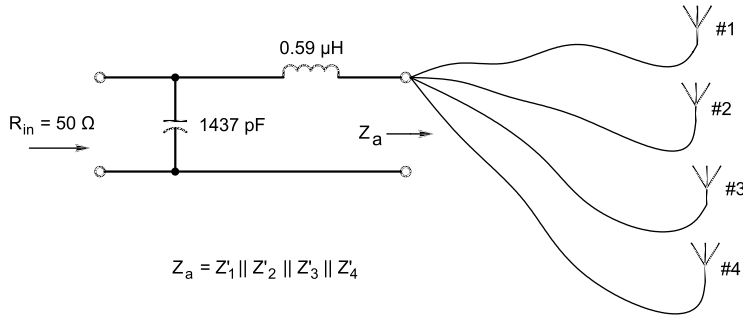
Figure 12—The complete circuit which enables the array to generate an omni-directional (circular) radiation pattern.
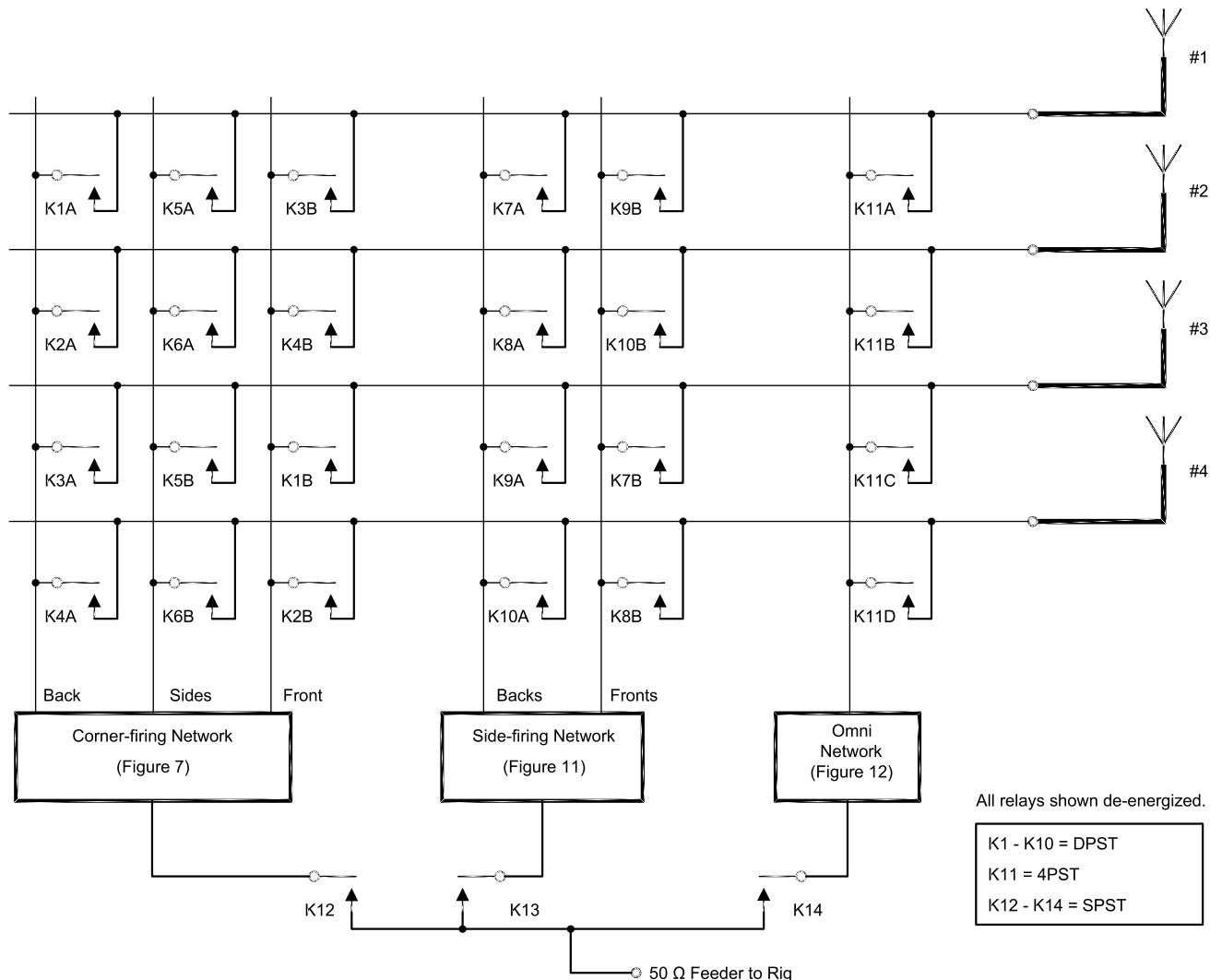
Figure 13—A complete block diagram, showing the networks and the RF wiring for the switching relays. The antenna elements are oriented as shown in Figure 1. With all relays de-energized, no RF reaches the antenna.
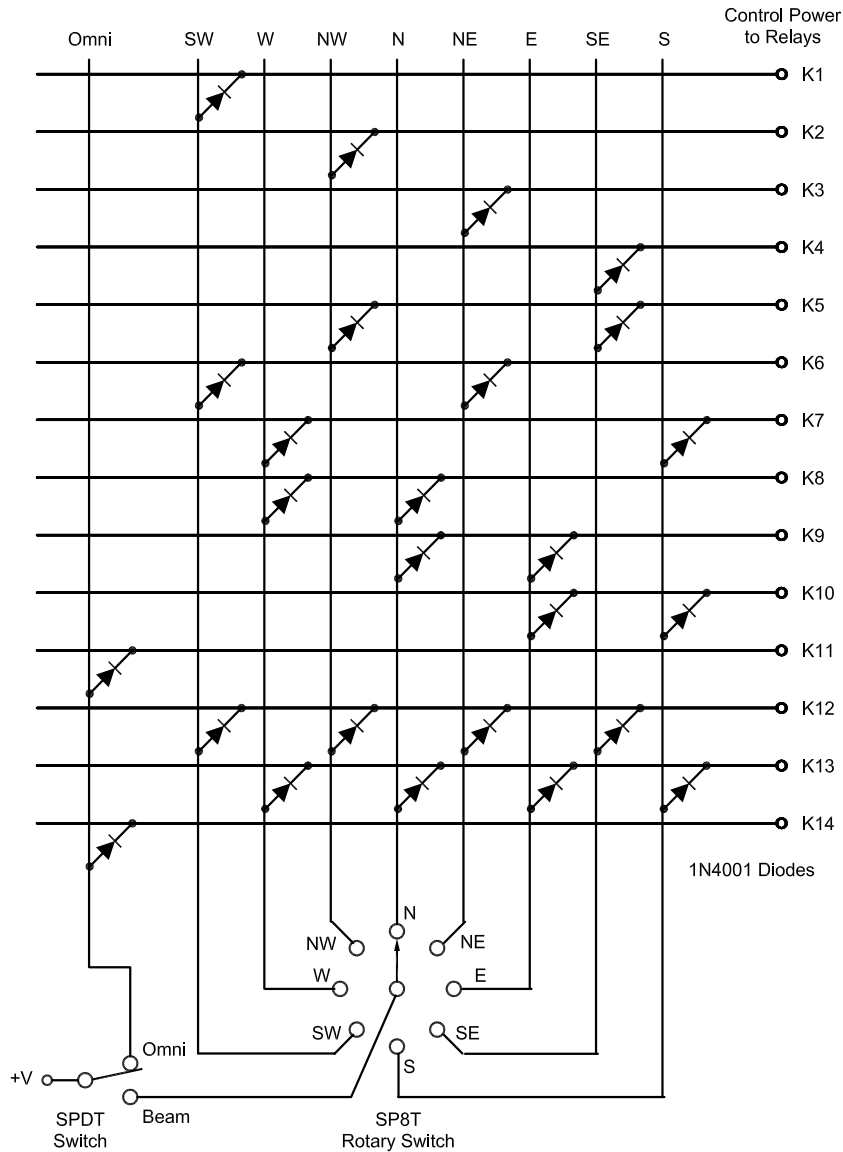
Figure 14—Relay control wiring for the block diagram of Figure 13.

Table 7

Relay-control Arrangement for the Block Diagram shown in Figure 15. In the event that control power is lost, the array will beam to the northeast.

Direction of Fire	Energized Relays
NE	None
E	K3, K6, K9, K10, K12, K13
SE	K3, K4, K5, K6
S	K3, K6, K7, K10, K12, K13
SW	K1, K3
W	K3, K6, K7, K8, K12, K13
NW	K2, K3, K5, K6
N	K3, K6, K8, K9, K12, K13
Omni	K3, K6, K11, K12, K14

Table 8

Data for the Array when Firing through the Corners, when 50-Ω phasing lines are used.

$Z_1 = 59.42 + j\,59.51\ \Omega$ $I_1 = 1{<}{-}180°$ front
$Z_2 = 42.98 - j\,18.47\ \Omega$ $I_2 = 1{<}{-}90°$ side
$Z_3 = -0.298 - j\,19.36\ \Omega$ $I_3 = 1{<}0°$ back
$Z_4 = 42.67 - j\,21.19\ \Omega$ $I_4 = 1{<}{-}90°$ side

$Z_1' = 21.00 - j\,21.04\ \Omega$
$Z_2' = 49.10 + j\,21.10\ \Omega$
$Z_3' = -1.99 + j\,129.10\ \Omega$
$Z_4' = 47.00 + j\,23.34\ \Omega$

Phase-shift network:
$X_{ser} = 29.19\ \Omega$ (1.23 µH at 3.79 MHz)
$X_{sh} = -19.95\ \Omega$ (2105 pF at 3.79 MHz)

Impedance-matching network:
$X_2 = 8.14\ \Omega$ (0.34 µH at 3.79 MHz)
$X_1 = -32.10\ \Omega$ (1308 pF at 3.79 MHz)
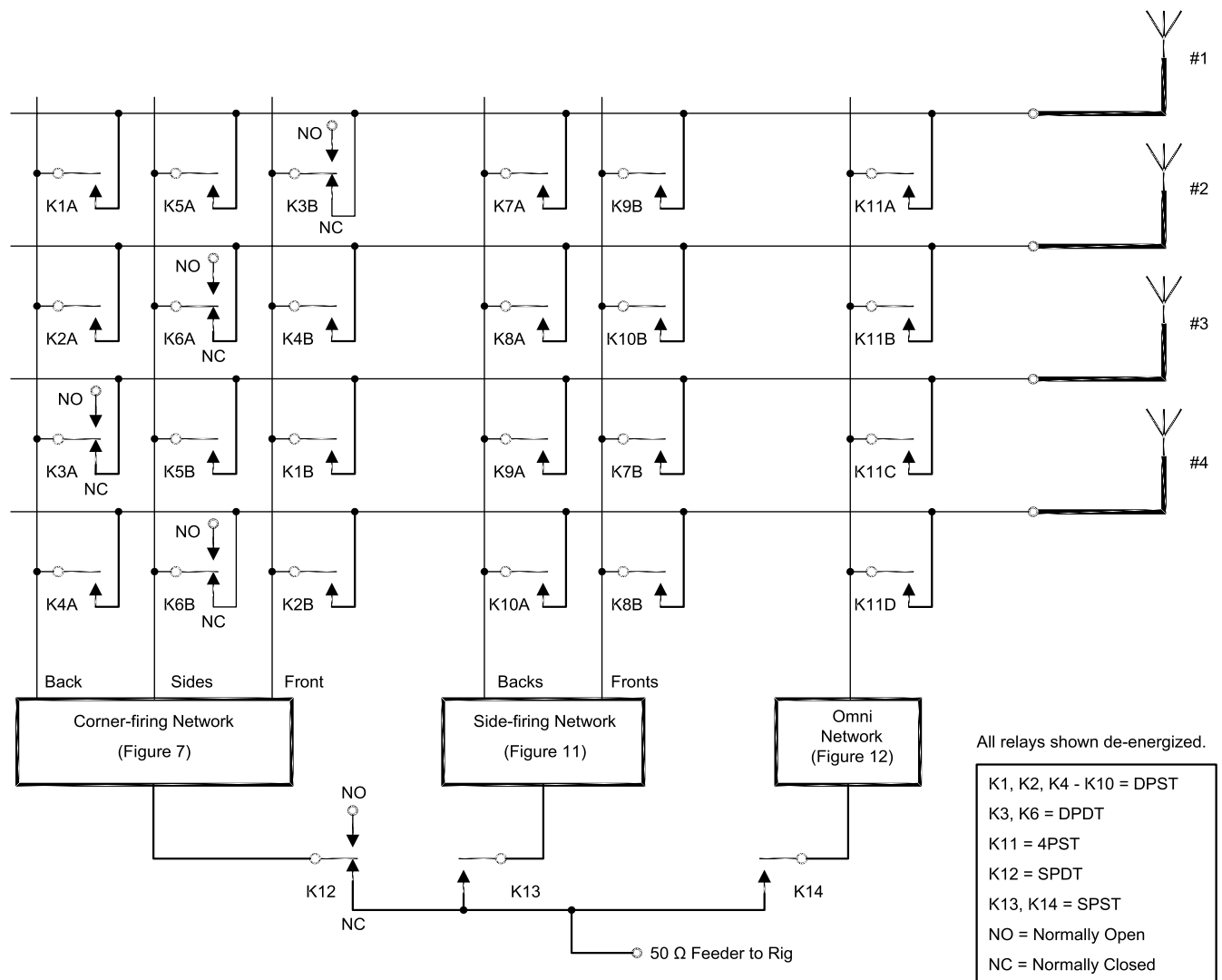
Figure 15—A complete block diagram, showing the networks and the RF wiring for the switching relays. The antenna elements are oriented as shown in Figure 1. With all relays de-energized, the array fires northeast.

All relays shown de-energized.

| K1, K2, K4 - K10 = DPST |
| K3, K6 = DPDT |
| K11 = 4PST |
| K12 = SPDT |
| K13, K14 = SPST |
| NO = Normally Open |
| NC = Normally Closed |

Table 9

Data for the Array when Firing through the Sides, when 50-Ω phasing lines are used.

$Z_1 = 89.63 + j\,13.04\ \Omega$	$I_1 = 1<-90°$	front
$Z_2 = 89.39 + j\,11.64\ \Omega$	$I_2 = 1<-90°$	front
$Z_3 = 21.01 - j\,41.21\ \Omega$	$I_3 = 1<0°$	back
$Z_4 = 20.93 - j\,42.55\ \Omega$	$I_4 = 1<0°$	back

$Z_1' = 27.31 - j\,3.97\ \Omega$
$Z_2' = 27.50 - j\,3.58\ \Omega$
$Z_3' = 24.55 + j\,48.15\ \Omega$
$Z_4' = 23.27 + j\,47.31\ \Omega$

Phase-shift network:

$X_{ser} = 13.96\ \Omega$ (0.586 µH at 3.79 MHz)
$X_{sh} = -16.20\ \Omega$ (2592 pF at 3.79 MHz)

Impedance-matching network:

$X_2 = 10.34\ \Omega$ (0.434 µH at 3.79 MHz)
$X_1 = -20.14\ \Omega$ (2085 pF at 3.79 MHz)

Table 10

Data for the Array when Firing in an "Omni" pattern, when 50-Ω phasing lines are used.

$Z_1 = 81.36 - j\,46.85\ \Omega$	$I_1 = 1<0°$
$Z_2 = 81.17 - j\,48.14\ \Omega$	$I_2 = 1<0°$
$Z_3 = 80.90 - j\,49.46\ \Omega$	$I_3 = 1<0°$
$Z_4 = 80.70 - j\,50.76\ \Omega$	$I_4 = 1<0°$

$Z_1' = 23.08 + j\,13.29\ \Omega$
$Z_2' = 22.79 + j\,13.51\ \Omega$
$Z_3' = 22.49 + j\,13.75\ \Omega$
$Z_4' = 22.20 + j\,13.96\ \Omega$

Common-point impedance:

$Z_a = 5.66 + j\,3.41\ \Omega$ (very low)

Impedance-matching network:

$X_2 = 12.43\ \Omega$ (0.522 µH at 3.79 MHz)
$X_1 = -17.86\ \Omega$ (2351 pF at 3.79 MHz)

At a frequency of 3.79 MHz, this negative reactance corresponds to a capacitance of 1437 pF.

Figure 12 shows the schematic diagram for the L-network.

Putting It All Together

Figure 13 is a complete system block diagram, which includes all of the phasing/matching networks and the RF wiring for the 14 relays. Table 6 shows which relays must be energized for each direction of fire, and Figure 14 is a schematic diagram for the control circuitry for those relays. In this configuration, the antenna will not work if control power is lost, because all of the relays are single-throw, meaning that their contacts are "open" when de-energized.

An alternative arrangement is provided in Figure 15, whereby "northeast" is the "default" direction of fire. Here, DPDT relays are needed for K3 and K6, and a SPDT relay for K12. The normally-closed contacts of these relays are wired so that the corresponding circuits are "made" when the control power is off. Table 7 shows which relays must be *on* for each direction of fire. Now, relay K3 must be *on* for all directions of fire except NE, relay K6 must be *on* for all directions of fire except NE and SW, and relay K12 must be *on* for N, S, E, W, and OMNI. Figure 16 is a wiring diagram for the relay control power.

If 50-Ω coaxial cable is used for the quarter-wave phasing lines, then impedances throughout the system will be lower. Tables 8 through 10 list the pertinent information. Notice that the common-point impedance (Z_a) for the omni-directional network is very low, so the current will be quite large.

It was mentioned previously that the *actual* feed-point current magnitudes weren't needed, only their *relative* values. However, when selecting network components, it is important that the actual current and voltage amplitudes be known. When the array is firing through the corners of the square, the feed-point currents have a magnitude of 3.219 A, for a power input of 1500 W at the terminals of the vertical elements. When firing through the sides of the square, 2.606 A flows into each element, and 2.151 A when in the "omni" mode.

Conclusions

This article has reviewed the procedures and mathematics that are necessary to design the phasing and matching circuitry for a 4-square phased-vertical array that can fire in 8 azimuthal directions, and also pro-

vide a circular radiation pattern. All of the impedance data mentioned here was derived from a computer model, and your measured values will probably be different. The actual impedances depend upon the length/diameter ratio of the vertical elements, the quality of the ground system, and the electrical characteristics of the soil.

A variety of software packages are available to reduce the mathematical drudgery involved in this effort. For instance, ON4UN's *New Lowband Software*[6] can handle loss-less and real coaxial cables, transform circuit parameters from one end of the cable to the other, do parallel-resistance calculations, design L-networks, etc. I used it to double-check much of the algebra that was demonstrated in the text.

Figure 16—Relay control wiring for the block diagram of Figure 15.

Notes
[1]Al Christman, K3LC, "A Four-Square with Eight Directions of Fire," *National Contest Journal*, Volume 32, Number 2, March/April 2004.
[2]Roy Lewallen, W7EL, "Quadrature-Fed Elements in Larger Arrays," *The ARRL Antenna Book*, American Radio Relay League, 2000, page 8-21.
[3]Several versions of *EZNEC* are available from Roy Lewallen, W7EL, PO Box 6658, Beaverton OR 97007.
[4]Roy Lewallen, W7EL, "A Preferred Feed Method," *The ARRL Antenna Book*, American Radio Relay League, 2000, page 8-15.
[5]Forrest Gehrke, K2BT, "Vertical Phased Arrays: part 4," *Ham Radio*, October 1983, page 39.
[6]John Devoldere, ON4UN, *New Lowband Software*, available either directly from ON4UN, or from George Oliva, K2UO. □□

Antenna Options:
A Yagi Case Study Part 2—
Element Material Options

By L. B. Cebik, W4RNL

1434 High Mesa Drive
Knoxville, TN 37938-4443
cebik@cebik.com

I n the first episode of this *Tale of Three Yagis*, we explored the design options for a 3-element 2-meter Yagi with intended field use and restricted to a 30-inch or smaller boom. Our options included high-gain, high-front-back, and wide-band versions of the antenna. For each option we provided design dimensions for round-tubing elements ranging from 0.125 inch up to 0.5 inch in diameter. In this episode, we shall examine some of the element materials other than round tubing that we may use and how we may go about the process of correlating these materials to the dimensions in the first part of this exercise on antenna options.

However, let's make no mistake—the design options presented do not represent a comprehensive view of all of the Yagi design variations that we might bring to the planning table. There are designs with wider bandwidths and designs with higher gain—all generally within the initial guidelines for the exercise.

For example, we may develop a very wide-band Yagi by slaving a second driver to the original driver. Technically, this becomes a 4-element Yagi if we view the driver as a parasitic element, but it is not a true director except at the very low end of the operating passband. Table 1 shows the dimensions for such a very-wide-band Yagi using 0.125-inch diameter elements. The performance figures appear in Table 2 and in Fig 1 and Fig 2. As the table shows, the antenna is capable of very acceptable performance for at least the 140 to 150-MHz range, with lesser performance beyond. The first graph—taken from an *EZNEC* frequency sweep and displayed on AC6LA's *EZPlot*—shows the relatively even gain, which varies by only 0.4 dB across the passband. The line marked "front/sidelobe ratio" actually provides the worst-case front-to-back value, in contrast to the 180° front-to-back ratio that shows higher values across part of the operating passband. The second graph records the modeled feed-point resistance, reactance and 50-Ω SWR values from 140 to 150 MHz. Note that the SWR does not rise to 1.3:1 within the passband. The performance overall is comparable to the wide-band design in Part 1, but with a much wider pass-band. However, in exchange for the

Table 1—4-Element Very-Wide-Band Yagi Dimensions for 0.125" Round Elements

Dimensions: L = Element half-length—double the L-value to obtain the full element length. Dimensions in inches—multiply by 25.4 to obtain dimensions in millimeters.

Ref L	Dri L	Dir 1 L	Dir 2 L	R-Dr Sp	R-Dir 1 Sp	R-Dir 2 Sp
21.01	21.20	18.69	17.76	7.41	8.89	21.16

extended passband, the design requires an extra element and exceptionally careful construction and field adjustment to achieve the performance promised by the model. In the rigors of field operation, the chances of maladjustment due to bumps and other accidental deformations are too great for inclusion in the design pool.

There are ways to achieve higher gain from the same boom length as our three original designs. One technique is to use a pair of phased elements as a driver, as exemplified by the design in Table 3. The antenna is essentially a *phagi*, that is, a phased horizontal array with one or more parasitic elements. We may also call this a log-cell Yagi, although the phased driver set is not large enough to constitute a true LPDA on its own. The dimensions specify 0.1875-inch diameter elements for 2 meters. The phase line between the two rear elements consists of a 50-Ω line with a reversal between elements. The electrical length is 20.26 inch, allowing lines with a 0.66 velocity factor to meet the need. The native feed-point impedance at the 146-MHz design frequency is about 15 + j23 Ω. Since the impedance is inductive reactance, we may apply beta-match techniques to raise the impedance to 50-Ω resistive—or close to that value. A shunt capacitor with about - j35.5 Ω reactance across the feed-point gap will do the job. At 146 MHz, this amounts to about 30.7 pF, the equivalent of a 12.27-inch electrical length of 50-Ω transmission line used as an open stub.

Table 4 tabulates the performance between 145 and 147 MHz, while Figures 3 and 4 provide a graphical view of the same data. The design provides almost an extra dB of forward gain relative to the high-gain design in Part 1, while preserving a high front-to-back ratio within the listed passband. Typical of most Yagi designs—the worst-case front-to-back ratio is relatively even across the passband, while the 180° value tends to peak at a high value. As with many higher gain Yagi designs, the SWR and impedance curves suggest that the antenna may be useful below the lower limit of the passband, but the performance graphs suggest that the use is limited by decreasing gain and front-to-back ratios.

I have not included this design in our general pool because it involves phasing techniques. To construct the phagi would require extensive measurement and adjustment, for example, to determine the precise velocity factor of the line used for phasing the rear-ward elements. Listed velocity factor values are simply not accurate enough from one batch of line to the next to ensure proper line length to achieve the modeled performance. The phase line becomes an extra element to carry into the field, not to mention the need for connectors at each end as part of the antenna structure.
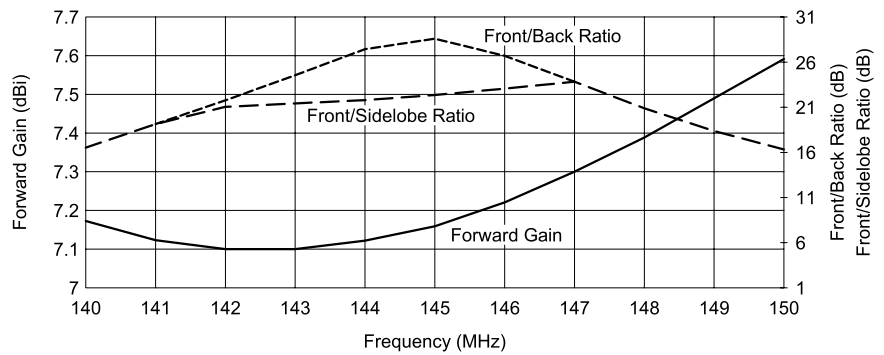
Fig. 1—Very-wide-band 4-element Yagi gain and 180° worst-case FB ratios.
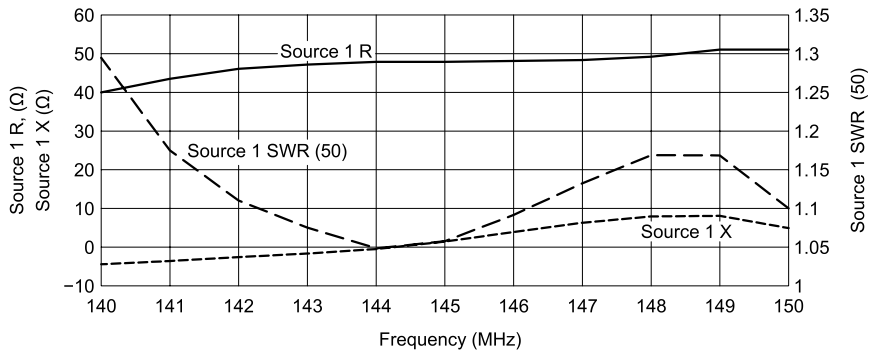
Fig. 2—Very-wide-band 4-element Yagi feed-point resistance and reactance; 50-Ω SWR.

Table 2. 4-Element Very-Wide-Band Yagi Modeled Performance Across 2 Meters

0.125" Diameter Elements

Freq. MHz	Free-Space Gain dBi	Front-to-Back Ratio dB	Feedpoint Z R +/- jX Ω	50-Ω SWR
140	7.17	16.51	39.5 - j4.7	1.294
142	7.10	21.78	45.9 - j3.0	1.110
144	7.12	24.61	47.7 - j0.6	1.050
146	7.22	26.80	48.0 + j3.6	1.089
148	7.39	20.92	49.5 + j7.7	1.167
150	7.59	16.33	51.1 + j4.7	1.100

Table 3—3-Element Phagi Dimensions for 0.1875 inch Round Elements

Dimensions: L = Element half-length—double the L-value to obtain the full element length. Dimensions in inches—multiply by 25.4 to obtain dimensions in millimeters. The elements marked "Ref" and "Dri" actually form a phased pair of driven elements.

Ref L	Dri L	Dir L	R-Dr Sp	R-Dir Sp
19.80	19.45	17.63	10.25	28.70

Nevertheless, these two brief examples of alternative designs are reminders that we do not exhaust the full set of design options in the ones that we included in Part 1. Rather, these options only scratch the surface of a wide variety of Yagi and related designs. We chose them only because they form a relevant collection of straightforward designs that promise relative ease of replication in most home shop settings. As a final design reminder, all of the designs in both this part and the first episode involve elements that are insulated and isolated from a metallic boom and indeed prefer a non-metallic boom. However, to say more about boom materials would leap into the last part of this series and skip our trips to the home improvement center and our survey of element materials.

Part 2—Element Materials for the Three Yagi Designs

It would seem on the surface that the range of rod and tubing sizes reported in the dimension tables of Part 1 would cover the territory indicated by the Part 2 subtitle. We have already noted that one may use aluminum, brass, or copper tubing or rods for the elements with no significant change in performance. Once an element reaches a certain diameter for a given frequency, the differential in material losses for common conductive materials no longer makes a difference to performance. At 2 meters, that semi-critical element size is about $1/8$ inch.

I have not included common metric sizes of tubing and rod material. For example, the common 4-mm material used in Europe for VHF arrays is about 0.1575 inch in diameter, half way between $1/8$ inch and $3/16$ inch US sizes. I have also omitted AWG wires sizes, although AWG #8 (0.1285 inch) would make a usable substitute for $1/8$-inch elements with no design modification. Elements smaller than $1/8$ inch tend to be flimsy, while those larger than $1/2$ inch tend to be physically impractical. As a result, the range of sizes that we have provided in the dimension tables covers most of the reasonable materials for 2-meter Yagi construction.

Some might assume that builders want to use elements having a circular cross section. I have learned over the years that we should never make this assumption. Antenna builders will latch onto almost any material at hand, including dime-store collapsible whips, flat stock, L-stock, and even channel and square stock. For special purposes, some antenna builders will use the metal tape that comes in
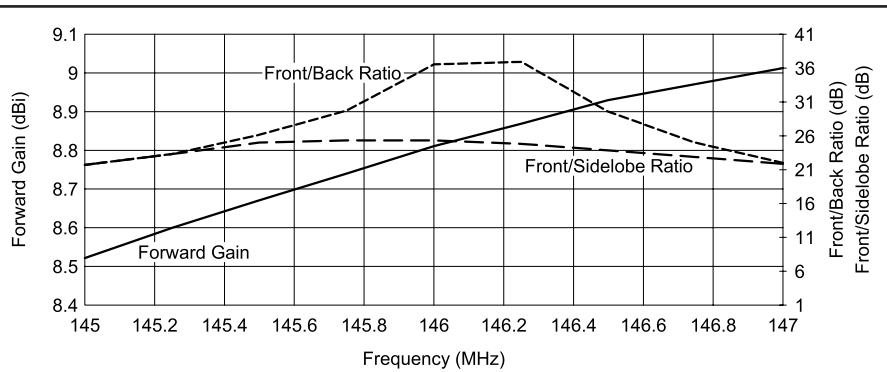
Fig. 3—Gain and 180° worst-case FB ratios for 3-element phagi.
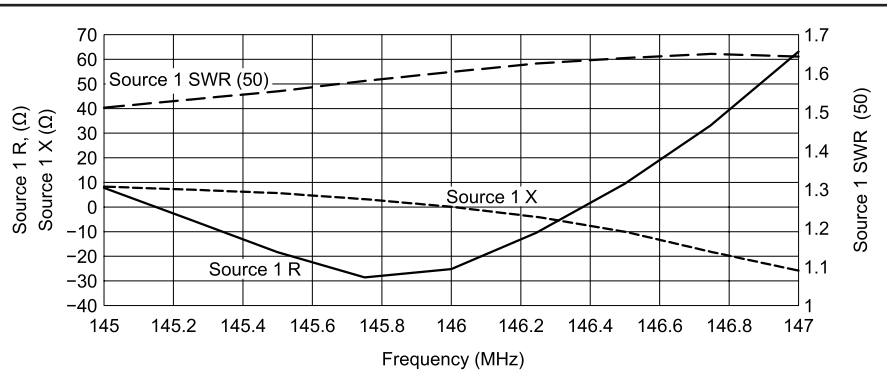
Fig. 4—Feed-point resistance and reactance; 50- Ω SWR for 3-element phagi.
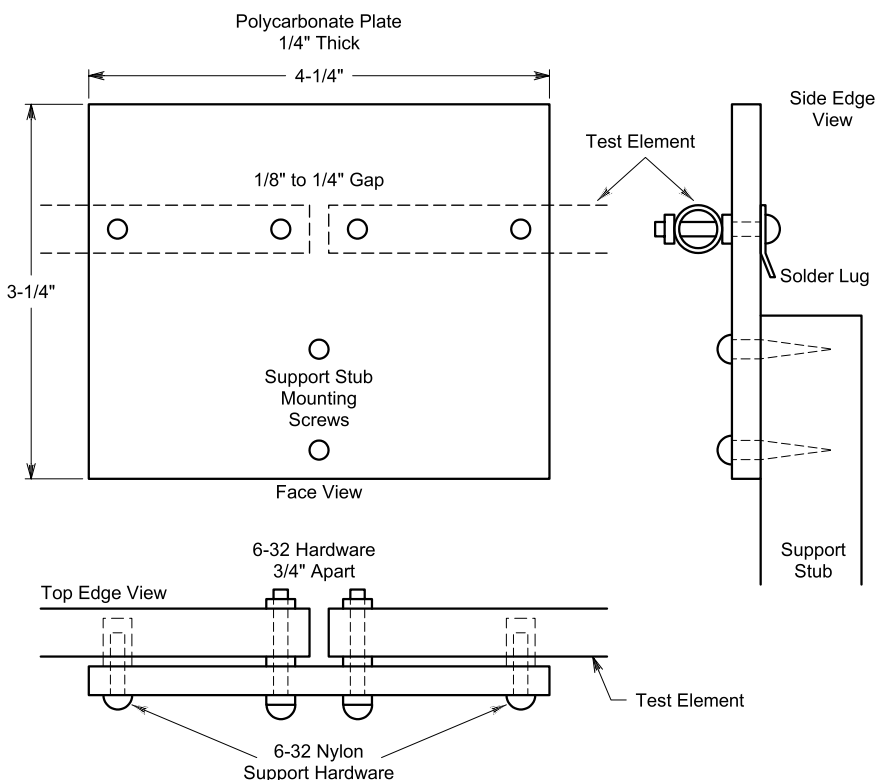
Fig. 5—A sketch of the test dipole mounting plate assembly.

spring-loaded tape measures.

Proposals to use these materials come with one question—with what round element size does the size of each variant material equate? The notes in this section will present a few of my findings for some of the materials at 146 MHz. More important than the results is the procedure that I used to determine them. I shall outline a very practical procedure for use on 2 meters that will allow anyone to replicate my experiments and to find the best approximation of a round conductor that matches a novel material proposal. All that we require is a reasonably accurate antenna analyzer, a standardized center hub for a dipole, and a mast-stand fixture on which to perform the experiments.

The method that I used to compare a variety of materials was to create dipoles resonant at 146 MHz. Using an MFJ-259B analyzer, first calibrated to my station receiver, I made and pruned dipoles for each round conductor listed in the dimension tables of Part 1 and then made and pruned dipoles for each variant material that I could think of and easily obtain. I added a round 0.75 inch diameter dipole to the group, because many substitute materials are close in performance to this size round element. The key feature of the procedure is not absolute agreement with modeled predictions for the round

conductors, but instead a method that would ensure consistency from one dipole to the next.

The dipole hub assembly that I used is designed to provide a consistent dipole-center environment from one test to the next. Fig 5 shows the general outline of the plate, which I made from a scrap of $\frac{1}{4}$-inch thick polycarbonate. Hence, there is no magic, but only convenience, in the plate length and width. Each dipole candidate mounts both physically and

electrically by way of the two #6-32 nuts and bolts at the upper plate center. For each dipole, I used a bolt length to have the least excess threaded length beyond the limits of the dipole material. The two outer holes in the plate use nylon screws into threaded plastic tubes that sit within holes in the dipole for support of the element. I removed the support tubes for the tape elements, since they are too thin to support drilling $\frac{1}{4}$-inch holes. For the rod elements, I used

Table 4—3-Element Phagi Modeled Performance from 145 to 147 MHz.

0.1875" Diameter Elements

Freq. MHz	Free-Space Gain dBi	Front-to-Back Ratio dB	Feedpoint Z R +/- jX Ω	50-Ω SWR
145	8.52	21.57	40.8 + j7.8	1.305
145.5	8.67	26.82	47.2 + j5.6	1.137
146	8.81	36.48	54.7 + j0.0	1.093
146.5	8.93	29.55	60.9 - j10.5	1.315
147	9.01	21.89	61.2 - j25.7	1.652
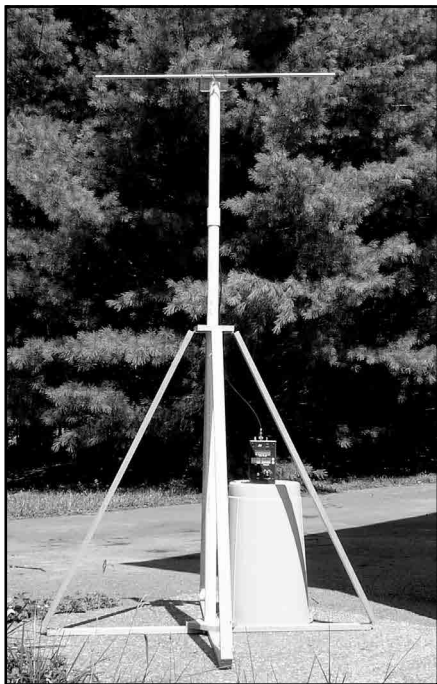
Photo A—The complete test assembly with a tubular dipole attached and the antenna analyzer stationed closer to the ground.
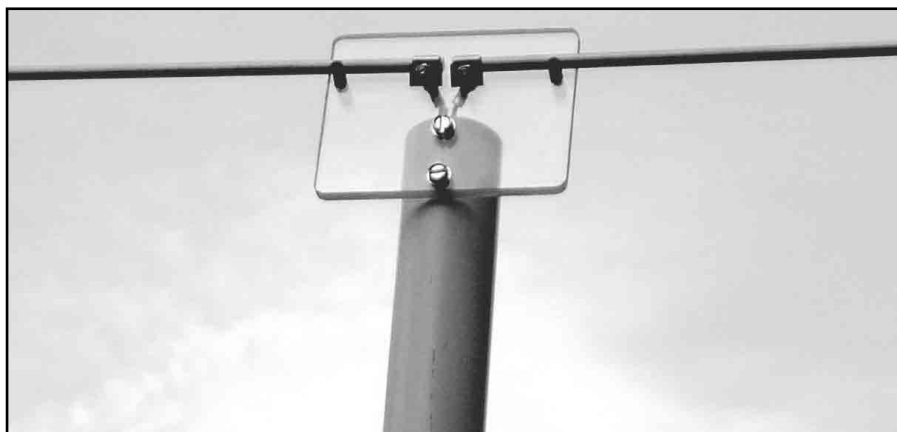
Photo B—A close-up of the center plate with a thin rod element clamped in place and supported by the outer posts.

Photo C—The same assembly as in Photo B, but with an L-stock element—the outer support posts pass though holes in the element.

square washers at the inner screws to electrically clamp the inner rod ends, while the rod itself rested on top of the outer tubes.

The plate mounts to a section of PVC with a pair of sheet-metal screws. Because the assembly is only temporary, you can use any clean hardware. The area above the support stub and behind the dipole center is clear so that I could mount a length of coax with solder lugs, avoiding the use of a connector at this point. The coax length is $\frac{1}{2}$ λ, allowing for the velocity factor of the RG-8X that I used. (Note that RG-8X has different velocity factors from different makers. However, do not rely on manufacturer's specifications for velocity factor. Measure the line for an electrical $\frac{1}{2}$ λ. My line had a listed velocity factor above 0.8, but measured about 0.735. The distant line end should replicate the feed-point impedance at the dipole terminals, while minimizing body effects during measurements.)

I have a wood test stand that I use for various purposes. It appears in the photos. It holds a 5-foot section of $1\frac{1}{4}$ inch Schedule 40 PVC for this test. The upper section of the mast, using a coupling (not cemented), is a 2-foot section of the same material, and that is the support stub to which I attached the dipole plate. For pruning, I simply lifted the upper section off, carried it into the shop, and sawed, clipped, or sanded the element ends, according to which material was under test.

The 7 foot total height of the assembly placed the antenna about 1 λ above ground, a sufficient height to minimize ground effects on the dipole's resonant frequency. For each test, I placed the test stand in the same position with the dipoles oriented the same way. The goal was not laboratory precision, but usable consistency from one test to the next.

Photo A shows the complete assembly with a tubular dipole attached and the antenna analyzer stationed closer to the ground. Photo B is a close-up of the center plate with a thin rod element clamped in place and supported by the outer posts. The last picture in this series, Photo C, shows the same assembly with an L-stock element—the outer support posts pass though holes in the element.

You may replicate this type of system—adding your own improvements—to test any number of materials for comparison with the round elements presumed by antenna modeling software. In the interim, the following notes record the results that I obtained.

Round Conductors

Table 5 shows the results of tests with round conductors that form the reference values for all of the subsequent tests. Also included in the table are the *NEC-4* modeled values for the lengths of each size of tubing.

Round conductors offer the best combination of strength vs weight and ability to slip the wind to minimize loading from that source. As well, they tend to resist ice build-up better than most flat or L-stock elements. Hence, for a long-term station installation, I would recommend them. For most purposes 6061-T6 and 6063-T832 aluminum stock, available by mail order if not in stock locally, are the best antenna element materials. Never-

theless, there are reasons and occasions for using other materials.

Interestingly, the round elements all measure well within 0.5% of the *NEC-4* modeled lengths, except for the $\frac{3}{4}$-inch tubing, which comes in with under 1.0% variance relative to the modeled value.

Table 6 provides the measured data on all of the tested alternatives to round conductors. The table lists not only the length of the dipole that turned out to be resonant on 146 MHz, but as well the size of the most nearly equivalent measured round conductor. This value permits the builder to refer to the dimensions in Part 1 that most closely approximate the dimension needed for the alternative material.

Table 5—Modeled and tested resonant lengths of round-element 146 MHz dipoles.

El. Diameter (inches)	Modeled Length (inches)	Tested Length (inches)
0.125	38.42	38.31
0.1875	38.28	38.25
0.25	38.10	38.06
0.375	37.80	37.81
0.5	37.60	37.44
0.75	37.30	36.94

Table 6—Tested 146-MHz resonant lengths of alternative element materials.

Material	Tested Length (inches)	Nearest Round Element
Aluminum Flat Stock (size in inches)		
$\frac{1}{2}$ by $\frac{1}{16}$	37.31	0.5
$\frac{1}{2}$ by $\frac{1}{8}$	37.19	0.5
$\frac{3}{4}$ by $\frac{1}{16}$	37.06	0.75
Aluminum L-Stock (size in inches)		
$\frac{1}{2}$ by $\frac{1}{2}$ by $\frac{1}{16}$	37.44	0.5
$\frac{3}{4}$ by $\frac{3}{4}$ by $\frac{1}{16}$	37.00	0.75
Collapsible Whips (size in inches)		
1. 5-section TV "rabbit ear," maximum extension 48.5 inches with "button" tip. Approximate diameters: 0.25, 0.219, 0.1875, 0.125, 0.0625		
a. With largest sections fully extended	37.88	0.375
b. With smallest section fully extended	40.00	<0.125
2. Radio Shack 5-section cordless telephone replacement (#270-1405A); maximum extension 23 inches with button tip. Approximate diameters: 5 mm, 4.125 mm, 3.25 mm, 2.375 mm, 1.5 mm		
Roughly equal section extension	38.88	<0.125
Metal Measuring Tapes (size in inches)		
1 ($\frac{15}{16}$ with curve)	37.38	0.5
$\frac{3}{4}$ ($\frac{11}{16}$ with curve)	37.63	0.375 to 0.5
$\frac{5}{8}$ ($\frac{9}{16}$ with curve)	37.88	0.375
$\frac{1}{2}$ ($\frac{15}{32}$ with curve)	38.25	0.1875

Flat Stock

Flat stock holds two advantages for home construction. First, it is readily available at home centers. Second, it is flat. Hence, we can drill it easily on any equally flat surface and avoid the difficulty of drilling a round surface. The disadvantage of this stock is that the $^1/_{16}$ inch thick type is very flimsy and bends all too easily. The $^1/_8$ inch thick type is sufficiently sturdy for a permanent installation, but may be needlessly heavy for field use.

The flat stock plays very close to its measured round counterparts. Some modelers advocate using round wires having the same surface area as the flat stock. The closest round wire to $^1/_2$ inch by $^1/_{16}$ inch flat stock is 0.375 inch tubing. However, the measured lengths for both the $^1/_{16}$ inch and $^1/_8$ inch flat stock is 0.5 inch tubing, which has about 1.4 times the surface area per unit length. As well, the $^3/_4$-inch by $^1/_{16}$-inch flat stock measures closest to the 0.75 inch round tube.

L-Stock

L-stock that is $^1/_{16}$-inch thick combines the benefits of offering flat surfaces to drill with excellent rigidity and easy availability at home centers. In addition to Yagi service, builders have used the stock for both the horizontal element-portions of quads and for Moxon rectangles. It is half the weight of square stock with equal outer dimensions. The down side of L-stock is that it offers considerably more wind resistance than a round conductor. It also is prone to snagging in field exercises, such a fox hunts in wooded areas.

As with flat stock, L-stock appears to approximate its round counterpart element material in both the measured half-inch wire and the modeled $^3/_4$-inch wire. Within the limits of my measurements ($^1/_{16}$ inch), there is no significant difference between the flat stock and the L-stock.

Collapsible Whips

For field antennas, collapsible whips offer a certain convenience, since we can shorten the elements to the whip's minimum length for transport. In addition, most whips adapted from TV and cell-phone replacement service have a plug in the lower end. The plug has a mounting hole, which permits the builder to swivel the elements in line with the boom for an even more compact assembly during transport to and from the working site.

For this test, I salvaged whips from very old TV rabbit ears as a test of larger diameter versions. Since the whips extended to about 48 inches, I performed two tests—one with the larger section dominating the element length at 146 MHz, the other with the thinnest sections fully extended. I also obtained two Radio Shack cell-phone whips that extend only to 28 inches per unit. These whips give an indication of equivalent lengths for the thin-whip style. In both cases, I used the square washer clamp method of fastening that I used with aluminum rods in the initial tests.

With the large whips using their fattest sections, the dipole length is closest to $^3/_8$ inch round wire. The same whip using its inner largest-diameter section (about 0.25 inch) and its smallest section (about $^1/_{16}$ inch) requires a length of 40.0 inches, which is longer than needed for 0.125-inch uniform-diameter material. The small whip required a dipole length of 38.88 inches, also longer then needed by the smallest round element tested.

The excess length required by collapsible whips, even with fat button ends, owes to the stepped-diameter structure on each side of the dipole centerline. The first test used the fattest large-whip sections, resulting in the smallest step, and the result is the shortest of the required whip lengths. The second large-whip test had the greatest step in diameter, and yields the longest resonant overall length. The cell-phone replacement begins with a smaller diameter, from which we might expect a longer overall length. However, the steps in diameter are small and regular so that its length is shorter than required for the second large-whip test. All of these results coincide with fundamental theory regarding elements that taper from the center to their tip.

Measuring Tapes

The final group of tests involves a material used almost exclusively by foxhunters—cannibalized measuring tape. Although the tape is steel, it is satisfactory for field antennas. By judiciously buying a few bargain tapes and replacing some very worn tape measures in the shop, I managed to find four tape widths. Measuring tape is very thin, but the exact thickness may vary with brand and age. Hence, the values shown in the table are indicative, but not absolute, for each width.

The advantage of a tape-measure element is its ability to bend at a field snag and to bounce back to position with no damage (at least, no damage in the short run). Because a 3-element, 2-meter Yagi, perhaps of the maximum front-to-back design, requires about 10 feet of tape for its elements, a single long tape measure provides material for many replacement elements or for several individual Yagis. Replacement tapes without the cases and mechanisms are difficult to find locally these days, so expect to destroy a complete tape-measure unit if you opt for this element material. However, bargain tape measures abound.

The measured resonant lengths for tape-measure material all indicate an equivalence to round conductors about half as much in diameter as the tapes were wide. Unlike the flat stock, which had a significant thickness, the tapes are very thin. Hence, their wide surfaces alone did not suffice to bring them close to the resonant lengths of round conductors with the same cross dimension.

Summary of Findings

The measured values for the alternative materials held a few surprises. Perhaps the performance of flat stock was the most dramatic. Nevertheless, I would not claim that the near-equivalencies at 2-meters would hold up at HF, where one might trade the greater difficulty of constructing the requisite number of long dipoles for finer gradations of measurement.

The survey of alternative element materials is not by any means complete or ultra-precise. However, the technique used to find their nearest equivalent round conductor has proven quite reliable in adapting designs. Reliability here means that the results are usable for the adaptation of round wire designs to alternative stock used in the home-construction of antennas. Neither my tape measure nor my antenna analyzer meets anything like laboratory standards, and the testing circumstances are not of calibrated range or chamber quality.

One final caution is in order. With non-round conductors, the inter-element coupling between adjacent elements may not be identical to the coupling from round elements. Hence, some final field adjustment of element lengths may be necessary, even for materials listed as equivalent to a round conductor. This caution is especially true of the driver-director relationship, where small director length adjustments tend to yield considerable changes in the Yagi performance curves at 2 meters.

Field adjustment, of course, presumes that we have already built our Yagi design of choice. Even within the constraints of this exercise, we have options. Some of those options will be the subject of "Part 3—Building 3-Element Yagis for Different Uses." ☐☐

Tech Notes

By Ray Mack, WD5IFS
QEX Contributing Editor

A Look at Current Feedback Amplifiers

I have seen very little in print about current feedback amplifiers. Most manufacturer application notes begin with a description that "even seasoned engineers tend to stay away from current feedback amplifiers because they seem to be more difficult than voltage feedback amplifiers."

The original operational amplifiers were tube-based designs from the 1960s. A major breakthrough occurred when the µA709 integrated opamp became commercially available. Opamps are voltage feedback devices and the basic circuit is the same for all types of active devices (vacuum tubes, bipolar transistors, JFETs). Figure 1 shows the internal design of the LM324 opamp. The input stage (Q1-Q6) is a differential amplifier with high input impedance that operates as a voltage to current converter. The output stage (Q7-Q13) provides appropriate gain, current to voltage conversion, and conversion to a single-ended power output stage. Figure 2 shows a model of an ideal opamp. The resistance between the inverting and non-inverting inputs is infinite in an ideal opamp, but many hundreds of kohms or greater in a real amplifier. The voltage controlled voltage source has
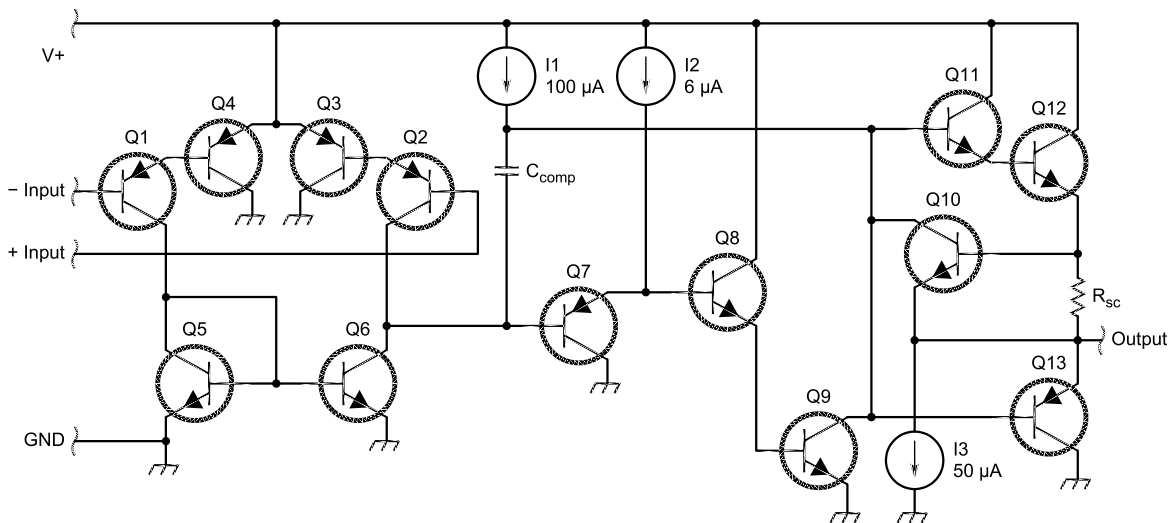
Figure 1—The internal design of the LM324 opamp.
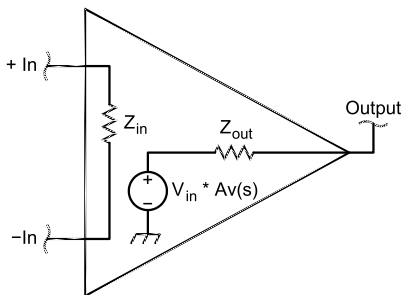
Figure 2—A model of an ideal opamp.
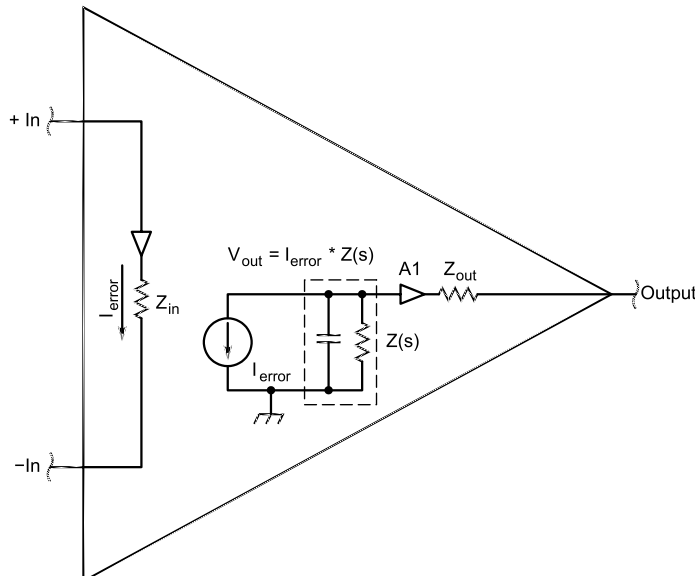
Figure 3—The ideal circuit of a current feedback amplifier.
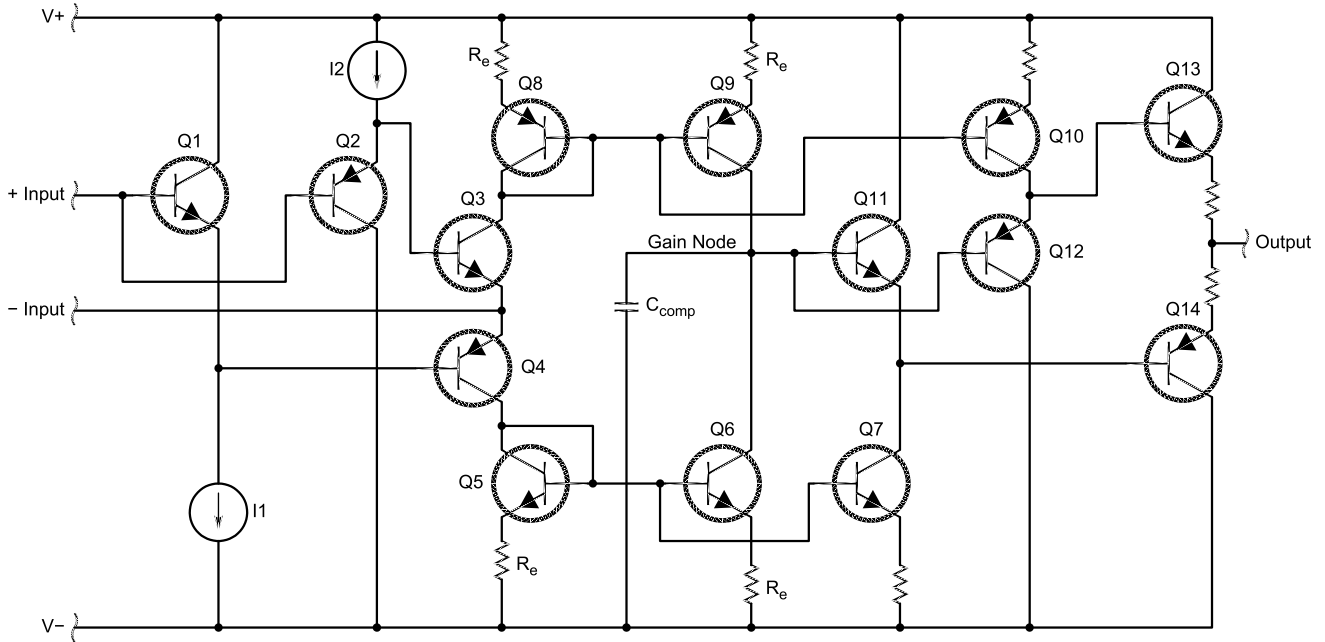
Figure 4—The internal circuit of a representative current feedback amplifier.

infinite gain in an ideal opamp, but a modern real device will have gain on the order of 100,000 or more.

Opamps are always used with a feedback loop to produce a closed loop system (except when used as low performance comparators). There are many hundreds of examples of closed loop circuits for op-amps. National Semiconductor is one of the best sources of application notes. If you are interested in op-amp applications, you should keep your eyes open for the blue National Linear Device data books at hamfests. The voltage between the two input pins of an opamp is forced to be essentially zero by the very high gain.

A current feedback amplifier expands on the concepts for an opamp using high gain, high input impedance, low output impedance and feedback to produce a well behaved closed loop system.

Circuit Comparison

Fig 3 shows the ideal circuit of a current feedback amplifier. The first stage is a unity gain buffer. An ideal unity gain buffer has a gain of exactly one, an infinite input impedance and zero output impedance. In a real world amplifier the gain will be less than one, but so close that it is not measurable. The input impedance will be large but not infinite, and the output will have some small amount of impedance. The middle stage is a current
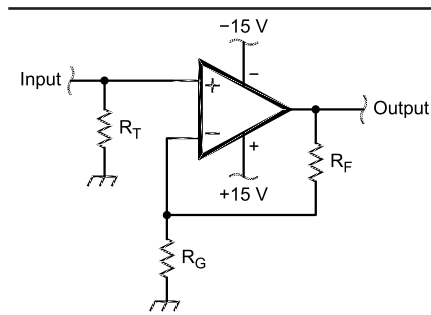
Figure 5—A non-inverting amplifier.
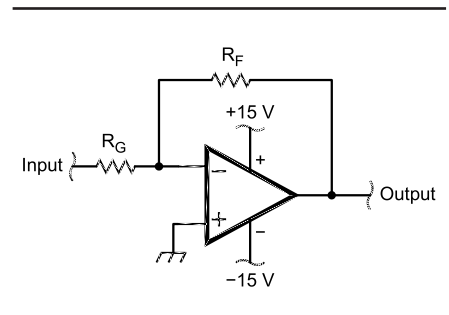
Figure 6—An inverting amplifier.
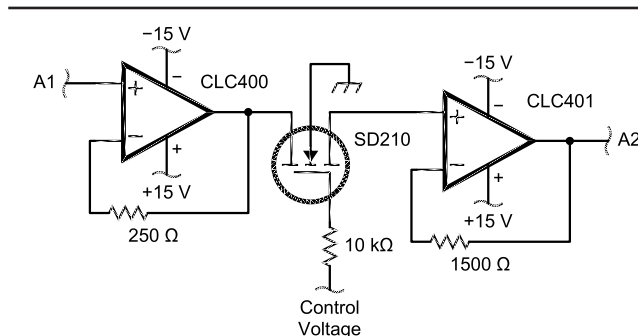
Figure 7—A variable gain amplifier using an FET to control gain.

controlled current source with a frequency dependent impedance in parallel. The output of the middle stage is presented to the input of the unity gain power amplifier.

Fig 4 shows the internal circuit of

a representative current feedback amplifier. Q1 and Q2 provide symmetrical input buffering. The input impedance of an emitter follower is equal to the emitter impedance times the gain. Since a current source has

essentially infinite impedance, the current sources in the emitters of these two amplifiers provide infinite input impedance at the non-inverting input. The current through Q3 and Q4 is the average of the currents in Q1 and Q2. The emitter follower output formed from Q3 and Q4 provides a low output impedance for the input buffer. Q8/Q9 and Q5/Q6 form current mirrors that implement the current controlled current source. The connection of the two current mirrors becomes the gain node where the actual amplification occurs. Q7 and Q10 provide bias current for the output unity gain amplifier, and Q11 through Q14 implement the output unity gain buffer.

The voltage gain of a current mode amplifier is generated by the error current times the generator impedance. This is shown in Fig 4 as $Z(s)*i_{error}$. The actual gain is called transimpedance gain because the voltage is a function of impedance. This impedance is very high at DC and decreases with frequency due to a primary pole at a low frequency.

Advantages

In general, the opamp and current mode amplifier have the same characteristics:

• infinite impedance between the non-inverting pin and ground,

• infinite voltage gain,

• zero current flow between the inverting and non-inverting inputs.

These characteristics mean that the current mode amplifier can be used in most circuits just as you would use an opamp.

When current feedback amplifiers were first introduced in the 1990s they generally offered bandwidth significantly higher than voltage feedback opamps at much lower prices. Semiconductor technology has increased the gain bandwidth of voltage feedback amplifiers to the point where bandwidth is no longer much of an advantage. Check out the TI web page for a comparison of cost for voltage mode and current-mode amplifiers (**focus.ti.com/lit/ml/slob088a/slob088a.pdf**).

The real advantage of current mode amplifiers is in slew rate. The 100 µA source in Figure 1 limits the output voltage slew rate of an opamp. The rate of charging the compensation capacitor is what limits the slew rate. The error current of the current feedback amplifier charges the compensation capacitor, so increasing the input voltage also increases the charge current. A second-order improvement comes from the output current that is supplied through R_F by the input amplifier while the system is unbalanced.

In general, current feedback amplifiers provide lower distortion at high frequencies than opamps. This comes from the advantages of negative feedback in the two unity gain amplifier stages.

The open loop gain of a current feedback amplifier is set by the feedback resistor. The open loop gain bandwidth is a constant. Increasing R_F raises the open-loop gain and reduces bandwidth in the same manner we are used to affecting gain bandwidth with closed loop gain for an opamp. The consequence is that closed loop bandwidth is always equal to the open loop-bandwidth set by R_F. Closed loop gain does not affect the bandwidth of the final amplifier.

Disadvantages

In real opamps there is always a very small error voltage between the input pins to force the output voltage. A current-mode amplifier always has a small error current that flows out of the inverting input to force the output voltage. The cookbook examples always assume there is no error, but the output of real amplifiers is always equal to the error signal times the open-loop gain.

A current feedback amplifier uses the error current to set the gain. There can be no error current if R_F is not present. There must always be some
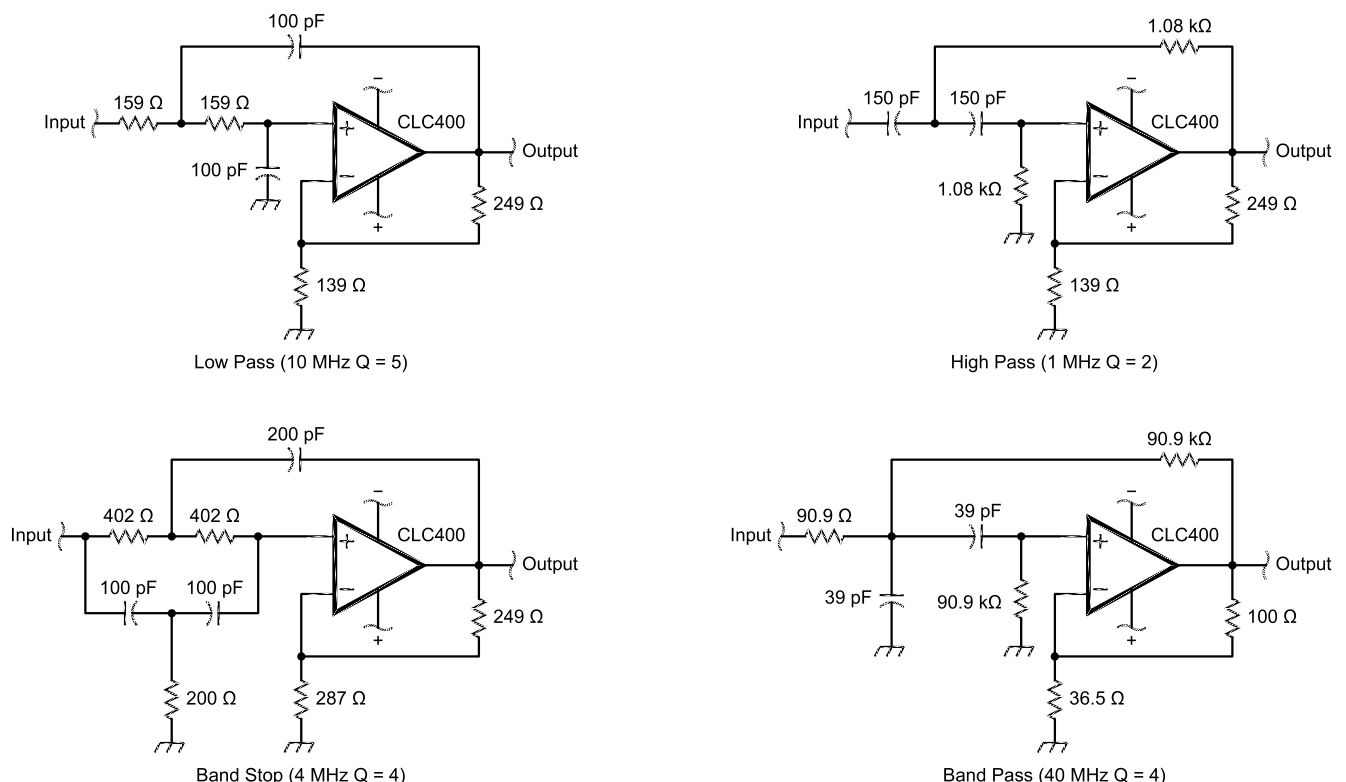
Figure 8—Op-amp realization of low-pass, high-pass, band-stop and band-pass filters.

impedance between the output pin and the inverting input pin for the amplifier to be stable. Any feedback circuit that has a zero in the response (this causes the impedance to be zero) will cause the circuit to become unstable. The requirement for no zeros limits the applications for filtering to those that put the reactances in the non-inverting input path. This means that the typical integrator implemented with a capacitor from output to non-inverting input cannot be implemented.

The value of R_F is usually suggested on the data sheet to give optimum performance. It is generally on the order of a few hundred to a few kohms.

Capacitance from inverting input to ground cause a pole in the response that usually interacts with the primary pole in the gain response. When this pole approaches the pole in the gain response, the amplifier starts to exhibit frequency peaking and ringing in the transient response. For low gain values the capacitance must be smaller than a few pF. This places a stringent requirement on layout to keep the capacitance at the inverting input as low as possible. The small amount of capacitance means that you should never use a socket for a current feedback amplifier.

Current mode amplifiers should not be used for applications that require close DC matching. An op-amp has symmetrical inputs and the effects of the bias currents from the input transistors can be offset by ensuring that the same resistance appears to ground for both inputs. This eliminates one source of DC offset for opamps. The same is not true for current feedback amplifiers. Trying to connect equal resistances to ground will have no effect since the –In pin is actually the output of an amplifier stage.

Current mode amplifiers do not drive high capacitance loads well. Driving a capacitor will cause phase shift at very high frequencies and cause the system to ring or oscillate in the same way capacitance at the inverting input will cause instability. If you need to drive a high capacitance load it must be isolated by a small resistor on the order of 30 ohms.

Basic Applications

Fig 5 shows a non-inverting amplifier. The voltage across R_G must be exactly equal to the input voltage because of the input buffer. If we start from the assumption that zero current flows out of the non-inverting input, then the output voltage must be equal to:

$$V_{OUT} = V_{in} * \frac{R_F + R_G}{R_G} = V_{in}\left(1 + \frac{R_F}{R_G}\right) =$$

(Eq 1)

This is exactly the same equation that you would use for an opamp. The input termination is only necessary if the driving circuit requires the termination. Otherwise the input is a high impedance. Fig 6 shows an inverting amplifier. The input impedance is equal to the value of R_G.

Fig 7 shows a variable gain amplifier using an FET to control gain. Since bandwidth is independent of closed loop gain, this circuit will maintain constant bandwidth over a very large gain range.

Fig 8 shows how to implement low-pass, high-pass, band-stop, and band-pass filters. Notice that all of these filters keep the reactances out of the negative feedback loop.

More Information

The pioneers in current feedback amplifiers were Elantec and Comlinear. These companies are now part of Intersil and National respectively. You can find application information by visiting the websites for Intersil (**www.intersil.com**) and National Semiconductor (**www.national. com**). ☐☐

Letters to the Editor

Resistance—The Real Story (Jul/Aug 2004)

Doug,

That was a great article in the July/ August *QEX* about resistance. Rephrased, you can say resistance is the inverse of speed, or conductance is speed. You also discussed the impedance of electromagnetic fields as the ratio of electric to magnetic field strengths, which is well accepted, but be careful how you present it. We both understand that the impedance in a transmission line and free space is the ratio of the electric to magnetic fields, but we also understand we're talking about propagating waves. I was once corrected when I didn't specify "propagating wave," and had to admit that when used for dc, the field ratios in a transmission line are totally dependent on load and source, obviously. This applies to static fields in free space, too, of course.

I'm going to review your analysis more and may have additional comments later, but I just thought I'd mention that I really thought you did an interesting piece.—*J. Arthur Smith, WB9RWY;* 203 11th St S, Hudson, WI 54016-2040; **aSmith@dynatronix. com**

Hi Doug,

This is what I am trying to learn. Is the system of units that results in seconds over distance for resistance the same system of units that results in one ampere giving a force of 2×10^{-7} newtons per meter between infinite conductors one meter apart? Any help with the above question would be very much appreciated.—*Thanks, Fred Doran;* **freddoran@rogers.com**

Hi Fred,

Well, not quite, because all my stuff is in centimeter-gram-second units (CGS) and newtons and meters don't fit that system directly. You would need to use dynes for the force and centimeters for the distance to stay in CGS, applying a constant correction factor to get to the meter-kilogram-second (MKS) system.—*Doug Smith, KF6DX*

Doug,

I enjoyed your article about resistance. Not too many people think about the actual mechanism behind current flow. It would be great if there were more articles discussing fundamentals like this in *QEX*. However, I am bothered by the units of seconds for resistivity. You mention "Field strength can also be expressed as charge/cm^2" and then use this to derive the resistivity units of seconds. If I remember correctly, charge/cm^2 is usually surface charge density and although an electric field will be generated by the surface charge, it isn't the same as the electric field.

Am I missing something? I would appreciate more details. Regardless, thanks for writing the article. That kind of stuff takes time.—*73, Phil Bondurant, WA7ZWD, 16433 SE 264th St Kent, WA 98042-8388;* **wa7zwd@comcast.net**

Hi Phil,

You are right that charge per square centimeter is surface charge density, but it is directly proportional to the electric field strength. My references on this point seem pretty solid to me. Thanks for the note.—*Doug, KF6DX*

Improved Remote Antenna Impedance Measurement (Jul/Aug 2004)

Sir:

I thoroughly enjoyed the first article, and appreciate the second even more. I'd been analytically pursuing a similar method of using two known values to eliminate the need to measure coax loss and length. Your solution is much more elegant and practical than what I was approaching. Thank you and congratulations — this is good, important work.

I have a question and a comment:

1. Is the spreadsheet available electronically somewhere? I found no reference to a source in your otherwise well documented article. I've used your first spreadsheet extensively.

2. I think I've found an error (or misprint) in the derivation on the left-hand side of page 35. In the first line, you equate $\tanh(\gamma\times L)$ with values from the two different measurements. The second line shows the result of a cross-multiplication to simplify; unfortunately, the algebra doesn't seem to work. Then, I notice that the third line does not follow from the second line, either. if I work the derivation independently, however, I *do* arrive at the third line. So, it appears to me that there's an error in the second line. It *appears* that Rh–Zh, on the left of the equality and Rl–Zl on the right-hand side should, in fact, be Rh•Zh and Rl•Zl, respectively. It appears that perhaps the editors or printers misread your submission.

If you agree with my assessment of the error, I request a clarification.— Thanks and very 73, *Jim Sanford, WB4GCS, 10 Sugar Run Rd, Eighty Four, PA 15330-2550;* **wb4gcs@ amsat.org**

Hi Jim,

Thanks for your e-mail and the kind remarks about my article; I'm pleased that you put my previous spreadsheet to good use.

In reply to your point 1, the spreadsheet is now on the ARRL Web site **www.arrl.org/qexfiles/**.

Regarding your point 2, you are correct in your assumption; it is a printing error. There was an error on the proof, which was corrected, but in making the correction, we introduced another error, which you have identified. I didn't see the corrected version until it appeared in the magazine, and I was unaware of it until I read your e-mail.

I would be interested to know your facilities for measuring impedance and what your observations are on the effect of frequency on velocity factor, which I reported in the article.—*73, Ron G4JNH,* **ron.g4jnh@ talk21. com**

Ron,

A reference you might find of interest is H. N. Dawirs, "Application of the Smith Chart to General Impedance Transformations," *Proceedings of the IRE*, Vol 55, July 1957, p 954. It discusses use of the Smith Chart with networks having complex image impedances—not of much practical importance now. It dates from the time before powerful desktop computers, when graphical techniques were the only practical way to solve many problems.

I still can't put my hands on the reference using the Weisfloch transformer theorem. Weisfloch's theorem, at least in its simplest form, states that an unsymmetrical network can be represented by a symmetrical network in series with an ideal transformer. The reference replaced an antenna with a resistive load of some value near the antenna impedance and tuned the input end of the transmission line to produce a resistive output equal to the nominal impedance of the impedance measuring device, say typically 50 Ω.

Via Weisfloch, this arrangement became equivalent to an ideal transformer and a section of matched transmission line. Then the transmission-line length was adjusted to be a multiple of one-half wavelength.

Suppose the resistive load was 300 Ω. Then the arrangement was equivalent to an ideal transformer with a turns ratio of the square root of 6 and a line length of zero. If the antenna showed an impedance of $350 + j65$, the impedance measurement would read $58.3 + j10.8$, very handy.

The authors were working at microwave frequencies and using low-loss components such as screw tuners, slotted lines and wave guides. There was some brief mention of losses that I never understood.

I have tried to figure a way to use this in what my number-two son calls "the DC band" (200 MHz and down!), figuring to replace the line stretcher with calculations and using a typical antenna tuner, but the tuner is hardly low loss, and neither is the coaxial transmission line. I have never (yet) found a way to account for the losses.—*73, Bert Weller, WD8KBW; 1325 Cambridge Blvd, Columbus, OH 43212-3206;* **aeweller@att.net**

A Low-Cost 100-MHz Vector Network Analyzer (Jul/Aug 2004)
Doug,

There was an interesting article in the issue that just arrived (Jul/Aug). However, I went over it many times in the days since it arrived, and I seem to be missing something. Is this a construction article, a review of a commercial item, or something to whet our appetite for a kit offering? Was it the second part of some article that I missed, or a first of a series with the rest to follow?

I am quite baffled. On page 2, under "In This Issue," you said "If you build it…." That implies that we are to build it. I see a block diagram but no schematic. *QEX* claims to be an experi-menter's journal, but expecting us to build something from just a block diagram really "separates the men from the boys." I see no reference to an online schematic anywhere, no indication that kits are available or will be, no hint of where to buy it, or that it's a commercial product. What's going on here?

About the only clue of any sort is the picture of the rear that has the TAPR URL printed on it. I see that the TAPR ad in that issue of *QEX* has no mention of it, so it's obviously not a thinly disguised new product promotion. The TAPR Web site does mention it, but only says that plans are underway to produce it and ten beta kits are being assembled. (Of course nothing in the text prompted me to go there; I only did it because of the picture.)

Somehow, I expect a lot more from

ARRL and *QEX*. Apparently, this article really is a thinly disguised promotion for a semi-commercial product after all? The lack of a schematic strongly suggests that, but there is no hint as to where or how they can be procured, not even any leads to the TAPR site except for a picture! Maybe it's just me, but that certainly seems a bit obscure. (Beta kits? What if problems develop and it never becomes available for one reason or another? I'd at least expect them to wait until it's a real product before advertising it.)

Surely we can do better than this. I know I certainly expect better from *QEX.—73 de Mike Czuhajewski, WA8MCQ ,7945 Citadel Dr, Severn, MD 21144-1566;* **wa8mcq@comcast.net**

Dear Mike,

The code and schematics are now on our download site at **www.arrl.org/qexfiles/** as **VNA.zip.**—*Doug.*

Antenna Options (Jul/Aug 2004)
Sir:

Although I haven't designed or built any complex antennas (that is, other than dipoles, etc.), I always enjoy reading articles about them. Most interesting, what tradeoffs are made—either deliberately or accidentally? The three Yagis in W4RNL's article are good examples. The differences are clear from the drawings, yet the rationale for going in a given path seems less obvious. I would maintain that, for most uses, front-to-back ratio (F/B) is the most important criteria. I say that because: First, a gain optimized antenna is rarely more than 1 dB better than other optimizations, and that 1 dB won't ever be noticed. Second, that 1 dB probably only applies over a much narrow range of frequencies than will likely be used in practice, so is of even less value. F/B, however, can vary by many decibels and allows rejection of strong signals while receiving much weaker ones.

However, the notion of F/B as simply being a sharp null 180° from the angle of maximum gain fails to accomplish the above purposes. The form of F/B that really matters is either the worst-case front to anything else ratio, or, alternately, the front to average of everything else" ratio. Obviously, both of these are a little hard to quantify, being related to beam width and the complexities of side lobes in some designs. Maybe that is why they are rarely considered. For most Amateur operation, however, this is really what will make the difference between good and mediocre antennas.

The third example, the one with

very wide bandwidth, is a real joke, and it is a sad commentary on far too much antenna design. I have even seen this misconception rampant in commercial and military design specifications. The antenna may be broadband, but that only means that its gain is lousy over a wide range of frequencies. Compared to the other two designs, neither the gain, nor the F/B are significantly better, even at the band edges, and they are far worse in the middle. The design criteria was low SWR, but the SWR of the other designs (over the band of interest) was probably well within the range that would allow a transmitter to deliver full power to the load, with minimal feed-line loss. It puzzles me why our industry is so fixated on keeping VSWR so low.

Beyond designing for good front-to-everything-else ratio, I would submit that the second criteria for antenna design in most cases should be designing for that ratio, and, secondarily, best gain over the widest possible frequency band. Unless SWR or other parameters become very bad, they can be mostly ignored in the process. Likewise, given the number of excellent matching and transformation techniques available, the unmatched impedance should be a relatively minor concern.—*73, Wilton Helm, WT6C, 11425 E Caribou Dr, Franktown, CO 80116-8523;* **whelm@compuserve.com**

The Author Replies:

The use of very general criteria—such as maximum F/B and gain-bandwidth—might have been the limits of amateur Yagi design thinking one to two decades ago. They emerged from simplified cutting formulas and cut-and-try development techniques. Today, however, the design tools at our disposal are good enough that we can design and successfully build for goals that are much more specifically suited to the particular uses to which we put antennas. There is no longer a need to use over-generalized criteria. Similarly, there is no need to accept a poor match (especially at VHF and up) when we can design a good match. (This may be accomplished with the established matching systems for low-impedance designs or through the natural 50-Ω match of a wide-band design). A 20-meter Yagi is large enough that we may need the best compromise among all of the initial design goals. For a 3-foot-long $20 2-meter Yagi, there is no reason why we cannot create truly function-specific designs and antennas. —*73, L. B. Cebik, W4RNL, QEX Contributing Editor, 1434 High Mesa Dr, Knoxville, TN 37938-4443,* **cebik@cebik.com**. □□

Out of the Box

By Ray Mack, WD5IFS
QEX Contributing Editor

Watts Unlimited PS-2500A

Watts Unlimited is producing a high voltage switching power supply that is intended to replace the HV supply in tube amplifiers. This design was originally presented in February 1991 *QEX*. Tim has updated the design since that article. The supply is available either built and tested or in kit form.

The stock design produces 3600 V with 110 mA of idle current and drops to 2500 V at the full load current of 1.1 A. The supply has line and load regulation that is very similar to the stock power supply in most tube amplifiers. Even though the supply uses switching technology, it is not a regulated supply. The supply can be ordered with other output voltages if your amplifier requires a value other than 2500 V.

The design is very conservative and should have no problem giving years of service. There are several interesting features of the design. The first is that Watts Unlimited has paid close attention to ensuring that the supply does not produce RFI. The supply output is intended to be turned off when not transmitting. The output is electronically controlled and can respond very quickly to the control signal. This allows for full QSK on CW. Amplifiers should run significantly cooler than with the stock supply because the tubes do not draw any current during receive. There is full thermal protection to ensure that the supply does not fail if the fan fails or the ambient temperature is too high for proper operation. The fan runs on a voltage from 8 to 12 Vdc, but this voltage is not supplied by the PS-2500A. Likewise the control voltage for the output circuit must be externally supplied. Data modes that use 100% duty cycle require derating the maximum output current to 500 mA. The supply must run on 240 Vac for full output, but this is normal for 1500 W PEP class amplifiers. It is possible to run the supply on 120 Vac if you need 1350 W or less.

The supply is intended to replace the transformer and rectifier assembly inside the cabinet of your amplifier. It can be used outboard, but you will need to provide additional wiring and protection. Operation as an outboard supply is definitely not plug-and-play. Watts Unlimited gives well written and detailed instructions for both inboard and outboard mounting.

The supply measures 11.75×6×5 inches and weighs only 10 pounds. It might be a little difficult to fit this supply in a small amplifier such as a Heath SB-200 or similar small 1 kW amplifier. Larger amplifiers such as the Heath SB-220 and SB-230 should be just fine.

The kit instructions show that the author has built more than a few Heathkits. The instructions are very well written and presented. The biggest task in building the kit is to wind the power transformer. It is a stacked set of toroids and requires you to use a shuttle to wind the wire onto the transformer.

My only reservation about this supply is the design of the power transformer. The wire used has heavy Teflon insulation on both the primary and secondary windings. Watts Unlimited has verified the dielectric should withstand up to 11 kV. The stock iron transformer in your amplifier has almost certainly been designed and tested to Underwriters Laboratory (UL) standards even if your amplifier is not UL certified. UL requires that there are two levels of insulation protection between the power line and any user exposed portions of the circuit. These are called primary insulation and secondary insulation (easily confused with primary and secondary windings). UL certification is a costly and difficult process and most manufacturers do not seek it unless there is a compelling reason. However, most still design to UL standards.

The Teflon is the primary insulation in this design. There is no secondary insulation for the PS-2500A transformer. If the Teflon insulation fails, there can be a direct short from the primary winding to the ferrite core of the transformer. While this is very unlikely, it is not impossible. One problem with Teflon is that it cold flows and the insulation could fail from stress where the turns go from the inside to outside of the core. The transformer design can be improved by wrapping either mylar tape or kapton tape around the core before winding the primary. The primary should also be covered with mylar or kapton tape before the secondary is wound. This is a difficult task with a toroid.

Price: $698 built and tested, $585 kit, postage paid in the USA. Contact: Watts Unlimited, 886 Brandon Lane, Schwenksville, PA 19473. Tel 610-764-9514, e-mail **wattsunlimited@aol.com**, **www.wattsunlimited.com**. □□

In the next issue of QEX/Communications Quarterly

John Champa, K8OCL, and John Stephensen, KD6OZH, outline recent developments in high-speed multimedia (HSMM) using 802.11 and other types of equipment. A lot of their work has grown out of the ARRL HSMM Working Group. Be sure to check it out. KD6OZH also contributes a piece on software-defined radio. Randy Evans, KJ6PO, gives us a look at phase-locked loop (PLL) design and implementation. Karl-Otto Müller, DG1MFT, discusses coaxial traps for antennas. □□